COO-4433-2
Distribution Category UC-96

THEORETICAL STUDIES ON HETEROGENEOUS COMBUSTION

Progress Report

for Contract No. EG-77-S-02-4433.A000

Covering the Period of March 1, 1978 - Feb. 28, 1979

Prepared by

Chung K. Law
Department of Mechanical Engineering
and Astronautical Sciences
Northwestern University
Evanston, Illinois 60201

NOTICE
This report was prepared as an account of work sponsored by the United States Government. Neither the United States nor the United States Department of Energy, nor any of their employees, nor any of their contractors, subcontractors, or their employees, makes any warranty, express or implied, or assumes any legal liability or responsibility for the accuracy, completeness or usefulness of any information, apparatus, product or process disclosed, or represents that its use would not infringe privately owned rights.

For Review by

Division of Chemical Sciences
Office of Basic Energy Sciences
U.S. Department of Energy

DISTRIBUTION OF THIS DOCUMENT IS UNLIMITED

DISCLAIMER

This report was prepared as an account of work sponsored by an agency of the United States Government. Neither the United States Government nor any agency Thereof, nor any of their employees, makes any warranty, express or implied, or assumes any legal liability or responsibility for the accuracy, completeness, or usefulness of any information, apparatus, product, or process disclosed, or represents that its use would not infringe privately owned rights. Reference herein to any specific commercial product, process, or service by trade name, trademark, manufacturer, or otherwise does not necessarily constitute or imply its endorsement, recommendation, or favoring by the United States Government or any agency thereof. The views and opinions of authors expressed herein do not necessarily state or reflect those of the United States Government or any agency thereof.

DISCLAIMER

Portions of this document may be illegible in electronic image products. Images are produced from the best available original document.

TABLE OF CONTENTS

I. Summary of Program Objectives and Present Status

In most of the liquid-fueled chemical power plants the fuel is usually introduced into the combustor in the form of a spray jet consisting of an ensemble of droplets. The spray subsequently ignites and burns, releasing chemical energy to perform work and, at the same time, producing trace pollutants which are subsequently exhausted. Hence in order to improve the combustor performance in terms of, say, cleanliness and efficiency, understanding of the combustion characteristics of fuel spray is essential. The present program then aims to study, from theoretical viewpoint, the various heterogeneous processes involved during (1) vaporization, ignition, deflagration, and extinction of single fuel droplets in the reactive environment simulating the spray interior, and (2) the vaporization and ignition of the spray as a whole.

During the reporting period we have completed the numerical modeling of unsteady droplet combustion in a reactive environment simulating the spray interior. From the fundamental viewpoint this is the first systematic study on the combustion characteristics of a system exhibiting both diffusional and premixed burning. From the practical viewpoint it provides useful information on such pertinent questions as the ignition lag, burning rate, and flame size for droplets burning or vaporizing within the spray environment.

This numerical study has also yielded much physical insight which is useful for further analytical studies. For example, examination of the numerical results has led us to question a basic feature of the classical droplet combustion theory, that is the instantaneous rate of

fuel vaporization from the droplet is equal to the rate of fuel consumption at the flame. We have subsequently formulated a theory which demonstrates that a significant portion of the fuel vaporized is actually used in filling up the space between the droplet and the flame instead of being consumed at the flame. Therefore by adopting the classical droplet combustion theory in modeling spray combustion, grossly inaccurate estimates of the chemical heat release rate may result.

We have also started our studies on spray vaporization. We have first investigated the effect of possible condensation of ambient moisture on the spray vaporization rate. This possibility has been overlooked in the past although we have shown that the potential enhancement of the fuel vaporization rate through water moisture condensation is significant, particularly for a cold and dense spray. It also has important implications on the ignition delay of a spray.

In the following the highlights of these three projects are discussed in more detail.

II. Numerical Modeling of Droplet Ignition and Combustion in a Reactive Environment

The extensive amount of literature on droplet combustion has all assumed an oxidizing environment. In reality, however, the environment which the droplet responds to within the spray interior also consists of fuel vapor produced prior to ignition and is therefore reactive. It is obvious that depending on the fuel vapor concentration, quantitative

or even qualitative changes on the droplet combustion characteristics can result. For example when the environment becomes excessively fuel rich, droplet combustion, or even pure vaporization, may be inhibited. Indeed, recent experimental evidence does seem to indicate that the single droplet combustion mode is not favored in the fuel rich region of the spray core.

From the fundamental viewpoint fuel droplet combustion in an environment consisting of some of its own vapor is also an interesting chemical system to study. This is because part of fuel present in the system is premixed with the oxidizer in the ambiance whereas the rest is perpetually being released from the droplet and has to diffuse outward and mix with the oxidizer before reaction can take place. Therefore the expected combustion mode is neither strictly diffusional nor strictly premixed. One would then expect that this hybrid system will exhibit diffusional-like combustion for low levels of fuel vapor concentration and premixed-type combustion when the environment fuel-oxidizer concentration approaches stoichiometric.

In order to provide the needed physical insight to the problem, a numerical study on the vaporization and combustion of a fuel droplet in a reactive environment with varying reactant concentrations has been conducted. The problem considered is as follows. At time $t = 0$ a pure fuel droplet of constant temperature T_s is introduced into a hot, stagnant, isobaric environment with initial temperature T_{∞_o} and mass fractions of oxidizer and fuel vapor, $Y_{O\infty_o}$ and $Y_{F\infty_o}$, respectively. The droplet, being at a lower temperature, receives heat from the

environment and in turn releases fuel vapor to the gas medium. The subsequent processes of vaporization, heat and mass transport, and the chemical reactions between the fuel and oxidizer are studied. The governing equations are the spherically-symmetric, isobaric, transient-diffusive-convective-reactive conservation relations for species concentration and energy.

The numerical study shows that when the ambiance is fuel lean, diffusion-like burning generally can be identified. Ignition takes place close to the droplet and early in the droplet lifetime, when less than 1% of the droplet mass has vaporized. After ignition the flame propagates outward, with the fuel vapor released from the droplet being partly consumed at the flame and partly stored in the inner region to the flame. In the case of a fuel-rich environment, diffusional burning is not possible.

Considerable simplification in estimating the droplet behavior also results if the ambiance is either weakly or intensely reactive. If it is weakly reactive then the environment is essentially frozen during the droplet lifetime. Then the droplet undergoes either purely diffusional burning if the ambiance is fuel lean or pure vaporization if it is fuel rich. If the environment is intensely reactive, one of the reactants will be rapidly depleted. Then the subsequent phenomena of interest are again either purely diffusional burning or pure vaporization, except now the ambient temperature is the adiabatic flame temperature and is therefore much hotter. Homogeneous ignition theory can be used to assess the reactivity of the ambiance.

This work is detailed in Appendix A, which has been submitted for consideration for publication.

III. Re-examination of the Classical d^2-Law of Droplet Combustion

In our numerical study of droplet combustion we noticed that after ignition the flame-front standoff distance $\tilde{r}_f$, defined as the ratio of the flame diameter to the droplet diameter, continuously increases. This is the case even when the ambiance is devoid of any fuel vapor and therefore is strictly oxidizing. This is contrary to the result of the classical d^2-law of droplet combustion which states that $\tilde{r}_f$ is a constant. A continuously increasing $\tilde{r}_f$ has actually been observed by Kumagai and his co-workers by conducting the experiment in a freely-falling chamber.

Waldman, and Crespo and Linan, attributed this to be caused by the gas-phase unsteadiness as a result of the finite magnitude of the gas density compared with the liquid density such that during the characteristic gas-phase transport time the droplet surface does regress a little. This then implies that rather than being quasi-steady as assumed in the d^2-law model, the gas-phase transport processes are intrinsically unsteady. Crespo and Linan further showed that these finite-density effects are expected to be important in the region located at $\tilde{r} > 0(\sqrt{\rho_\ell/\rho_g})$ away from the droplet. In this region the gas velocity becomes comparable with the droplet radial regression rate such that the flow changes from being convective-diffusive in the interior, quasi-steady, region to being transient-diffusive here.

Therefore any process of significance occurring in this far field region is expected to render the bulk combustion characteristics unsteady.

However, an examination of the data of Kumagai et al. in light of the above discussion yields the following dilemma. Using $\rho_\ell/\rho_g = 0(10^3)$, the transient-diffusive region is expected to be at least 30 droplet radii away. However, the experimental flame size is $\tilde{r}_f < 10$. Therefore the flame characteristics, as well as other bulk combustion parameters, should exhibit quasi-steadiness with small perturbations of the order of $\sqrt{\rho_g/\rho_\ell}$. This, of course, is contrary to the observation that the flame continuously propagates outward. Therefore the finite-density effect is not adequate to explain the experimental flame behavior.

In response to the above dilemma, we have recently identified an additional, unsteady process which we believe is of importance under all situations and indeed is quite adequate to explain the observed flame behavior without accounting for the finite-density effect. The process of interest is the transient build-up of the fuel vapor profile in the inner region to the flame as it approaches the d^2-law location. Obviously prior to ignition the fuel vapor concentration in the vicinity of the droplet is quite low, especially for the spark-ignition experiment of Kumagai et al. conducted in a cold environment. However, after ignition this concentration will have to be significantly increased in order to sustain combustion. Therefore immediately after ignition most of the fuel vaporized is stored in the inner region rather than

being actually consumed at the flame. Due to the insufficient amount of fuel supplied, the flame will lie in close proximity to the droplet during this period. As the fuel vapor concentration increases, more fuel vapor can then be used for combustion and the flame subsequently propagates outward.

Formulation of the theory parallels with that of the d^2-law, except now distinction must be made between the rates of fuel vaporization and consumption. The overall mass balance for the fuel then consists of three terms representing respectively the amount vaporized, consumed, and accumulated. The last term is absent in the d^2-law model.

Results of the theory agree with the above reasoning, particularly the existence of a continuously increasing $\tilde{r}_f$. Furthermore, since the rate of vaporization exceeds the rate of combustion initially but eventually the trend is reversed, therefore by assuming these two rates are identical in the d^2-law, the rate of chemical heat release can be grossly mis-estimated in spray combustion studies.

It is important to note that recently we have also obtained experimental evidence which substantiates our theoretical findings.

This work is summarized in Appendix B, which has been submitted for external publication considerations.

IV. Enhancement of Fuel Spray Vaporization Rate through Condensation of Water Vapor

The rate of combustion of a fuel spray is frequently controlled by the rate with which the individual droplets within the spray interior

vaporize. In general the primary driving force to effect vaporization is the sensible heat of the hot environment within which the spray is introduced. Through conductive-convective heat transport the originally cold fuel droplets subsequently heat up and vaporize, producing fuel vapor which is mixed with the oxidizer gas to render combustion possible.

There is, however, another potentially important source of heat whose utilization can significantly enhance the spray vaporization rate. This arises from the possibility that during vaporization the spray interior may be chilled to such an extent that the water vapor present in the gas medium may condense and release the associated heat of condensation, which can then supplement the heat needed for fuel vaporization.

This condensation-enhanced vaporization is expected to be particularly beneficial for spray vaporization in a relatively cold, humid, environment, for example during carburetion of the automotive engine. For systems similar to this it has been found that under most situations the spray interior rapidly becomes saturated with fuel vapor, leading to complete termination of vaporization. Since it is generally recognized that incomplete fuel vaporization during carburetion causes maldistribution and other deleterious heterogeneous combustion characteristics, the possible minimization of these heterogeneous effects through water vapor condensation is significant. Similar arguments can also be extended to the direct injection systems because the environment of the spray core is likely to be cold and fuel rich due

to the slow rate of entrainment.

It is also reasonable to expect that the extent of augmentation in the fuel spray vaporization rate can indeed be substantial. This is because firstly the air-fuel mass ratio for near-stoichiometric combustion of typical hydrocarbon fuels (e.g. gasoline) is usually a large number, around 15. Therefore for a sufficiently humid environment the moisture content is of the same order as the liquid fuel introduced. Furthermore the specific latent heat of vaporization of water is much larger than those of the hydrocarbon fuels. It is then obvious that the water vapor present in the environment does contain sufficient latent heat of condensation which when released can supply a significant portion of the energy needed for fuel vaporization. Finally, it is also of interest to note that since water is a major product of hydrocarbon combustion, the water vapor generated at the hot combustion zone may diffuse back to the cold, vaporization region where it condenses.

The above concepts have been substantiated and quantified through a study of monodisperse spray vaporization in an environment initially containing some water vapor. Two models have been formulated to bracket the limiting behavior of spray vaporization in the presence of water condensation. In the fastest limit, termed the heterogeneous condensation mode, condensation of water vapor is assumed to occur at the surface of the fuel droplets which, being colder than the gas, are ideally suited as heterogeneous nucleation sites. Since in this limit the condensation heat release is directly supplied to the droplet,

the droplet vaporization rate is expected to be maximally enhanced. In the slowest limit, termed the homogeneous condensation mode, condensation occurs with the gas medium at the saturation temperature. This implicitly assumes that there exist some heterogeneous nucleation sites (e.g. dust particles) in the gas other than the fuel droplets. In this limit the increase in the droplet vaporization rate is caused by an increase in the gas temperature relative to the case of no water condensation. Due to the large amount of air mass that needs to be heated, the extent of increase in the gas temperature, and hence the droplet vaporization rate, are not expected to be as significant as the heterogeneous mode.

The formulation of each model consists of a description of the vaporization of an individual droplet, possibly in the presence of water condensing at its surface, in an environment whose properties are continuously being modified by the vaporization of all the droplets and also the depletion of water vapor. Therefore conservation equations for heat and mass are needed both for the individual droplet and also the spray as a whole.

Sample solutions were obtained for an heptane spray vaporizing in air with initial temperatures of 280^{o}K, 300^{o}K, and 320^{o}K, and which can be either fully humid, half-humid (on molar basis), or completely dry. The results substantiate our initial reasoning. For example, for a 300^{o}K, fully-humid environment, the presence of heterogeneous condensation can enhance the spray vaporization rate by almost a factor of two. The increase is less drastic for the homogeneous mode, about

10%. However, it can be argued that even this small amount of increase can be significant for a spray which otherwise cannot achieve complete vaporization. The present study also emphasizes the potential complications on spray experimentation caused by condensation of water either from the inducted air or generated through combustion. Water condensation may result in larger droplet sizes due to heterogeneous condensation or in high droplet number density due to homogeneous nucleation.

This work is detailed in Appendix C and will be published in International Journal of Heat and Mass Transfer.

V. Publications Resulting from Present Program

(1) "Deflagration and Extinction of Fuel Droplet in a Weakly-Reactive Atmosphere," by C.K. Law, J. Chem. Phys. 68, 4218 (1978).

(2) "Ignition of a Combustible Mixture by a Hot Particle," by C.K. Law, AIAA J. 16, 628 (1978).

(3) "Fuel Spray Vaporization in Humid Environment," by C.K. Law and M. Binark, to appear in International Journal of Heat and Mass Transfer.

DROPLET COMBUSTION IN A REACTIVE ENVIRONMENT

P. Botros and C. K. Law
Northwestern University
Evanston, Illinois 60201

W. A. Sirignano
Princeton University
Princeton, New Jersey 08540

ABSTRACT

The transient processes of evaporation, ignition, and combustion of a fuel droplet in a hot, reactive fuel-oxidizer environment simulating the spray interior are studied numerically, with emphasis on the relative importance of diffusional burning in the droplet vicinity and premixed burning in the ambiance. It is shown that for a fuel-lean environment diffusional burning is generally possible and is initiated rapidly, whereas for a fuel-rich environment only premixed burning is possible. For a sufficiently reactive environment one of the reactants is rapidly depleted such that during most of the droplet lifetime the environment is really non-reactive. The present numerical study yields much physical insight useful for further modeling efforts.

I. INTRODUCTION

Much research have been conducted on the combustion of single fuel droplets in oxidizing environments [1,2]. In reality, however, the environment which the droplet responds to within the spray interior also consists of fuel vapor produced prior to ignition and is therefore reactive. It is obvious that depending on the fuel vapor concentration, quantitative or even qualitative changes on the droplet combustion characteristics can result. For example when the environment becomes excessively fuel rich, droplet combustion, or even pure vaporization, may be inhibited. Indeed recent experimental evidence does seem to indicate that the single droplet combustion mode is not favored in the fuel rich region of the spray core [3].

From the fundamental viewpoint fuel droplet combustion in an environment consisting of some of its own vapor is also an interesting chemical system to study. This is because part of fuel present in the system is premixed with the oxidizer in the ambiance whereas the rest is perpetually being released from the droplet and has to diffuse outward and mix with the oxidizer before reaction can take place. Therefore the expected combustion mode is neither strictly diffusional nor strictly premixed. One would then expect that this hybrid system will exhibit diffusional-like combustion for low levels of fuel vapor concentration and premixed-type combustion when the environment fuel-oxidizer concentration approaches stoichiometric.

When the environment is only weakly-reactive and fuel-lean, the combustion characteristics are expected to resemble those of the classical Godsave's d^2-law model [4], with perturbations being proportional to the ambient fuel vapor concentration. The steady combustion and extinction characteristics in this weakly-reactive limit have been analyzed recently [5]. The results show that with increasing fuel vapor concentration the flame temperature and

size both increase although the droplet burning rate is only minimally affected. These results are amenable to experimental verification.

When the environment becomes more reactive, chemical reactions are not confined to a thin flame region close to the droplet and the phenomena of interest are more complex. Therefore in order to provide the needed physical insight to the problem, a numerical study on the vaporization of a fuel droplet in a reactive environment with varying reactant concentrations has been conducted and the results are reported herein. The governing equations and the numerical details are presented in the next Section. Results and discussions are given in Section III.

II. FORMULATION

Governing Equations

The problem considered is as follows. At time $t = 0$ a pure fuel droplet of constant temperature T_s is introduced into a hot, stagnant, isobaric environment with initial temperature $T_{\infty o}$ and mass fractions of oxidizer and fuel vapor, $Y_{O\infty o}$ and $Y_{F\infty o}$, respectively. The droplet, being at a lower temperature, receives heat from the environment and in turn releases fuel vapor to the gas medium. We are interested in the subsequent processes of vaporization, heat and mass transport, and the chemical reactions between the fuel and oxidizer. The governing equations for this spherically-symmetric, isobaric, transient-diffusive-convective-reactive gaseous system are as follows [6].

Continuity:
$$\frac{\partial \rho_g}{\partial t} + \frac{1}{r^2}\frac{\partial}{\partial r}\left(\rho_g v r^2\right) = 0 \tag{1}$$

Species:
$$\rho_g\left(\frac{\partial Y_i}{\partial t} + v\frac{\partial Y_i}{\partial r}\right) - \frac{1}{r^2}\frac{\partial}{\partial r}\left(\rho_g \mathcal{D} r^2 \frac{\partial Y_i}{\partial r}\right) = -\nu_i W_i \omega \tag{2}$$

Energy: $$\rho_g\left(\frac{\partial H}{\partial t} + v\,\frac{\partial H}{\partial r}\right) - \frac{1}{r^2}\,\frac{\partial}{\partial r}\left(\lambda r^2\,\frac{\partial T}{\partial r}\right) = \nu_F W_F Q\omega \qquad (3)$$

State: $$p = \rho_g (R^o/\bar{W})T \qquad (4)$$

where $$\omega = BT^{a_T}\left(\frac{X_O p}{R^o T}\right)^{a_O}\left(\frac{X_F p}{R^o T}\right)^{a_F} \exp\left(-\frac{E}{R^o T}\right) \qquad (5)$$

is the production term for a one-step overall irreversible reaction between the fuel and oxidizer, and where r is the radial co-ordinate, ρ the density, v the velocity, X_i the molar fraction, Y_i the mass fraction, T the temperature, p the pressure, H the enthalpy, Q the heat of reaction per unit mass of fuel consumed, C_p the specific heat, $\mathcal{D}$ an average mass diffusivity, λ the thermal conductivity, W_i the molecular weight, $\bar{W}$ an average molecular weight, ν_i the stoichiometric molar coefficient, B the pre-exponential constant for the Arrhenius reaction, R^o the universal gas constant, E the activation energy, L the specific latent heat of vaporization, and a_T, a_O and a_F are constant exponents. The subscripts O, F, g, ℓ, s, ∞ and o respectively designate the oxidizer, the fuel, the gas phase, the liquid phase, and the states at the droplet surface, the ambiance, and the initial instant.

Boundary and Initial Conditions

Since $\rho_g \sim 1/T$ as given by Eq. (4), the unknowns T, Y_i and v are to be solved from Eqs. (1) to (3) subject to the following boundary and initial conditions.

(a) Boundary Conditions at Droplet Surface ($r = r_s$).

Mass Conservation:

$$\frac{d}{dt}\left(\frac{4}{3}\,\pi r_s^3 \rho_\ell\right) = -\,4\pi r_s^2 \rho_{gs}\left(v_s - \frac{dr_s}{dt}\right) \qquad (6)$$

Fuel Conservation:

$$\left(\rho_g \mathcal{D} \frac{\partial Y_F}{\partial r}\right)_s + \rho_{gs}\left(v_s - \frac{dr_s}{dt}\right)(1 - Y_{Fs}) = 0 \tag{7}$$

Oxidizer Conservation:

$$\left(\rho_g \mathcal{D} \frac{\partial Y_O}{\partial r}\right)_s - \rho_{gs}\left(v_s - \frac{dr_s}{dt}\right) Y_{Os} = 0 \tag{8}$$

Energy Conservation:

$$\left(\lambda \frac{\partial T}{\partial r}\right)_s - \rho_{gs}\left(v_s - \frac{dr_s}{dt}\right) L = 0 \tag{9}$$

Constant Droplet Temperature:

$$T(r = r_s) = T_s \tag{10}$$

(b) Boundary Conditions at Ambiance ($r = \infty$).

For the present system the states at the ambiance continuously change with time. Therefore the proper boundary conditions to be imposed there are the vanishing of the gradients, viz.

$$\left(\frac{\partial Y_F}{\partial r}\right)_\infty = \left(\frac{\partial Y_O}{\partial r}\right)_\infty = \left(\frac{\partial T}{\partial r}\right)_\infty = 0 \tag{11}$$

(c) Initial Conditions ($t = 0$).

At the initial instant T, Y_i and v can assume arbitrary profiles given by

$$T(r,0) = T_o(r) \tag{12}$$

$$Y_i(r,0) = Y_{io}(r) \tag{13}$$

$$v(r,0) = v_o(r) \quad , \tag{14}$$

and the droplet is of a given size

$$r_s(0) = r_{so} \tag{15}$$

The problem is well posed at this stage. In order to solve for T, Y_F, Y_O and v from Eqs. (1) to (3), we need three initial conditions as given by Eqs. (12) to (14), and seven boundary conditions as given by Eqs. (7) to (11). Equation (6) is used to determine $r_s(t)$ subject to Eq. (15).

Non-Dimensionalization

By defining the non-dimensional variables

$$\tilde{\rho} = \rho/\rho_{\infty o} \quad , \quad \tilde{T} = H/Q \quad ,$$

$$\tilde{r} = r/r_s(t) \quad , \quad R = r_s(t)/r_{so} \quad ,$$

$$\tilde{m} = \tilde{\rho}_g \tilde{v} \tilde{r}^2 R \quad , \quad \tilde{Y}_i = (\nu_F W_F/\nu_i W_i) Y_i \quad ,$$

$$\tilde{t} = (\lambda/C_p \rho_{\infty o} r_{so}^2) t \quad , \quad \tilde{v} = (\rho_{\infty o} C_p r_{so}/\lambda) v \quad ,$$

and by assuming that λ, C_p, and $\rho_g \mathcal{D}$ are constants, and that the Lewis number is unity, Eqs. (1) to (3) become

$$R^2 \frac{\partial \tilde{\rho}_g}{\partial \tilde{t}} + \frac{\tilde{m}_s}{\tilde{\rho}_\ell (1 - \tilde{\rho}_{gs}/\tilde{\rho}_\ell)} \tilde{r} \frac{\partial \tilde{\rho}_g}{\partial \tilde{r}} + \frac{1}{\tilde{r}^2} \frac{\partial \tilde{m}}{\partial \tilde{r}} = 0 \quad , \tag{1'}$$

$$\mathcal{L}\{\tilde{Y}_i\} = \mathcal{L}\{-\tilde{T}\} = -D \tilde{Y}_O^{a_O} \tilde{Y}_F^{a_F} \tilde{T}^{a_T} \exp(-\tilde{T}_a/\tilde{T}) \quad , \tag{2',3'}$$

where

$$\mathcal{L} \equiv \tilde{\rho}_g R^2 \frac{\partial}{\partial \tilde{t}} + \left[\frac{\tilde{m}_s (\tilde{\rho}_g/\tilde{\rho}_\ell)}{(1 - \tilde{\rho}_{gs}/\tilde{\rho}_\ell)} \tilde{r} + \frac{\tilde{m}}{\tilde{r}^2} - \frac{2}{\tilde{r}} \right] \frac{\partial}{\partial \tilde{r}} - \frac{\partial^2}{\partial \tilde{r}^2} \tag{16}$$

and the Damköhler number D is

$$D = \left(\frac{C_p r_{so}^2 R^2}{\lambda} \right) \left(\frac{B \nu_F W_F c^{a_O}}{W_O^{a_O} W_F^{a_F}} \right) \left(\frac{\bar{W}_p}{R^o} \right)^{(a_O + a_F)} \left(\frac{Q}{C_p} \right)^{(a_T - a_O - a_F)} \tag{17}$$

Similarly, the boundary conditions Eqs. (6) to (9) can be written as

$$R\,\frac{dR}{d\tilde{t}} + \frac{\tilde{m}_s}{\tilde{\rho}_\ell(1-\tilde{\rho}_{gs}/\tilde{\rho}_\ell)} = 0 \qquad (6')$$

$$\left(\frac{\partial \tilde{Y}_F}{\partial \tilde{r}}\right)_{\tilde{r}=1} + \frac{\tilde{m}_s}{(1-\tilde{\rho}_{gs}/\tilde{\rho}_\ell)}(1-\tilde{Y}_{Fs}) = 0 \qquad (7')$$

$$\left(\frac{\partial \tilde{Y}_O}{\partial \tilde{r}}\right)_{\tilde{r}=1} - \frac{\tilde{m}_s}{(1-\tilde{\rho}_{gs}/\tilde{\rho}_\ell)}\tilde{Y}_{Os} = 0 \qquad (8')$$

$$\left(\frac{\partial \tilde{T}}{\partial \tilde{r}}\right)_{\tilde{r}=1} - \frac{\tilde{m}_s}{(1-\tilde{\rho}_{gs}/\tilde{\rho}_\ell)}\tilde{L} = 0 \quad . \qquad (9')$$

In the above σ is the stoichiometric oxidizer-to-fuel mass ratio, $T_a = E/R^o$, and $\tilde{L} = L/Q$. It may also be noted that instead of $\tilde{v}$, we have used the mass flow rate $\tilde{m}$ as the unknown quantity to be determined. In the quasi-steady d^2-law model $\tilde{m}$ is a constant of the system and is proportional to the droplet surface regression rate.

Numerical Representation

The governing parabolic partial differential equations were represented in a central differencing scheme for the spacial derivatives and backward differencing for the temporal derivatives. An accurate numerical solution of this problem requires small $\Delta\tilde{r}$ close to the droplet in order to adequately resolve the curvature effects, and in the same time a large computational domain because of the large size of the flame. Therefore a linearly varying spacing represented by

$$\tilde{r}_n = \tilde{r}_{n-1} + 0.2 + 0.06(n-2) \quad , \quad n \geq 2$$

is used. The spacings vary from $\Delta\tilde{r} = 0.2$ at the surface to about $\Delta\tilde{r} = 6$ at $\tilde{r} = 350$, which is the end of the computational domain. The fine mesh used

necessitated the adoption of very small time steps in order to represent the diffusion term well, and subsequently results in a large number of time steps in the order of 2×10^4.

In the present numerical representation the Arrhenius term $\exp(-\tilde{T}_a/\tilde{T})$ is not quasi-linearized but is left as is and is therefore determined iteratively. We believe the process of quasi-linearization may render the tracing of the ignition period exceedingly difficult, if at all possible. This may be the source of difficulty in the failure of previous attempts [7] at tracing through the ignition process.

III. RESULTS

Sample solutions were obtained for a heptane droplet in an oxygen/nitrogen/heptane environment at 1 atm and 1000°K. The initial gas-phase conditions are simply $T_o(r) = T_{\infty}$, $Y_{io}(r) = Y_{i\infty}$, $v_o(r) = m_o(r) = 0$, with $Y_{O\infty} = 0.232$. The droplet temperature is at a constant value of $T_s = 364^{\circ}K$, which is the wet-bulb temperature of heptane in a 1 atm, 1000°K environment without any fuel vapor. The dependence of the wet-bulb temperature on the ambient fuel vapor concentration at such a high temperature is expected to be minimal. It may also be noted that in realistic situations the initial droplet temperature can be lower than the present value, whereas the final temperature can be higher as the environment becomes hotter. This results in a finite period of droplet heating spanning about 10-20% of the droplet lifetime [2,8,9]. Therefore by fixing the droplet temperature at a constant value the liquid-phase transient effects are suppressed such that the unsteady phenomena exhibited by the present results are strictly those of the gas phase.

The physico-chemical parameters used are:

W_F = 100 Kg/Kg-mole , W_O = 32 Kg/Kg-mole ,

$\bar{W}$ = 30 kg/kg-mole , ρ_ℓ = 611 Kg/m^3 ,

$L = 3.16 \times 10^5$ J/Kg , $Q = 4.46 \times 10^7$ J/Kg ,

$a_O = a_F = 1$, $a_T = 0$,

$E = 1.26 \times 10^8$ J/Kg-mole , $D = 2 \times 10^3$,

$C_p = 1.46 \times 10^3$ J/Kg-^oK .

Figures 1 and 2 show the development of the temperature and species profiles in an environment whose fuel-oxygen concentrations are given by $\varphi = \tilde{Y}_{F\infty O}/\tilde{Y}_{O\infty O} = 0.7$, where φ is the equivalence ratio defined as the fraction of the fuel-oxidizer mass ratio compared with the stoichiometric fuel-oxidizer mass ratio. The progress in time is represented by the parameter $\epsilon = 1 - R^3$, which is the fractional amount of droplet mass vaporized and is believed to be a more meaningful representation than the physical time $\tilde{t}$.

It is seen that at $\varphi = 0.7$ the premixed reaction at the ambiance and the diffusional combustion close to the droplet are both very efficient. All the fuel vapor at the ambiance are consumed when less than 5% of the droplet mass has vaporized and the ambient temperature attains an equilibrium value of $\tilde{T}_{\infty e}$. The diffusional burning, as indicated by the bulge in the temperature profile and the dip in the fuel vapor profile, is established even faster, when $\epsilon < 0.008$. This implies that when modeling the transient droplet ignition process even for an ambiance as reactive as the present one, it may still be a good approximation to consider the reaction at the ambiance to be frozen and focus only on the diffusive-reactive processes close to the droplet.

Since all the fuel vapor at the ambiance has been consumed at $\epsilon = 0.05$, the subsequent problem of interest is simplified to that of a fuel droplet undergoing combustion in an oxidizing environment with a higher temperature and lower oxidizer concentration than the initial values. In fact since the ignition of the droplet and the depletion of the ambient fuel vapor both occur so fast for the present intensely-reactive system, the combustion behavior for the bulk of the droplet lifetime can be simply obtained by considering the droplet is burning on an oxidizing atmosphere whose properties correspond to the equilibrium state of the original environment. On the other hand when the environment is only weakly-reactive, one may assume the ambient reactions to be completely frozen and results of Ref. 5 are applicable.

Realizing the fact that all the ambient fuel vapor is depleted at $\epsilon = 0.05$ and therefore unsteadiness caused by changes of the environment are eliminated, it is then of interest to note that the combustion process is still unsteady and is therefore in contrast with what is to be expected from the classical d^2-law model. For example d^2-law predicts the flame-front standoff ratio, $\tilde{r}_f$, is a constant, although Fig. 1 shows that the location of the maximum temperature continuously propagates outward in $\tilde{r}$-space. This unsteadiness is believed to arise from two sources as will be elaborated in the following.

The first source, widely recognized [10,11], is a consequence of the assumption in the d^2-law model that because the gas density is much lower than the liquid density, the gas velocity would be much greater than the droplet regression rate. Therefore during the characteristics gas-phase transport period the location of the droplet surface is essentially frozen. This assumption obviously breaks down in regions far away from the droplet where the gas velocity becomes comparable with the droplet regression rate.

The second source, which we believe is probably more important, is the finite amount of time required to build up the fuel concentration profile in the inner region to the flame. The fact that this transition time is substantial can be easily demonstrated by summing over the mass of the fuel vapor in the inner region, using the d^2-law results, and show that it is a significant fraction of the droplet mass. Therefore by assuming that the quasi-steady flame is instantaneous established, mass conservation is violated in the d^2-law model. In reality, after ignition has been achieved only part of the fuel vapor released from the droplet surface is consumed at the flame. The rest is used to build up the fuel vapor profile as the flame propagates outward to approach its quasi-steady location. This unsteady phenomenon is currently being studied in detail.

Figures 3 and 4 show the temperature and species profiles for a stoichiometric ambiance, with $\varphi = 1$. It is seen that although a distinct diffusional ignition event can still be barely identified at $\epsilon = 0.008$ in Fig. 3, the local temperature peak is rapidly eliminated as complete consumption of the ambient fuel and oxidizer is achieved. The subsequent situation is that of the fuel droplet vaporizing in an inert, fuel-free environment at the adiabatic flame temperature.

Figure 5 shows R^2 versus $\tilde{t}$ for $\varphi = 0.7$ and 1.0. The two sets of results are almost identical and therefore indistinguishable in the figure. The closeness is due to the facts that the maximum flame temperature for $\varphi = 0.7$ is about the same as the equilibrium ambient temperature for $\varphi = 1.0$, and that the flame is also sufficiently far away from the droplet. Therefore the heat fluxes arriving at the droplet surface, and subsequently the droplet burning rate, are about the same for both cases. It may also be noted that the slope of Fig. 5 is initially higher but rapidly approaches a constant value.

Finally, Fig. 6 shows the initial development of the temperature profile for various values of φ. Of particular interest are the fuel-rich cases ($\varphi > 1$) in which the droplet is essentially vaporizing in a hot, inert, fuel-enriched environment whose temperature decreases with increasing φ. There is obviously no individual droplet combustion in an environment with $\varphi > 1$ because the condition of $\varphi \simeq 1$ required for diffusional burning is not met throughout the entire flow field.

IV. DISCUSSIONS AND CONCLUSIONS

In the present paper we have numerically investigated the combustion characteristics of a fuel droplet after it is placed in a hot, reactive, environment containing various concentrations of an oxidizer gas and the fuel vapor. When the ambiance is fuel lean, with $\varphi < 1$, diffusion-like burning generally can be identified. Ignition takes place close to the droplet and early in the droplet lifetime, when less than 1% of the droplet mass has vaporized. After ignition the flame propagates outward, with the fuel vapor released from the droplet being partly consumed at the flame and partly stored in the inner region to the flame. In the case of a fuel-rich environment, with $\varphi > 1$, diffusional burning is not possible.

Considerable simplification in estimating the droplet behavior also results if the ambiance is either weakly or intensely reactive. If it is weakly reactive then the environment is essentially frozen during the droplet lifetime. Then the droplet undergoes either purely diffusional burning if the ambiance is fuel lean or pure vaporization if it is fuel rich. If the environment is intensely reactive, one of the reactants will be rapidly depleted. Then the subsequent phenomena of interest are again either purely diffusional burning or pure vaporization, except now the ambient temperature

is the adiabatic flame temperature and is therefore much hotter. Homogeneous ignition theory can be used to assess the reactivity of the ambiance [12,13].

The present study has suppressed the droplet heating process so as to isolate effects due to gas-phase transient. When droplet heating is accounted for we expect the analysis of the problem to actually become somewhat simpler. For example the ignition lag will be dominated by the period of droplet heating, which is much longer than the gas-phase ignition delay [14]. Furthermore for an intensely-reactive environment the ambient reactions will have been completed during this droplet heating period, so that when the droplet is eventually ignited it will be burning in an oxidizing environment.

Acknowledgement

This research has been sponsored by the Department of Energy under Contract No. EG-77-S-02-4433 to Northwestern University and by the Army Research Office under Grant to Princeton University.

References

1. Faeth, G. M., "Current Status of Droplet and Liquid Combustion," Prog. Energy Combust. Sci. 3, 191-224 (1977).

2. Sirignano, W. A., and Law, C. K., "Transient Heating and Liquid-Phase Mass Diffusion in Droplet Vaporization," Evaporation-Combustion of Fuels, ACS Advances in Chemistry Series, Vol. 166, J. T. Zung Ed., 1978, pp. 1-26.

3. Chigier, N. A., and McCreath, C. G., "Combustion of Droplets in Sprays," Acta Astro. 1, pp. 687-710 (1974).

4. Godsave, G. A. E., "Studies of the Combustion of Drops in a Fuel Spray: The Burning of Single Drops of Fuel," Fourth Symposium (International) on Combustion, Williams and Wilkins, Baltimore, 1953, pp. 818-830.

5. Law, C. K., "Deflagration and Extinction of Fuel Droplet in a Weakly-Reactive Atmosphere," J. Chem. Phy. 68, pp. 4218-4221 (1978).

6. Williams, F. A., Combustion Theory, Addison-Wesley, Reading, Mass., 1965.

7. Birchley, J. C., and Riley, N., "Transient Evaporation and Combustion of a Composite Water-Oil Droplet," Combust. Flame 29, pp. 145-165 (1977).

8. Law, C. K., "Unsteady Droplet Combustion with Droplet Heating," Combust. Flame 26, pp. 17-22 (1976).

9. Law, C. K., and Sirignano, W. A., "Unsteady Droplet Combustion with Droplet Heating. II: Conduction Limit," Combust. Flame 28, pp. 175-186 (1977).

10. Waldman, C. H., "Theory of Non-Steady State Droplet Combustion," Fifteenth Symposium (International) on Combustion, Combustion Institute, Pittsburgh, 1975, pp. 429-442.

11. Crespo, A., and Liñán, A., "Unsteady Effects in Droplet Evaporation and Combustion," Combust. Sci. Tech. 11, pp. 9-18 (1975).

12. Hermance, C. E., "Implications Concerning General Ignition Processes From the Analysis of Homogeneous Thermal Explosions," Combust. Sci. Tech. 10, pp. 245-260 (1975).

13. Kassoy, D. R., and Poland, J., "The Subcritical Spatially Homogeneous Explosion; Ignition to Completion," Combust. Sci. Tech. 11, pp. 147-152 (1975).

14. Law, C. K., "Theory of Thermal Ignition in Fuel Droplet Burning," Combust. Flame 31, pp. 285-296 (1978).

Figure Captions

Figure 1: Development of the temperature profile for a heptane droplet burning in a reactive environment with initial temperature of 1000°K and initial equivalence ratio $\varphi = 0.7$.

Figure 2: Development of the fuel concentration profile for a heptane droplet burning in a reactive environment with initial temperature of 1000°K and initial equivalence ratio $\varphi = 0.7$.

Figure 3: Development of the temperature profile of a heptane droplet burning in a reactive environment with initial temperature of 1000°K and initial equivalence ratio $\varphi = 1.0$.

Figure 4: Development of the fuel concentration profile of a heptane droplet burning in a reactive environment with initial temperature of 1000°K and initial equivalence ratio $\varphi = 1.0$.

Figure 5: The temporal variation of the droplet surface area for a heptane droplet burning in a reactive environment with initial temperature of 1000°K and initial equivalence ratios $\varphi = 0.7$ and 1.0.

Figure 6: Initial development of the temperature profile of a heptane droplet burning in a reactive environment with initial temperature of 1000°K and various initial equivalence ratios.

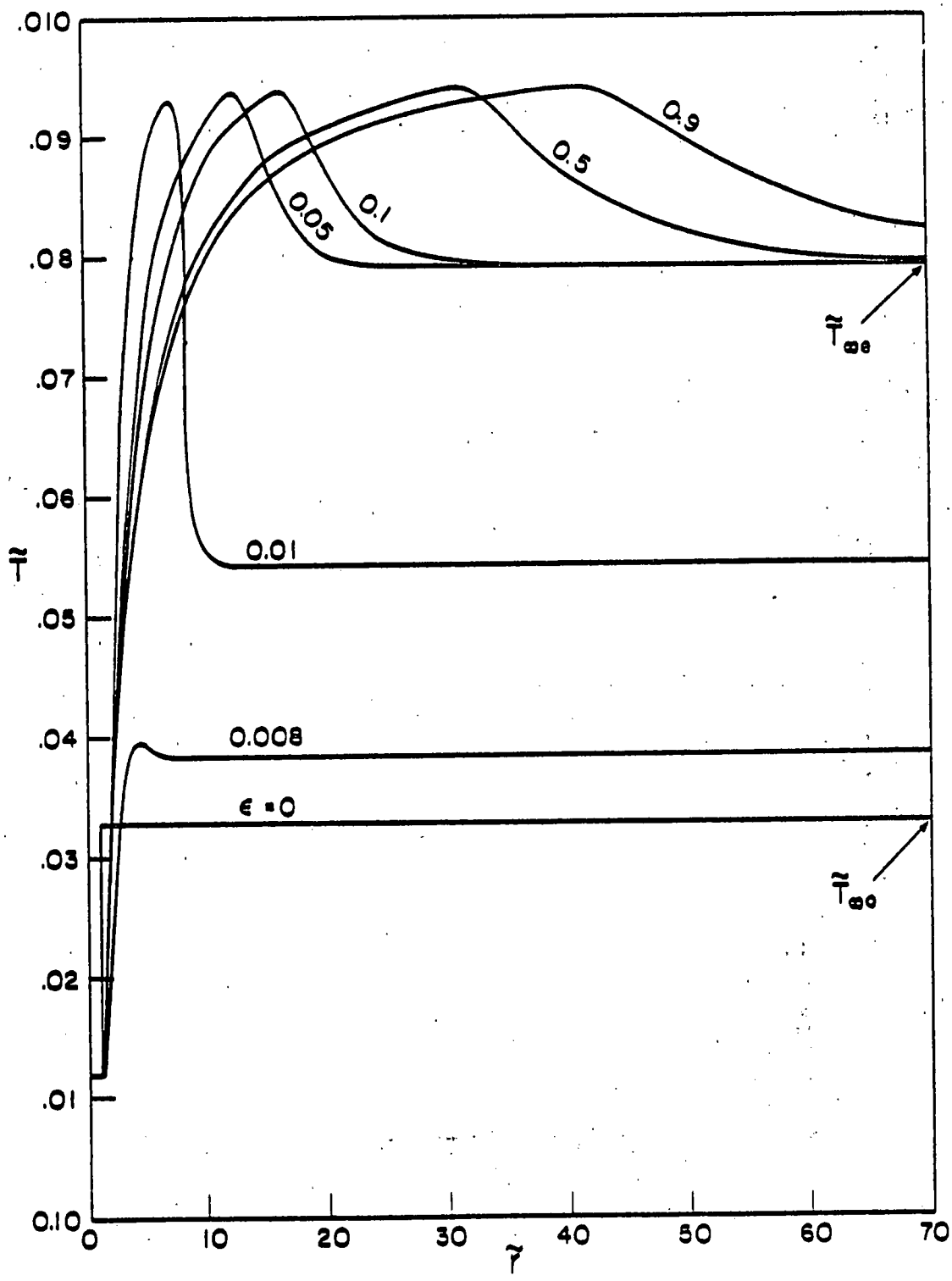
.010
.09
.08
.07
.06
.05
.04
.03
.02
.01
0.10
0
10
20
30
40
50
60
70
$\tilde{\tau}$
$\tilde{T}$
0.9
0.5
0.1
0.05
0.01
0.008
$\epsilon = 0$
$\tilde{T}_{\infty e}$
$\tilde{T}_{\infty 0}$

Figure 1

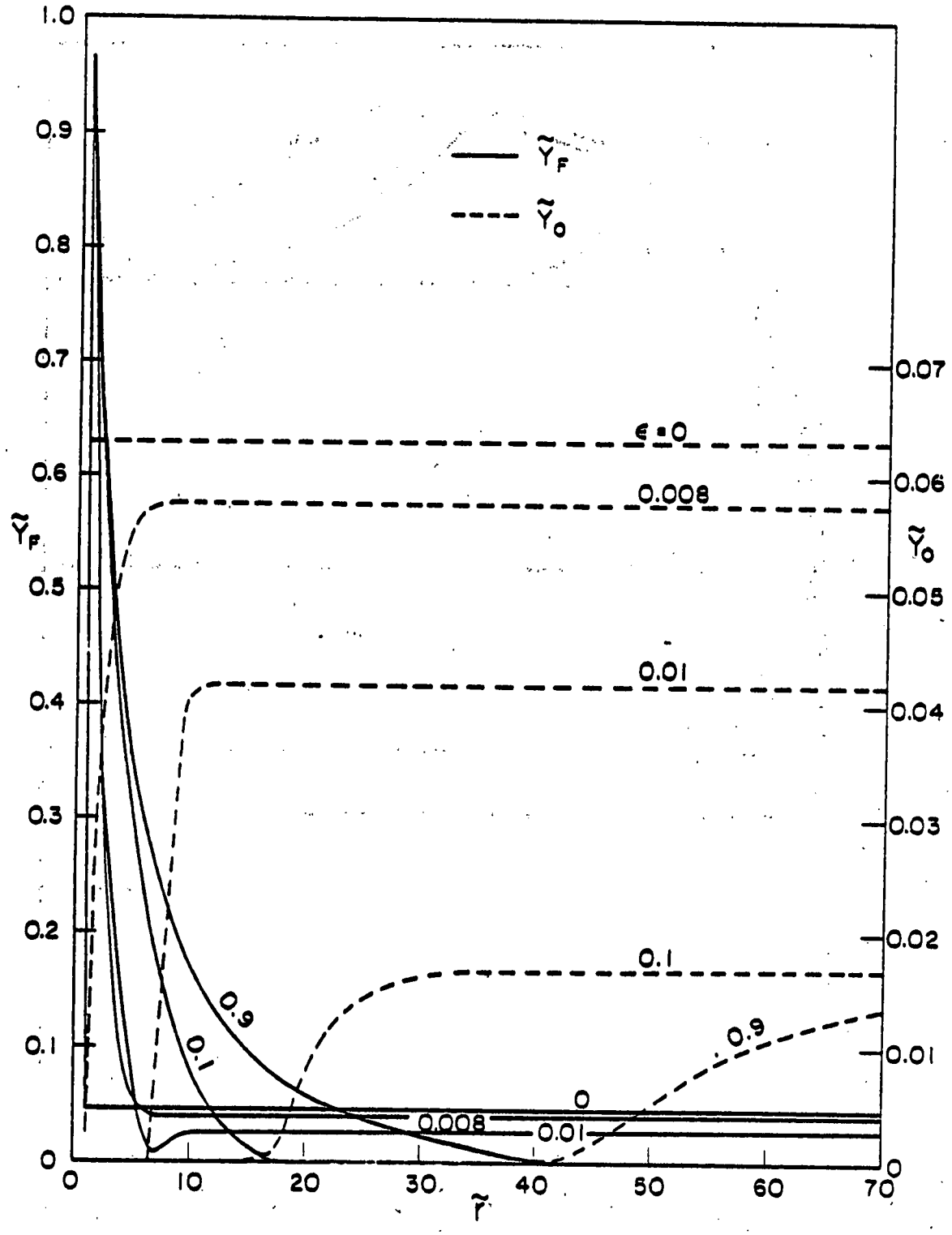
$\tilde{Y}_F$
$\tilde{Y}_O$
$\epsilon = 0$
0.008
0.01
0.1
0.9
0
0.008
0.01
0.9
0.1
$\tilde{Y}_F$
$\tilde{Y}_O$
$\tilde{r}$
0
0.1
0.2
0.3
0.4
0.5
0.6
0.7
0.8
0.9
1.0
0.01
0.02
0.03
0.04
0.05
0.06
0.07
0
10
20
30
40
50
60
70

Figure 2

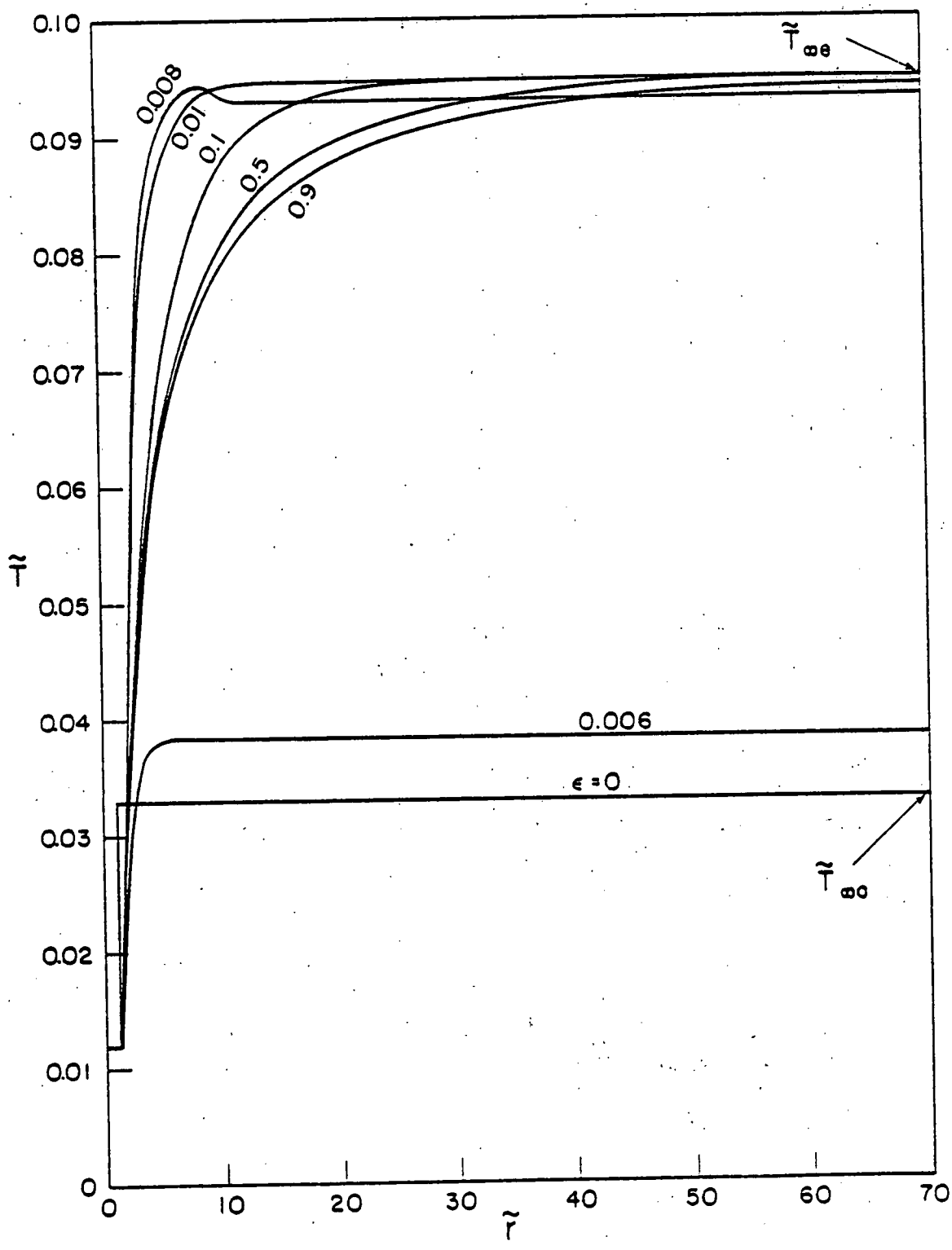
0.10
0.09
0.08
0.07
0.06
0.05
0.04
0.03
0.02
0.01
0
$\tilde{T}$
0
10
20
30
40
50
60
70
$\tilde{r}$
$\tilde{T}_{\infty e}$
0.008
0.01
0.1
0.5
0.9
0.006
$\epsilon = 0$
$\tilde{T}_{\infty 0}$

Figure 3

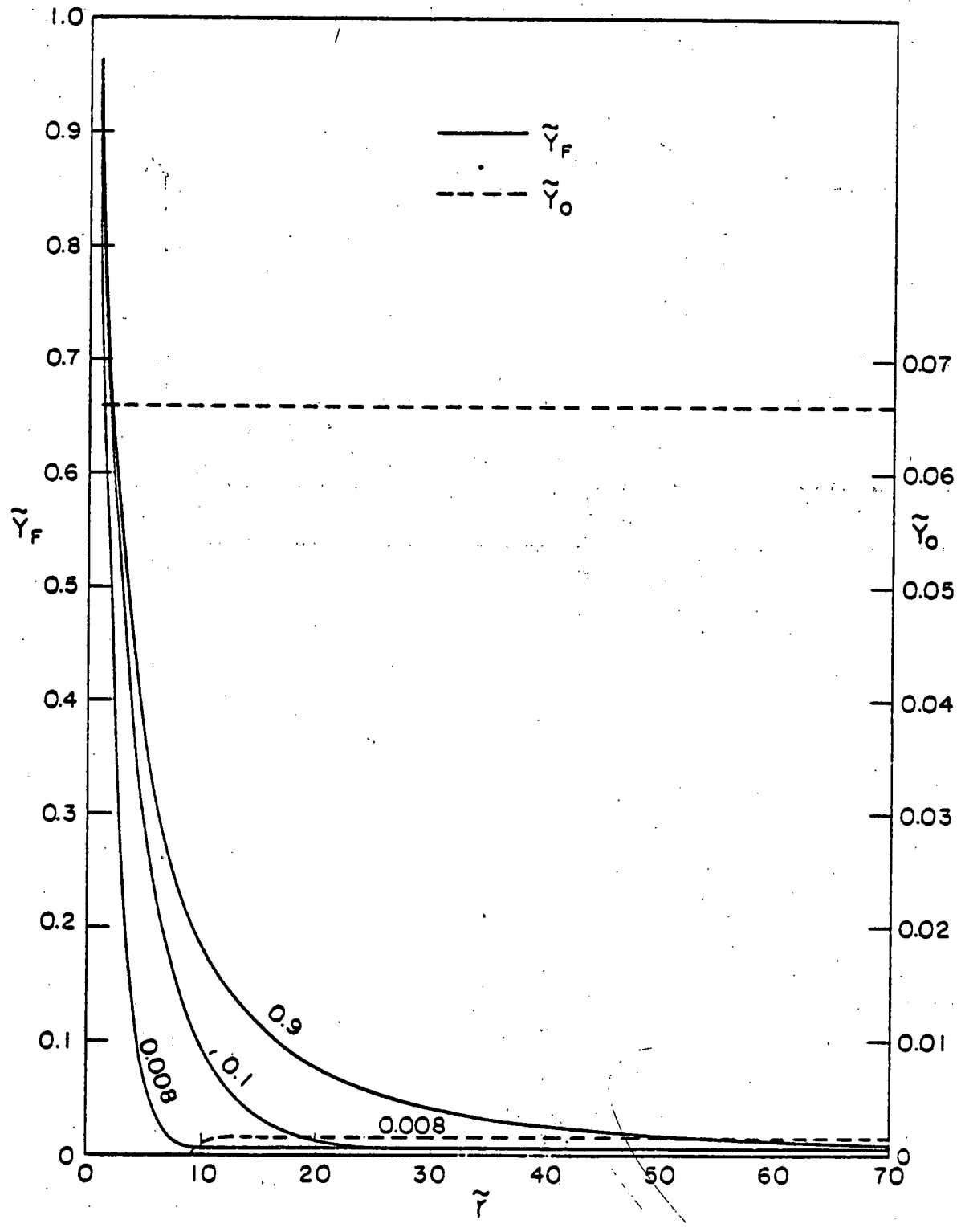
1.0
0.9
0.8
0.7
0.6
0.5
0.4
0.3
0.2
0.1
0
$\tilde{Y}_F$
$\tilde{Y}_F$
$\tilde{Y}_O$
0.07
0.06
0.05
0.04
0.03
0.02
0.01
0
0
10
20
30
40
50
60
70
$\tilde{r}$
0.9
0.1
0.008
0.008

Figure 4

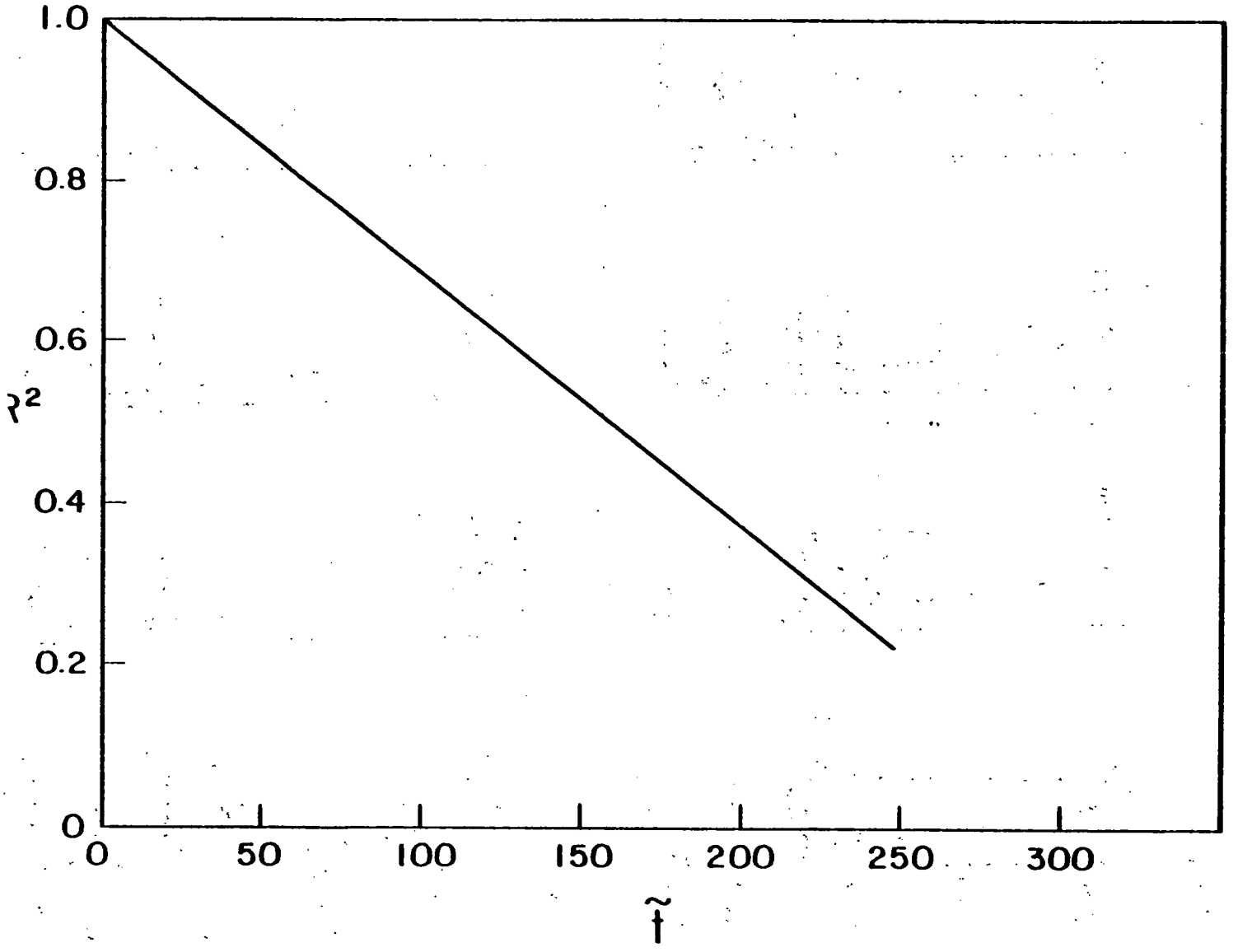

Figure 5

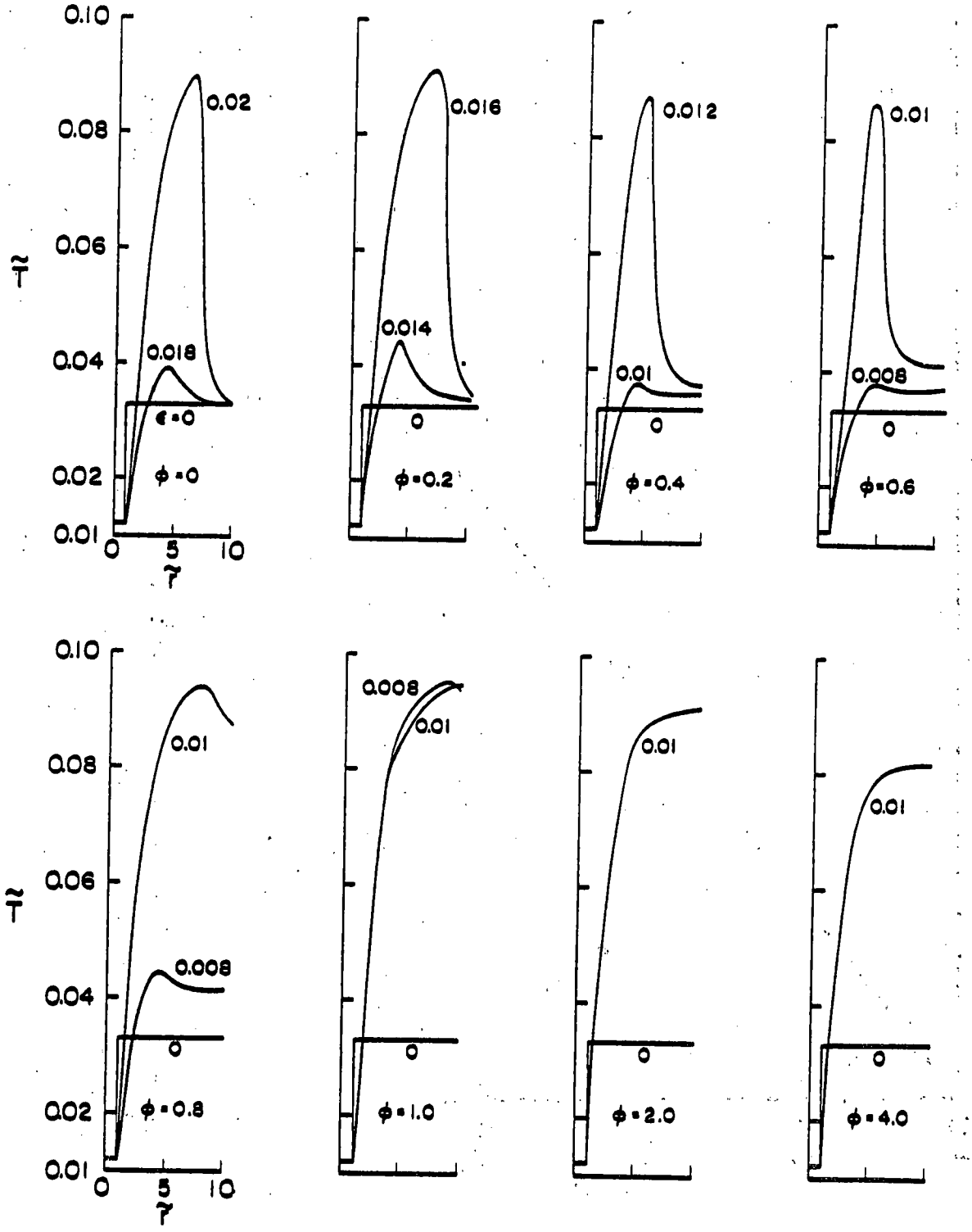
0.10
0.08
0.06
0.04
0.02
0.01
$\tilde{T}$
0
5
10
$\tilde{r}$
0.02
0.018
ϵ=0
ϕ=0
0.016
0.014
0
ϕ=0.2
0.012
0.01
0
ϕ=0.4
0.01
0.008
0
ϕ=0.6
0.01
0.008
0
ϕ=0.8
0.008
0.01
0
ϕ=1.0
0.01
0
ϕ=2.0
0.01
0
ϕ=4.0

Figure 6

THEORY OF TRANSIENT DROPLET COMBUSTION LEADING TO THE d^2-LAW STATE

C. K. LAW

Department of Mechanical Engineering
and Astronautical Sciences
Northwestern University
Evanston, Illinois 60201

ABSTRACT

The present investigation demonstrates that due to volume effects the amount of mass required for the transient build-up of the fuel vapor concentration leading to the d^2-law state of droplet combustion can be substantial. By properly accounting for this transient process, but still assuming gas-phase quasi-steadiness, simplified theories are formulated for droplet vaporization and combustion. The present results generally agree with those obtained from more detailed studies allowing for gas-phase unsteadiness, and with the experimental observation that the flame-front standoff ratio continuously increases for a significant portion of the droplet lifetime. It is emphasized that by assuming the instantaneous rate of fuel vaporization to be equal to that of fuel consumption at the flame, and therefore not accounting for the amount withheld in building up the fuel vapor concentration, the d^2-law can seriously over-estimate the rate of chemical heat release from droplet burning.

I. INTRODUCTION

In the study of the vaporization and combustion of fuel droplets and their applications to the modeling of spray-fueled combustors, the classical d^2-law model of Godsave [1] has provided much understanding on this apparently simple chemically-reacting system. The model assumes that the state of the droplet interior is constant; that the combustion process is spherically symmetric and isobaric; that because of the significant difference between the gas and liquid densities, under subcritical conditions, the gas-phase transport processes can be considered to be quasi-steady; and that chemical reactions are stoichiometric and confined to an infinitesimally-thin flame sheet which simply serves as a sink for the reactants and a source of heat and products. The resulting gas-phase diffusive-convective model predicts that the droplet surface regression rate, the ratio of the flame radius to the droplet radius Υ_f, and the flame temperature T_f are constants of the system as burning progresses.

A well-controlled experimental investigation on the extent of validity of the d^2-law model is difficult to be realized. A major obstacle is the presence of buoyancy which can severely distort the flame from its spherical shape that a meaningful identification of a flame radius is impossible. Furthermore since these buoyancy effects are droplet-size dependent, their continuous variation as the droplet size diminishes renders the combustion process to be intrinsically unsteady.

Recognizing the presence of these asymmetrical, unsteady buoyancy effects, Kumagai et al. [2] conducted the experiment in a freely-falling chamber and consequently observed spherically-symmetric combustion. Their data on the temporal variations of Υ_f and normalized droplet surface area, R_s^2, are shown in Fig. 1. When compared with results of the d^2-law model, these data show three important differences: (1) The droplet surface regression rate approaches a

constant only after an initial transient period spanning about 5-10% of the droplet lifetime, during which the burning rate is very slow; (2) The flame front standoff ratio Υ_f monotonically increases throughout the entire run which was terminated at $R_s^2 = 0.64$; (3) The value of Υ_f probably would not exceed 10 had the increasing trend continued, and therefore is in serious disagreement with the d^2-law value of about 40 for the heptane-air system investigated.

The data of Kumagai et al. [2] clearly demonstrate the existence of transient transport processes, in both the gas and liquid phases, during spherically-symmetric droplet combustion. Aiming to separate the transient effects caused by droplet heating from those of gas-phase unsteadiness, models were formulated by Law [3] and Law and Sirignano [4] allowing for droplet heating but still assuming quasi-steady gas-phase processes. The theoretical result on the regression rate [3] agrees very well with the data of Kumagai et al., although the predicted Υ_f still attains the d^2-law value of about 40, and at the much early instant when the droplet heating period is over.

Subsequently Law and Law [5,6] formulated a fairly rigorous model for droplet combustion allowing for realistic property variations, and showed that the abnormally large d^2-law value of Υ_f is strictly a consequence of the constant property, unity-Lewis number assumption. Specifically it is shown that by using the proper Lewis number, defined as the ratio of the thermal diffusivity in the inner region to the mass diffusivity in the outer region, then the predicted flame size is of the order of 10.

From the above discussions it can therefore be stated that the initial slow rate of burning as observed by Kumagai et al. [2] is primarily caused by droplet heating, whereas the abnormally large d^2-law flame size is a mathematical consequence rather than of a physical nature. These then lead to the conclusion that the behavior of the continuously increasing Υ_f, well past the droplet heating period, must be caused by some unsteady gas-phase processes. Indeed when the

gas-phase processes are treated as being unsteady, the approximate analytical results of Waldman [7] and Crespo and Linan [8], and the numerical results of Birchley and Riley [8], do show a continuously increasing $\mathfrak{r}_f$ over a significant portion of the droplet lifetime.

Waldman [6] and Crespo and Linan [7] attributed the gas-phase unsteadiness to be caused by the finite magnitude of the gas density compared with the liquid density such that during the characteristic gas-phase transport time the droplet surface does regress a little. This then implies that rather than being quasi-steady as assumed in the d^2-law model, the gas-phase transport processes are intrinsically unsteady. Crespo and Linan [7] further showed that these finite-density effects are expected to be important in the region located at $\mathfrak{r} > O(\sqrt{\rho_\ell/\rho_g})$ away from the droplet. In this region the gas velocity becomes comparable with the droplet radial regression rate such that the flow changes from being convective-diffusive in the interior, quasi-steady, region to being transient-diffusive here. Therefore any process of significance occurring in this far field region is expected to render the bulk combustion characteristics unsteady.

However, an examination of the data of Kumagai et al. [2] in light of the above discussion yields the following dilemma. Using $\rho_\ell/\rho_g = O(10^3)$, the transient-diffusive region is expected to be at least 30 droplet radii away. However, the experimental flame size is $\mathfrak{r}_f \lesssim 10$. Therefore the flame characteristics, as well as other bulk combustion parameters, should exhibit quasi-steadiness with small perturbations of the order of $\sqrt{\rho_g/\rho_\ell}$. This, of course, is contrary to the observation that the flame continuously propagates outward. Therefore the finite-density effect is not adequate to explain the experimental flame behavior.

In response to the above dilemma, we have recently identified an additional, unsteady process which we believe is of importance under all situations and indeed is quite adequate to explain the observed flame behavior without accounting for the finite-density effect. The process of interest is the transient build-up

of the fuel vapor profile in the inner region to the flame as it approaches the d^2-law location. Obviously prior to ignition the fuel vapor concentration in the vicinity of the droplet is quite low, especially for the spark-ignition experiment of Kumagai et al. [2] conducted in a cold environment. However, after ignition this concentration will have to be significantly increased in order to sustain combustion. Therefore immediately after ignition most of the fuel vaporized is stored in the inner region rather than being actually consumed at the flame. Due to the insufficient amount of fuel supplied, the flame will lie in close proximity to the droplet during this period. As the fuel vapor concentration increases, more fuel vapor can then be used for combustion and the flame subsequently propagates outward.

It is also easy to demonstrate that the amount of fuel vapor present in the inner region is significant when compared with the droplet mass, and therefore this relaxation process should be accounted for in droplet modeling. Take the quasi-steady profiles of the d^2-law solution as an example. It can be easily shown that the ratio of the mass of the fuel vapor to the droplet mass is given by

$$R_c = \lambda \int_1^{\tilde{r}_f} \left(Y_F/\tilde{T}\right) \tilde{r}^2 d\tilde{r} \tag{1}$$

where

$$Y_F = 1 - \left(1 + \tilde{Y}_{O\infty}\right)/\left(1 + B_c\right)^x \tag{2}$$

$$\tilde{T} = \left(\tilde{T}_s - 1\right) + \left(1 + B_c\right)^{(1-x)} \tag{3}$$

$$\tilde{r}_f = \left[\ell n\left(1 + B_c\right)\right]/\left[\ell n\left(1 + \tilde{Y}_{O\infty}\right)\right] \tag{4}$$

$$\lambda = 3\left(\rho_{gs}/\rho_\ell\right)\left(C_p T_s/L\right)$$

$$B_c = \tilde{T}_\infty - \tilde{T}_s + \tilde{Y}_{O\infty}\,\tilde{Q}$$

and $x = 1/\tilde{r}$. For a heptane/oxygen/nitrogen system, with $T_s = 372^{\circ}K$, $C_p = 0.35$ cal/gm-$^{\circ}K$, $L = 75.8$ cal/gm, $Q = 1.07 \times 10^4$ cal/gm, $\lambda = 0.03$, Fig. 2 shows R_c as a function of the transfer number B_c and oxidizer concentration $\tilde{Y}_{O\infty}$. For heptane burning in air, $\tilde{Y}_{O\infty} = 0.063$ and $B_c = 8.56$. Figure 2 shows convincingly that the amount of fuel vapor stored in the inner region can be of the same order of, if not more than, what is contained by the droplet itself. Physically it is also reasonable to expect that this amount is substantial because even though the gas density is much lower than the liquid density, volume effect dominates in this case due to the extended dimension of the flame. Therefore by assuming all the fuel vaporized is instantaneously consumed at the flame, the d^2-law model yields inaccurate results on the chemical heat release rate due to droplet burning in a spray.

Extending the above concept further, we have also evaluated the ratio R_v for the case of pure vaporization, for which

$$R_v = \lambda \int_1^{\tilde{r}_\infty} \left(Y_F/\tilde{T}\right) \tilde{r}^2 d\tilde{r} \tag{5}$$

$$Y_F = 1 - \left(1 - Y_{F\infty}\right)/\left(1 + B_v\right)^x \tag{6}$$

$$\tilde{T} = \left(\tilde{T}_s - 1\right) + \left(1 + B_v\right)^{(1-x)} \tag{7}$$

$$B_v = \tilde{T}_\infty - \tilde{T}_s \ .$$

The integral in Eq. (5) depends on the value used for $\tilde{r}_\infty$, the location of "infinity." Using $T_\infty = 900^{\circ}K$ and $Y_{F\infty} = 0$, Fig. 3 shows that R_v increases without bound as progressively larger values of $\tilde{r}_\infty$ are used. Therefore by letting $\tilde{r}_\infty = \infty$ in the study of droplet vaporization, an infinite amount of fuel vapor has been implicitly assumed to exist in the gas for a droplet of finite mass.

There is, however, an important difference between combustion and pure vaporization as revealed by the above results. For the case of combustion one

expects that since the amount of fuel vaporized will continuously decrease whereas the amount consumed at the flame will increase as burning proceeds, the d^2-law behavior will eventually be attained during the droplet lifetime. The relaxation time, of course, depends on the value of λ; smaller λ results in shorter times. On the other hand for the case of pure vaporization the d^2-law behavior may never be reached because it requires an infinite amount of fuel vapor to be present.

Finally, it is also reasonable to expect that the characteristic rate for appreciable changes in the fuel vapor content should be of the same order as the droplet regression rate, and is therefore much slower than the characteristic gas-phase transport rate for subcritical burning. Furthermore, the unsteady transport processes occurring in the far field region will also have small effects on the bulk combustion behavior, except probably towards the end of the droplet lifetime, because the dominant transport processes will occur close to the droplet as accumulation of the fuel vapor proceeds. These then imply the gas-phase processes can still be assumed to be quasi-steady; the transient fuel vapor accumulation process occurs at larger time scales.

We shall therefore present in the following a theory for droplet vaporization (Section II) and combustion (Section III), properly accounting for this transient accumulation effect. By further assuming that the gas-phase processes are quasi-steady, explicit analytical expressions can be derived for all quantities of interest. Finally, in order to isolate the phenomena of interest, we have also suppressed the effect of droplet heating by fixing the droplet temperature at a constant value T_s. Description of the droplet heating process can be grafted on to the present theory in a straightforward manner [3,4].

II. THEORY OF DROPLET VAPORIZATION

Formulation

The problem of interest is as follows. A droplet of constant temperature T_s and initial radius r_{so} undergoes pure vaporization after being introduced into an infinite environment of temperature T_∞ and fuel vapor concentration $Y_{F\infty}$. The quasi-steady gas-phase conservation equations for fuel vapor and energy are respectively given by the following [10].

$$\left.\begin{aligned} &\text{Fuel:} \quad \tilde{m}Y_F - \tilde{r}^2 dY_F/d\tilde{r} = \tilde{m} \qquad (8)\\ &\text{Energy:} \quad \tilde{m}\left(\tilde{T} - \tilde{T}_s\right) - \tilde{r}^2 d\tilde{T}/d\tilde{r} = -\tilde{m} \qquad (9)\end{aligned}\right\} \; 1 < \tilde{r} < \tilde{r}_\infty$$

where $\tilde{m} = m/(4\pi \rho_g D r_s)$, $\tilde{r} = r/r_s$, $\tilde{T} = C_p T/L$. The only difference between Eqs. (8) and (9), and the classical expressions, is that the outer boundary is now finite at $\tilde{r}_\infty$ rather than at infinity. Presently the location of $\tilde{r}_\infty$ continuously increases as the fuel vapor profile builds up and is to be determined through overall mass conservations.

Integrating Eq. (8) between $\tilde{r}$ and $\tilde{r}_\infty$, and Eq. (9) between 1 and $\tilde{r}$, we obtain

$$Y_F = 1 - \left(1 - Y_{F\infty}\right) \exp\left[-\tilde{m}\left(x - x_\infty\right)\right] \qquad (10)$$

and $$\tilde{T} = \left(\tilde{T}_s - 1\right) + \exp\left[-\tilde{m}(x-1)\right] \qquad (11)$$

Evaluating Eq. (11) at $\tilde{r} = \tilde{r}_\infty$, the mass evaporation rate is found to be

$$\tilde{m} = \left[\ell n\left(1 + B_v\right)\right]/\left(1 - x_\infty\right) \qquad (12)$$

Substituting Eq. (12) into Eqs. (10) and (11), we finally have

$$Y_F = 1 - \left(1 - Y_{F\infty}\right)/\left(1 + B_v\right)^{(x-x_\infty)/(1-x_\infty)} \qquad (13)$$

and $\tilde{T} = \left(\tilde{T}_s - 1\right) + \left(1 + B_v\right)^{(1-x)/(1-x_\infty)}$. (14)

Overall mass conservation states that the rate of change of the droplet mass should be equal to the negative of the rate of change of the fuel vapor in the gas, or

$$\frac{d}{dt}\left\{\frac{4}{3}\pi\, r_s^3\, \rho_\ell\right\} = -\frac{d}{dt}\left\{\int_{r_s}^{r_\infty} 4\pi\, r^2\left(\rho_g Y_F - \rho_{go} Y_{Fo}\right)dr\right\} \tag{15}$$

where $\rho_{go} = \rho_{g\infty}$ and $Y_{Fo} = Y_{F\infty}$.

Using the isobaric relation

$$\rho_g T = \rho_{gs} T_s \tag{16}$$

and after non-dimensionalization, Eq. (15) becomes

$$d\left\{\left(1 + \lambda f_v\right)R_s^3\right\} = 0 \tag{17}$$

where $R = r/r_{so}$ and

$$f_v = \int_1^{\tilde{r}_\infty} \tilde{r}^2\left(\frac{Y_F}{\tilde{T}} - \frac{Y_{Fo}}{\tilde{T}_o}\right) d\tilde{r} \tag{18}$$

with $Y_F(\tilde{r})$ and $\tilde{T}(\tilde{r})$ given by Eqs. (13) and (14). Integrating Eq. (17) and using the initial state that $f_{vo} = 0$ at $R_s = 1$, the dependence of the droplet size R_s on the location of the outer boundary $\tilde{r}_\infty$ is

$$R_s^3 = \left(1 + \lambda f_v\right)^{-1} \tag{19}$$

The problem is now completely expressed in terms of $R_s(\tilde{r}_\infty)$. To relate R_s to time t, we use the identity

$$\frac{d}{dt}\left\{\frac{4}{3}\pi\, r_s^3\, \rho_\ell\right\} = -\,4\pi\, \rho_g D r_s \tilde{m} \quad . \tag{20}$$

Integrating Eq. (20) yields

$$\tau = -\int_1^{R_s} \left(R_s'/\dot{M}\right) dR_s' \qquad (21)$$

where $\tau = (\rho_g D/\rho_\ell r_{so}^2)t$.

Therefore the solution to the problem can be most expediently sought in an inverse manner, that is for a given Υ_∞ the corresponding R_s and τ can be found from Eqs. (19) and (21) respectively.

Finally, it is worth noting that the only difference between the present formulation and that of the d^2-law model is the additional Eq. (15), which properly constrains the amount of fuel vapor that can exist so that overall mass conservation can be satisfied. Using Eq. (15) we are then able to determine the size, Υ_∞, of the sphere of influence of the transport processes. Equations (18) and (19) show that Υ_∞ is finite except at the instant of complete vaporization at which $r_s = 0$ and $\Upsilon_\infty = \infty$.

Results

The parameters used for study are the same as those of Fig. 3. The time to achieve complete vaporization for the present case is $\tau = 0.382$.

Figures 4 and 5 show the development of the fuel vapor and temperature profiles as evaporation proceeds, where $M = 1-R_s^3$ is the fractional amount of droplet mass vaporized and is a relevant indication of the progress in vaporization. It is found that during the initial 5% of the droplet lifetime rapid changes in the entire profile occurs. Subsequently the profiles in the droplet vicinity relax to almost steady behavior, with changes occurring primarily in regions further away. It is, however, significant to note that these changes persist throughout the entire droplet lifetime, implying that the d^2-law model is inadequate to provide accurate descriptions of the temperature and concentration profiles.

Figure 6 shows the temporal variations of $\tilde{m}$, R_s^2, and τ_f. It is seen that initially the evaporation rate $\tilde{m}$ is very high, being caused by the close proximity of the hot "ambiance" to the droplet. However, shortly after the droplet neighborhood is cooled by the released fuel vapor, the heat transfer rate to the droplet, and therefore $\tilde{m}$, are reduced. Subsequently $\tilde{m}$ decreases very slowly until complete droplet consumption. This behavior is further reflected in the R_s^2 curve, which shows a slightly steep initial slope, but assumes an almost linear variation afterwards.

The above results show that the d^2-law model is certainly accurate enough to predict the total evaporation time as well as the instantaneous vaporization rate, except during the initial period of rapid transient. Physically this is due to the fact that even though significant changes continuously occur in regions further away from the droplet, the droplet evaporation rate is primarily controlled by processes in its vicinity. As shown in Fig. 5, these properties rapidly achieve steady behavior after vaporization is initiated.

Finally, it is significant to note that towards the end of the droplet lifetime τ_∞ does attain very large values, implying the breakdown of the quasi-steady assumption here and the need to properly account for the transient processes in the far field region.

III. THEORY OF DROPLET COMBUSTION

Formulation

The problem to be studied is the following. At time t=0 a droplet of radius r_{so} and constant temperature T_s is ignited in an environment of temperature T_∞ and oxidizer mass fraction $Y_{O\infty}$. The initial ratio of the flame to the droplet radii is $\tilde{r}_{fo}$ and the initial fuel vapor concentration and temperature distributions in the inner region to the flame are $Y_{Fo}(\tilde{r})$ and $T_o(\tilde{r})$ respectively. These initial profiles may correspond to those of the pure vaporization case at the time of ignition. They provide information on the initial amount of fuel vapor present. The exact shapes of these profiles are irrelevant because, owing to the quasi-steady assumption, they will be instantly adjusted to the burning profiles constrained by the mass of fuel vapor they represent.

We shall also assume that initially part of the fuel vaporized is stored in the inner region, with the rest being stoichiometrically consumed with the inwardly-diffusing oxygen at an infinitesimally thin flame. During the later part of the burning process the fuel vapor initially stored will be made available for burning. The burning process is governed by the following equations.

Inner Region ($1 < \tilde{r} < \tilde{r}_f$).

$$\text{Fuel:} \quad \tilde{m} Y_F - \tilde{r}^2 dY_F/d\tilde{r} = \tilde{m} \tag{22}$$

$$\text{Energy:} \quad \tilde{m}\left(\tilde{T} - \tilde{T}_s\right) - \tilde{r}^2 d\tilde{T}/d\tilde{r} = -\tilde{m} \tag{23}$$

Outer Region ($\tilde{r}_f < \tilde{r} < \infty$) .

$$\text{Oxidizer:} \quad \tilde{m}_1 \tilde{Y}_O - \tilde{r}^2 d\tilde{Y}_O/d\tilde{r} = -\tilde{m}_1 \tag{24}$$

$$\text{Energy:} \quad \tilde{m}_1\left(\tilde{T} - \tilde{T}_s\right) - \tilde{r}^2 d\tilde{T}/d\tilde{r} = -\tilde{m} + \tilde{m}_1 \tilde{Q} \ . \tag{25}$$

In Eqs. (22) to (25) $\tilde{m}$ is the rate of vaporization and $\tilde{m}_1$ is the rate of consumption of the fuel vapor at the flame. In the d^2-law formulation $\tilde{m} \equiv \tilde{m}_1$. When

allowing for the fuel accumulation effect we expect $\tilde{m} > \tilde{m}_1$ until the d^2-law behavior is attained. Then the d^2-law results will be used for the subsequent combustion process.

Integrating Eq. (22) from $\tilde{r}_f$ to $\tilde{r}$, Eq. (23) from 1 to $\tilde{r}_f$, and Eqs. (24) and (25) from $\tilde{r}$ to ∞, we obtain

$$Y_F = 1 - \exp\left[-\tilde{m}\left(x - x_f\right)\right] \qquad (26)$$

$$\tilde{T} = \left(\tilde{T}_s - 1\right) + \exp\left[-\tilde{m}(x-1)\right] \qquad (27)$$

$$1 < \tilde{r} < \tilde{r}_f$$

$$\tilde{Y}_O = -1 + \left(1 + \tilde{Y}_{O\infty}\right)\exp(-\epsilon\,\tilde{m}x) \qquad (28)$$

$$\tilde{T} = \left(\tilde{T}_s - 1 + \epsilon\tilde{Q}\right) + \left(\tilde{T}_\infty - \tilde{T}_s + 1 - \epsilon\tilde{Q}\right)\exp(-\tilde{m}x) \qquad (29)$$

$$\tilde{r}_f < \tilde{r} < \infty$$

where $\epsilon = \tilde{m}_1/\tilde{m}$.

Evaluating Eqs. (27) to (29) at $\tilde{r} = \tilde{r}_f$, we obtain three equations from which the unknowns $\tilde{m}_1$, $\tilde{r}_f$ and $\tilde{T}_f$ can be solved as functions of ϵ, viz.

$$\tilde{m} = \ell n\left[\left(\tilde{T}_\infty - \tilde{T}_s + 1 - \epsilon\tilde{Q}\right) + \epsilon\tilde{Q}\left(1 + \tilde{Y}_{O\infty}\right)^{1/\epsilon}\right] \qquad (30)$$

$$\tilde{r}_f = \epsilon\tilde{m}/\ell n\left(1 + \tilde{Y}_{O\infty}\right) \qquad (31)$$

$$\tilde{T}_f = \left(\tilde{T}_s - 1 + \epsilon\tilde{Q}\right) + \left(\tilde{T}_\infty - \tilde{T}_s + 1 - \epsilon\tilde{Q}\right)/\left(1 + \tilde{Y}_{O\infty}\right)^{1/\epsilon} \qquad (32)$$

The remaining unknown in the problem, $\epsilon(\tilde{t})$, is to be determined from overall fuel conservation

$$4\pi\,\rho_g D r_s \tilde{m}(1-\epsilon) = \frac{d}{dt}\left\{\int_{r_s}^{r_f} 4\pi r^2 \rho_g Y_F dr\right\} . \qquad (33)$$

It is of interest to note that in the integral of Eq. (33) we need not subtract the initial mass because it is a constant for the present case. For the pure evaporation case the fuel vapor profile is built upon the fuel vapor originally

present in the environment. This amount continuously increases as the fuel vapor sphere propagates outwards and therefore needs to be subtracted out, as shown in Eq. (15).

Substituting Eq. (20) into Eq. (33) and rearranging, we obtain

$$-R_s^3 \frac{df_c}{dR_s^3} = f_c + (1-\epsilon)/\lambda \tag{34}$$

where $$f_c(\epsilon) = \int_1^{\tilde{Y}_f} \tilde{Y}^2 \left(Y_F/\tilde{T}\right) d\tilde{Y} \tag{35}$$

and $Y_F(\tilde{Y};\epsilon)$ and $\tilde{T}(\tilde{Y};\epsilon)$ are given by Eqs. (26) and (27) respectively.

Integrating Eq. (34) with the initial condition that $f_c = f_{co}$ when $R_s = 1$ yields

$$R_s^3 = \exp\left\{-\int_{f_{co}}^{f_c} \frac{df_c'}{f_c' + (1-\epsilon)/\lambda}\right\} \tag{36}$$

where f_{co} is either given or can be easily evaluated using Eq. (35) with the known initial profiles $Y_{Fo}(\tilde{Y})$ and $\tilde{T}_o(\tilde{Y})$.

Therefore the solution is again sought in an inverse manner, that is for a given ϵ we find the corresponding R_s. The relation between R_s and $\tilde{t}$ is given by Eq. (21).

Solutions for $\tilde{Y}_{O\infty} \ll 1$

For the hydrocarbon-air systems of interest to practical combustion, the parameter $\tilde{Y}_{O\infty}$ is usually a small number compared with unity. Then for $\epsilon > \tilde{Y}_{O\infty}$, Eqs. (30) and (32) can be simplied to

$$\tilde{m} \simeq \ell n\left(1 + B_c\right) \tag{37}$$

and

$$\tilde{T}_F \simeq \tilde{T}_\infty + \tilde{Y}_{O\infty}\tilde{Q} \tag{38}$$

with $\tilde{Y}_f$ still given by Eq. (31).

Equations (31), (37) and (38) show that except for the very initial period during which $\epsilon > \tilde{Y}_{O\infty}$ may not hold, the fuel accumulation process will essentially have no effect on $\tilde{m}$ and $\tilde{T}_f$. However, the influence on $\tilde{Y}_f$ is significant and is expected to persist until $\epsilon=1$. These features are in qualitative agreement with the observations of Kumagai et al. [2] and are also confirmed by our exact results presented in the following.

Results

The parameters used for study are the same as those of Fig. 2, with the additional condition that $Y_{Fo}= 0$ which implies that the flame starts propagating from the droplet surface. The time for burnout is $\tau = 0.22$.

Figures 7 and 8 show the development of the species concentration and temperature profiles as burning progresses. It is again seen that shortly after burning is initiated, the fuel vapor and temperature profiles in the droplet vicinity approach almost steady behavior. This results in the near-constant burning rate as shown in Fig. 9, in which the temporal variations of $\tilde{m}$, R_s^2, and ϵ are plotted. The behavior of $\tilde{m}$ and R_s^2 are qualitatively similar with those for the pure vaporization case. It is also seen that the state corresponding to d^2-law burning, $\epsilon=1$, is attained late in the droplet lifetime, when $\tau = 0.14$ and $M = 0.77$. Since ϵ indicates the rate of chemical heat release at the flame, by assuming $\epsilon=1$ the d^2-law will yield inaccurate estimates for this important parameter.

The above concept is further illustrated in Fig. 10 in which the fractional amount of the initial droplet mass that has actually been consumed at the flame,

$$\omega = -\int_1^{R_s^3} \epsilon \, dR_s'^3 \tag{39}$$

is plotted versus the fractional amount that has vaporized, $M = 1 - R_s^3$. It is clear that by allowing for the present fuel vapor accumulation process, the amount of fuel vapor burned substantially lags behind the amount of fuel vaporized. The

practical implication of this result on the rate of heat release during spray combustion is significant.

Figure 11 shows the temporal variations of $\tilde{r}_f$, $R_f = \tilde{r}_f R_s$, and T_f. It is seen that after the initial rise T_f levels off rapidly. This agrees with the analytical result of Eq. (38). However, the flame front standoff ratio continuously increases until the state of d^2-law burning is reached. This result is in qualitatively agreement with the experimental observations of Kumagai et al. [2] that the increase of $\tilde{r}_f$ persists throughout a significant portion of the droplet lifetime. The physical flame size, R_f, exhibits a maximum as should be.

Finally, it may be noted that the discontinuities in the curves of Figs. 10 and 11 are results of changing the description of the system from $\varepsilon < 1$ and $\tilde{r}_f$-varying to $\varepsilon = 1$ and $\tilde{r}_f$-fixed. It is reasonable to expect that when the gas-phase equations are treated completely unsteady, these discontinuities will be smoothed out as demonstrated by the numerical solutions of Birchley and Riley [9].

IV. CONCLUSIONS

In the present investigation we have identified the time required to build up the fuel vapor profile from an initial state of low concentration is significant and can have important transient effects on the droplet combustion characteristics. By further realizing that this transient process occurs at rates much slower than the gas-phase transport processes, at least in regions not too far from the droplet, simplified theories assuming gas-phase quasi-steadiness but properly allowing for the process of fuel accumulation have been formulated for both pure vaporization as well as combustion. Results show an initial period, spanning less than 5% of the droplet lifetime, during which rapid changes in all combustion characteristics occur. Subsequently the droplet surface regression rate and the flame temperature relax to values close to those of the d^2-law, although the flame size continuously increases throughout a significant portion of the droplet lifetime. The flame behavior satisfactorily explains the experimental observations of Kumagai et al. [2]. Finally, the present theory has also demonstrated that the actual amount of fuel consumed at the flame significantly lags behind the amount that has been vaporized. Therefore the adoption of the d^2-law, which assumes the two quantities are the same, may lead to incorrect estimates on the heat release rate during spray combustion.

When the droplet heating process is accounted for, it will completely dominate the higher initial vaporization rates as shown in Figs. 6 and 9 in that the initial rate of decrease of the droplet size will be very slow and therefore resembles the $R_s^2(t)$ results in Fig. 1. Furthermore, droplet heating will also reduce the initial values of $\tilde{Y}_f$; this will result in a higher initial rate of increase resembling the $\tilde{Y}_f(t)$ results in Fig. 1.

The present formulation assumes an infinite environment whereas in the spray interior the location of the "ambiance" is about (half of) the inter-droplet distance.

For the pure vaporization case the edge of the propagating fuel vapor sphere will then reach this ambiance much earlier. Afterwards the properties of this ambiance will change and this effect will also have to be accounted for through conservation relations for the bulk gaseous medium. For the combustion case the present results show that the flame is initially very small and therefore not overlapping, therefore the possibility of individual droplet combustion within the spray interior is enhanced. Finally, for both cases the quasi-steady gas-phase assumption is strengthened due to the limited extent of the inter-droplet spacings.

Results of the present investigation also indicate that whereas porous-sphere experiments can provide accurate estimates on the droplet burning rate and the flame temperature, they cannot describe the flame movement and the species and temperature profiles during the transient period which may well occupy the bulk of the droplet lifetime.

Acknowledgment

The support by the Division of Basic Energy Sciences, Department of Energy under Contract No. EG-77-S-02-4433 is gratefully acknowledged.

References

1. Godsave, G. A. E., "Studies of the Combustion of Drops in a Fuel Spray: The Burning of Single Drops of Fuel," Fourth Symposium (International) on Combustion, Williams and Wilkins, Baltimore, 1953, pp. 818-830.

2. Kumagai, S., Sakai, T. and Okajima, S., "Combustion of Free Fuel Droplets in a Freely Falling Chamber," Thirteenth Symposium (International) on Combustion, Combustion Institute, Pittsburgh, Pa., 1971, pp. 778-785.

3. Law, C. K., "Unsteady Droplet Combustion with Droplet Heating," Combust. Flame 26, pp. 17-26 (1976).

4. Law, C. K., and Sirignano, W. A., "Unsteady Droplet Combustion with Droplet Heating II: Conduction Limit," Combust. Flame 28, pp. 175-186 (1977).

5. Law. C. K., and Law, H. K., "Quasi-Steady Diffusion Flame Theory with Variable Specific Heats and Transport Coefficients," Combust. Sci. Tech. 12, pp. 207-216 (1976).

6. Law, C. K., and Law, H. K., "Theory of Quasi-Steady One-Dimensional Diffusional Combustion with Variable Properties Including Distinct Binary Diffusion Coefficients," Combust. Flame 29, pp. 269-275 (1977).

7. Crespo, A., and Linan, A., "Unsteady Effects in Droplet Evaporation and Combustion," Combust. Sci. Tech. 11, pp. 9-18 (1975).

8. Waldman, C. H., "Theory of Non-Steady State Droplet Combustion," Thirteenth Symposium (International) on Combustion, Combustion Institute, Pittsburgh, Pa., 1971, pp. 429-442.

9. Birchley, J. C., and Riley, N., "Transient Evaporation and Combustion of a Composite Water-Oil Droplet," Combust. Flame 29, pp. 145-165 (1977).

10. Williams, F. A., Combustion Theory, Addison-Wesley, Reading, Mass., 1965.

NOMENCLATURE

B_c	$\tilde{T}_\infty - \tilde{T}_s + \tilde{Y}_{O\infty}\tilde{Q}$
B_v	$\tilde{T}_\infty - \tilde{T}_s$
C_p	Specific heat
D	Mass diffusivity
d	Droplet diameter
f_c, f_v	Defined in Eqs. (35) and (18) respectively
L	Specific latent heat of vaporization
M	$1-R_s^3$
m	Mass evaporation rate
m_l	Mass consumption rate at flame
$\tilde{m}$	$m/(4\pi \rho_g D r_s)$
Q	Heat of combustion per unit mass of fuel
$\tilde{Q}$	Q/L
R_c, R_v	Defined in Eqs, (1) and (5) respectively
R	r/r_{so}
r	Radial distance
$\tilde{r}$	r/r_s
T	Temperature
$\tilde{T}$	$C_p T/L$
t	Time
$\tilde{t}$	$(\rho_g D/\rho_\ell r_{so}^2)t$
x	$1/\tilde{r}$
Y	Mass fraction
$\tilde{Y}_O$	νY_O

Greek Symbols

ϵ	m_l/m
λ	$3(\rho_{gs}/\rho_\ell)(C_p T_s/L)$
ν	Stoichiometric fuel-oxidizer mass ratio
ρ	Density
ω	Fraction of initial droplet mass burned, Eq. (39)

Subscripts

F	Fuel
f	Flame
g	Gas phase
ℓ	Liquid phase
O	Oxidizer
o	Initial state
s	Droplet surface
∞	Ambiance or effective ambiance

FIGURE CAPTIONS

Figure 1. Experimental results on the temporal variations of the normalized droplet surface area R_s^2 and the flame-front standoff ratio $\tilde{r}_f$ for a heptane droplet burning in gravity-free, standard environment [2].

Figure 2. Ratio of the mass of the fuel vapor to the mass of the droplet, as given by the d^2-law results, for a heptane droplet burning with different transfer numbers B_c and ambient oxidizer concentrations.

Figure 3. Amount of fuel vapor present, as given by the d^2-law results, for different locations of the ambiance, for a heptane droplet vaporizing in a 900°K fuel-free environment.

Figure 4. Typical fuel vapor profiles as pure vaporization proceeds.

Figure 5. Typical temperature profiles as pure vaporization proceeds.

Figure 6. Temporal variations of the vaporization rate $\tilde{m}$, surface area R_s^2, and edge of the outwardly propagating fuel vapor sphere $\tilde{r}_\infty$, for a heptane droplet vaporizing in a 900°K, fuel-free environment.

Figure 7. Typical fuel vapor and oxidizer profiles as combustion proceeds.

Figure 8. Typical temperature profiles as combustion proceeds.

Figure 9. Temporal variations of the vaporization rate $\tilde{m}$, fractional fuel consumption rate ϵ, and surface area R_s^2, for a heptane droplet burning in the standard atmosphere.

Figure 10. Comparison between the present theory and the d^2-law on the fractional amount of fuel reacted as a function of the fractional amount of fuel vaporized.

Figure 11. Temporal variations of the flame temperature T_f, the flame front standoff ratio $\tilde{r}_f$, and the physical dimension of the flame R_f, for a heptane droplet burning in the standard atmosphere.

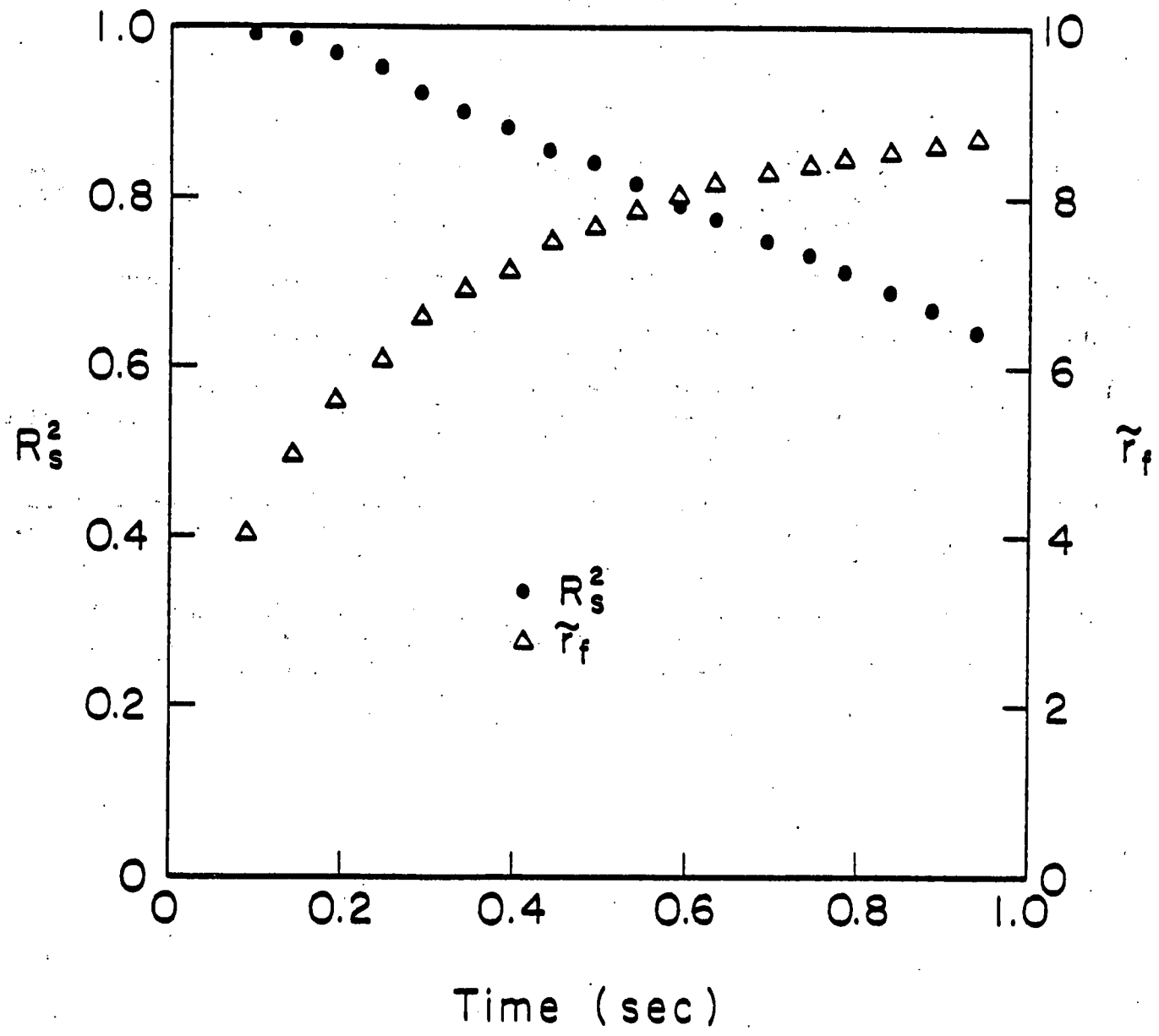
1.0
0.8
0.6
0.4
0.2
0
R_s^2
10
8
6
4
2
0
$\tilde{r}_f$
0
0.2
0.4
0.6
0.8
1.0
Time (sec)
R_s^2
$\tilde{r}_f$

Fig. 1

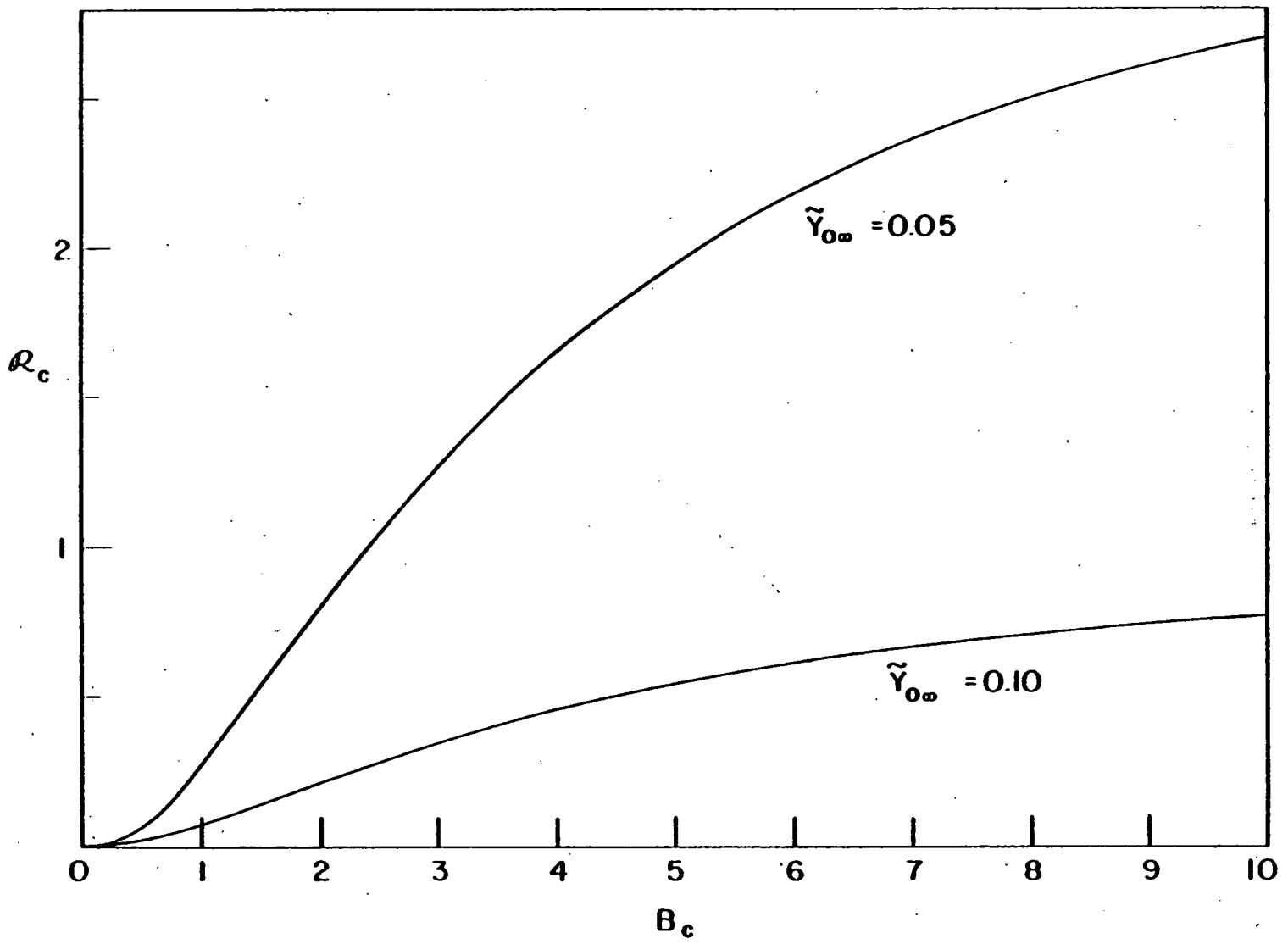
$\tilde{Y}_{0\infty}$ =0.05
$\tilde{Y}_{0\infty}$ =0.10
$\mathcal{R}_c$
B_c
0
1
2
3
4
5
6
7
8
9
10

Fig. 2

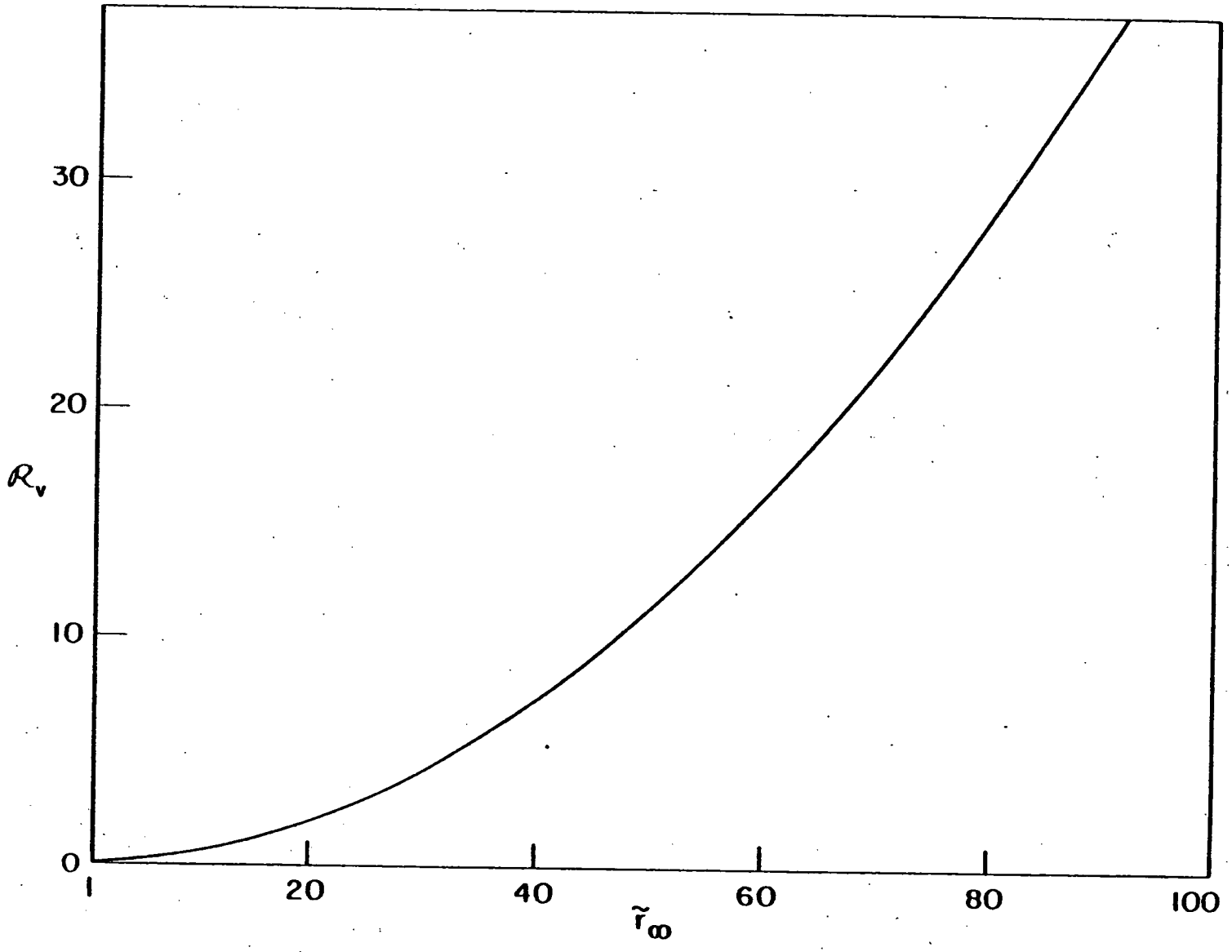

Fig. 3

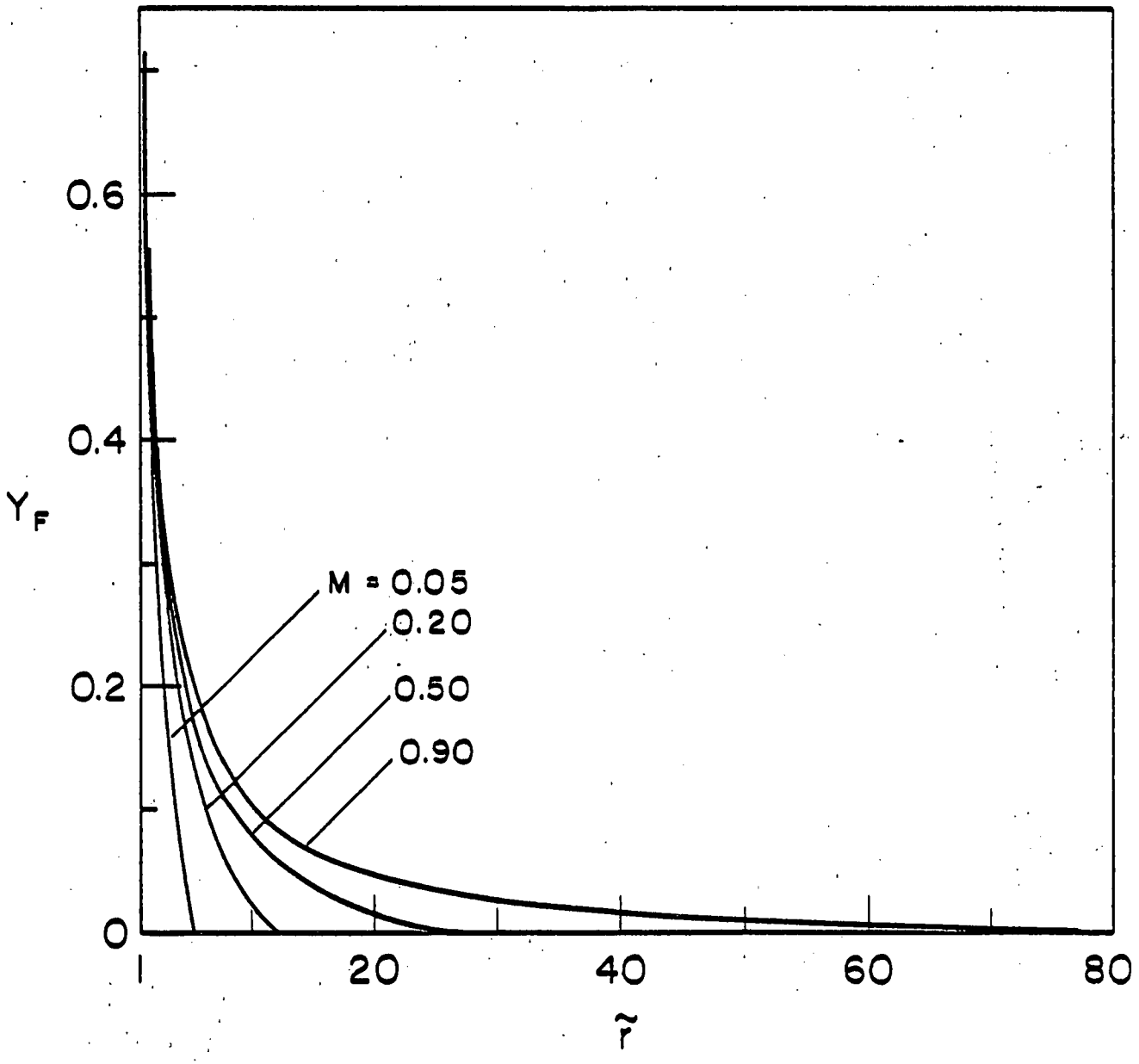

Fig. 4

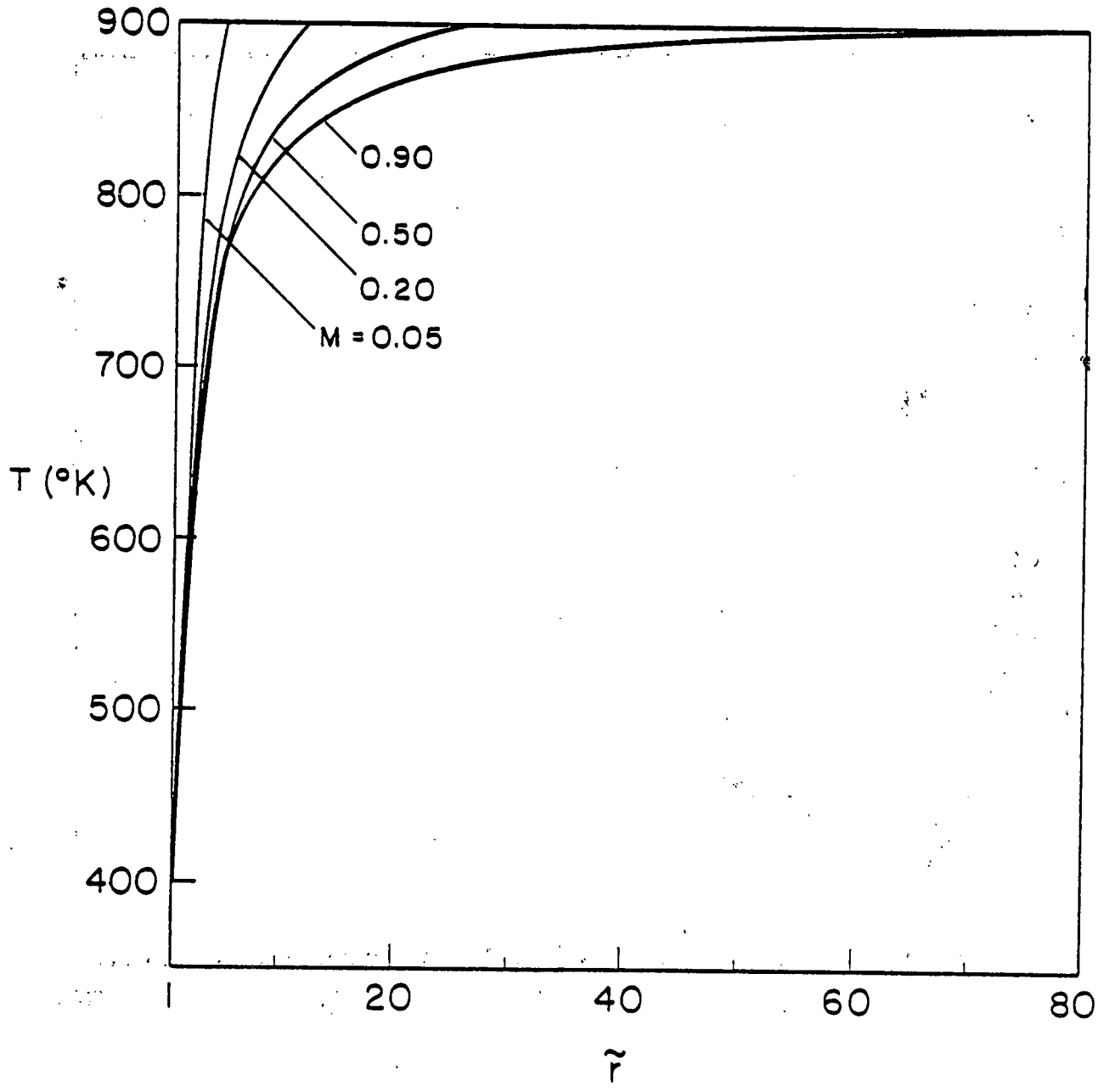

Fig. 5

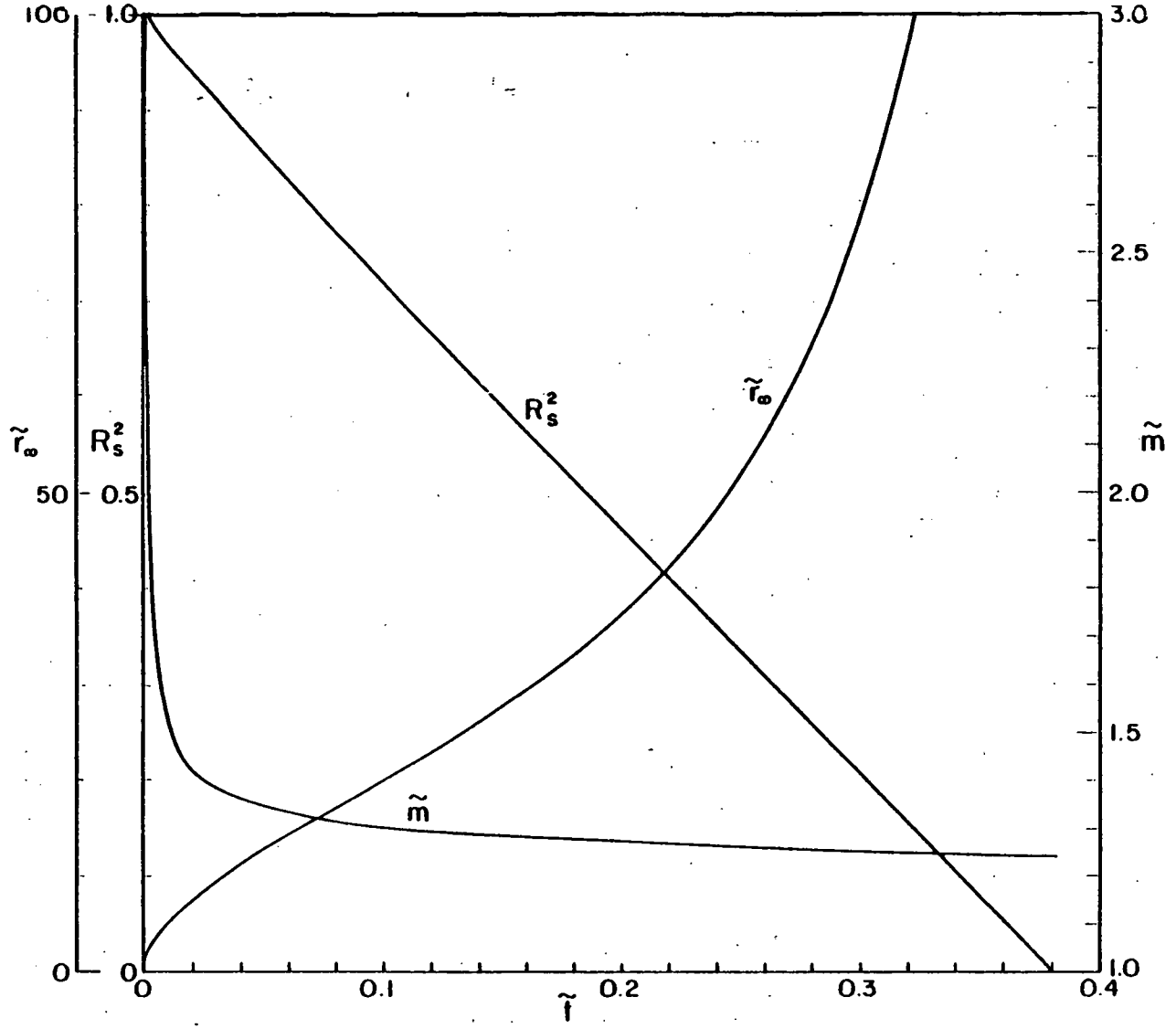
100
50
0
1.0
0.5
0
3.0
2.5
2.0
1.5
1.0
$\tilde{r}_\infty$
R_s^2
$\tilde{m}$
$\tilde{f}$
0
0.1
0.2
0.3
0.4

Fig. 6

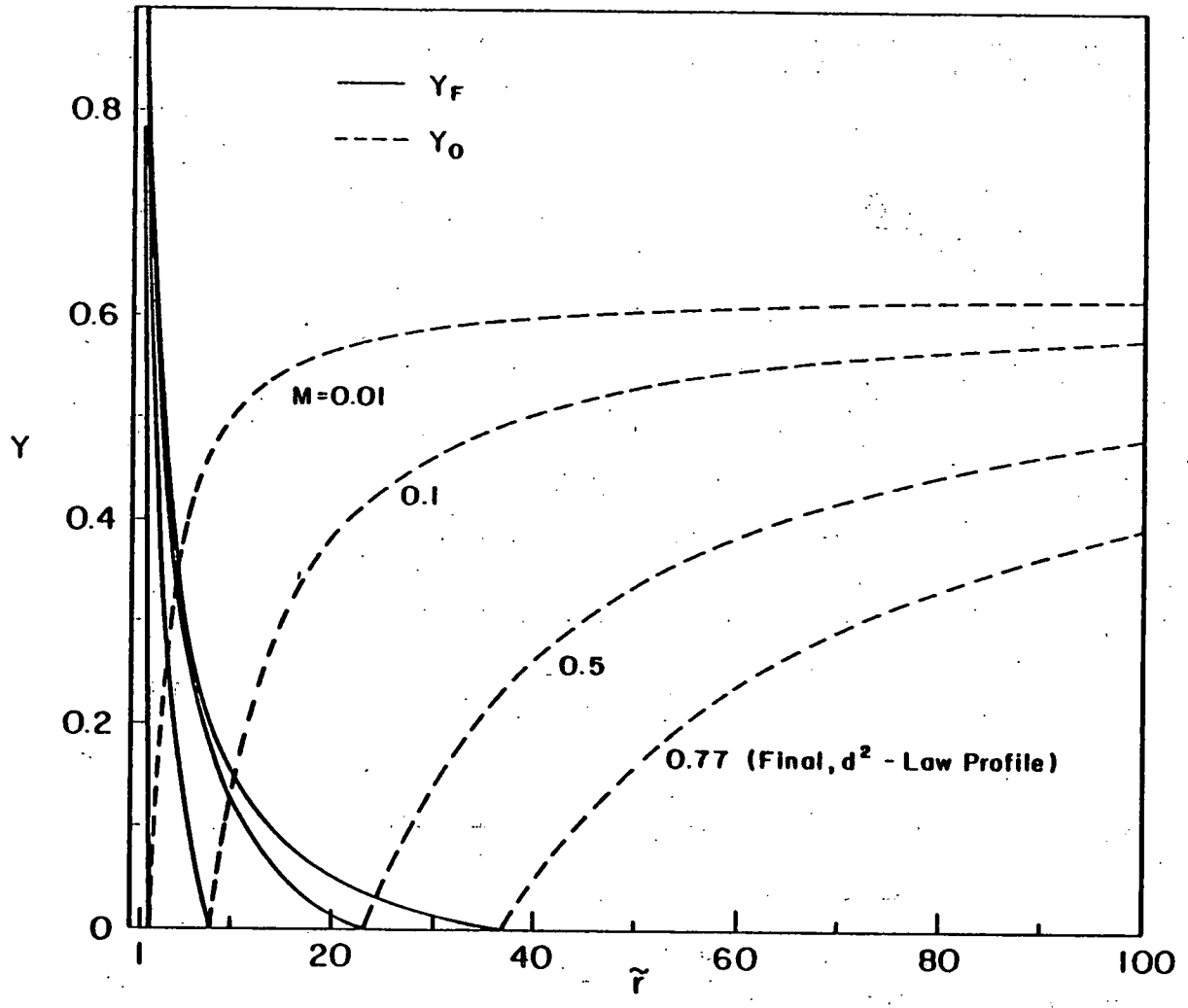
Y_F
Y_o
M=0.01
0.1
0.5
0.77 (Final, d^2 - Low Profile)
Y
$\tilde{r}$
0
0.2
0.4
0.6
0.8
1
20
40
60
80
100

Fig. 7

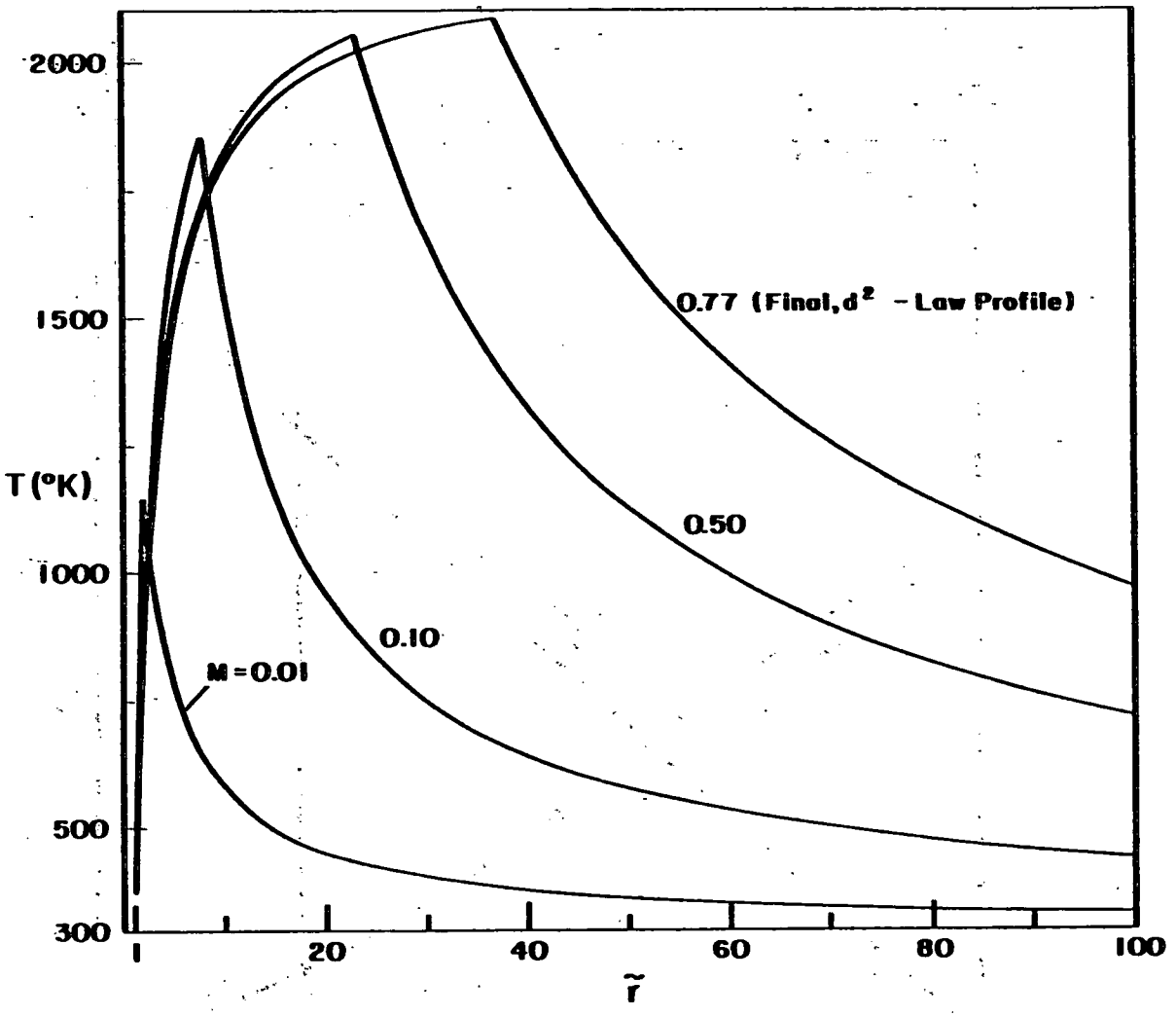
2000
1500
1000
500
300
T (°K)
0.77 (Final, d² - Law Profile)
0.50
0.10
M = 0.01
20
40
60
80
100
r̃

Fig. 8

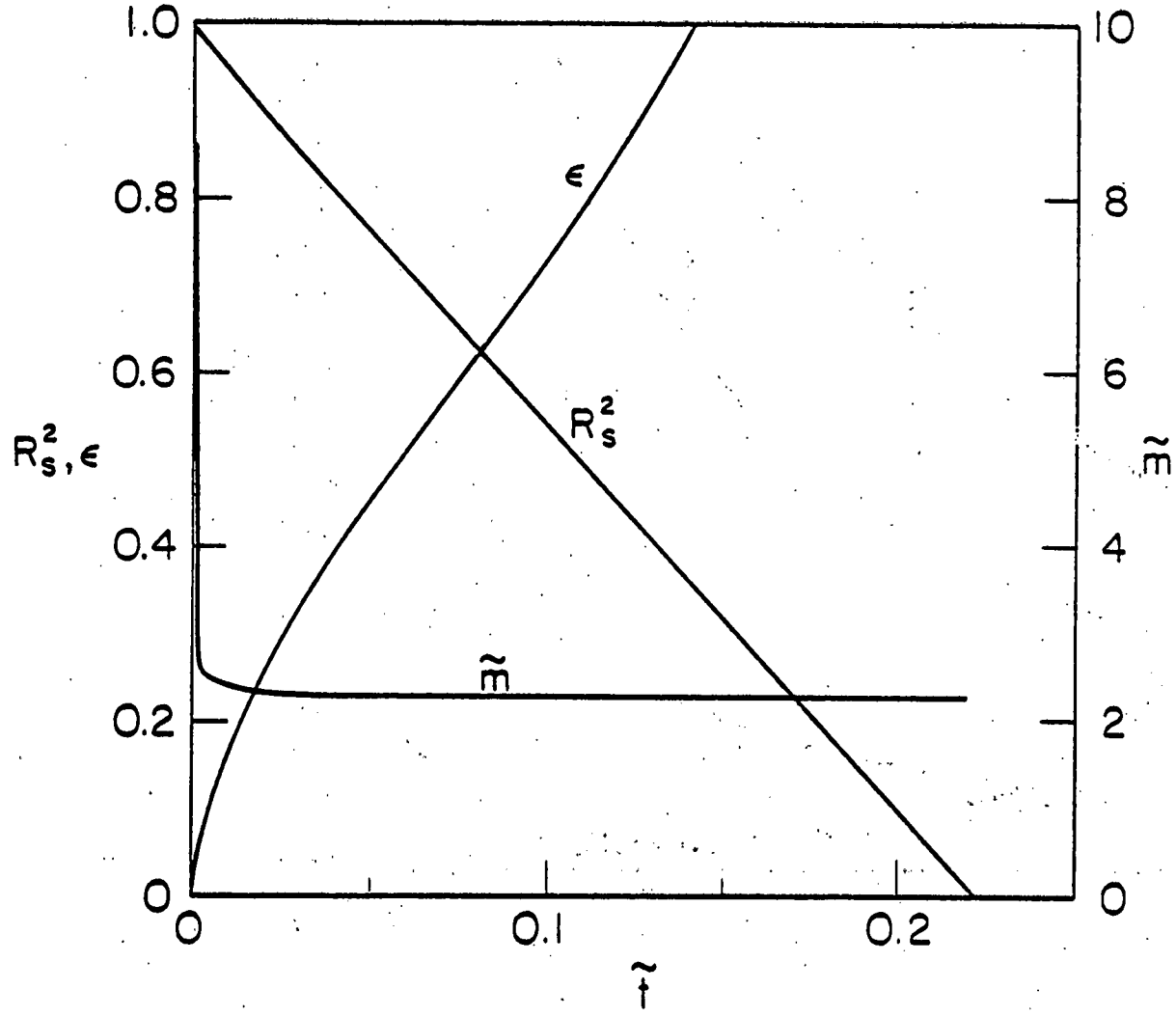
1.0
0.8
0.6
0.4
0.2
0
R_s^2, ϵ
10
8
6
4
2
0
$\tilde{m}$
ϵ
R_s^2
$\tilde{m}$
0
0.1
0.2
$\tilde{t}$

Fig. 9

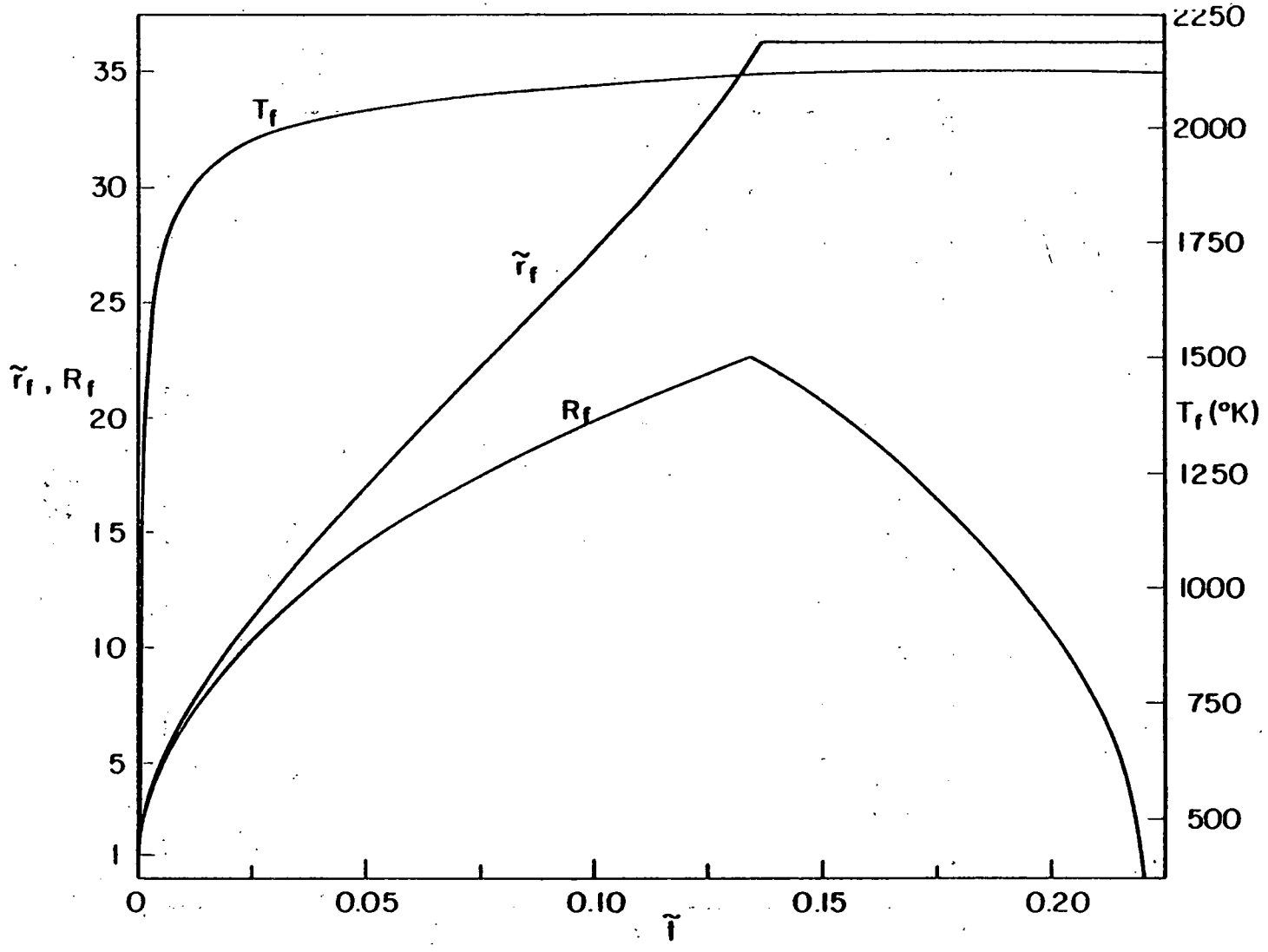
35
30
25
20
15
10
5
1
$\tilde{r}_f$, R_f
T_f
$\tilde{r}_f$
R_f
0
0.05
0.10
0.15
0.20
$\tilde{t}$
2250
2000
1750
1500
1250
1000
750
500
T_f (°K)

Fig. 10

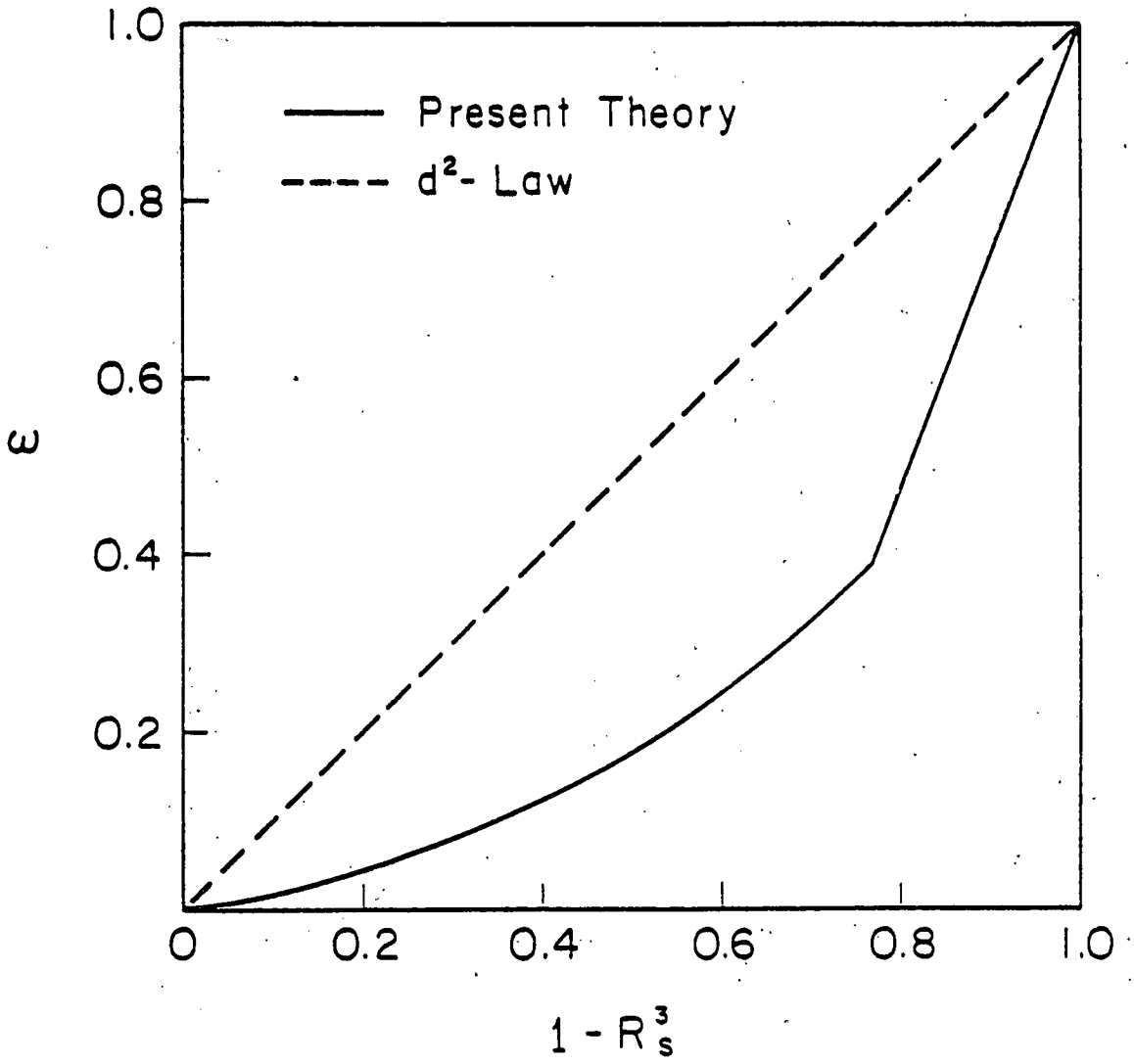

Fig. 11

FUEL SPRAY VAPORIZATION IN HUMID ENVIRONMENT

C. K. Law and M. Binark

Department of Mechanical Engineering
and Astronautical Sciences
Northwestern University
Evanston, Illinois 60201

ABSTRACT

The vaporization and transport of a monodisperse fuel spray in a cold, humid environment are analyzed, allowing for the possibility that the water vapor may condense, either heterogeneously at the droplet surface or homogeneously in the gas medium, as the spray interior is chilled through fuel vaporization. Results show that the associated condensation heat release is substantial and can significantly enhance the fuel vaporization rate, especially for the heterogeneous mode. It is further found that after initiation of vaporization the droplet temperature rapidly approaches a characteristic, constant value with heterogeneous condensation; this renders analytical solution possible. Potential complications caused by water condensation during spray experimentation are also discussed.

NOMENCLATURE

A_i, B_i, C_i	Antoine vapor pressure constants
A	area
$\hat{A}$	A/A_o
B	transfer number, Eq. (7)
$\hat{C}$	chamber function, Eq. (36)
C_p	specific heat
D	mass diffusivity
L_i	specific latent heat of vaporization/condensation
$\hat{L}_i$	L_i/L_W
L_H	heat utilized for droplet heating per unit change in droplet mass
$\hat{L}_H$	L_H/L_W
m_i	mass flow rate
m	$\Sigma\, m_i$
$\hat{m}_i$	$m_i/(4\pi\rho_g D_g r_s)$
p	pressure
Q_c	$1 + \epsilon_{Fc}(\hat{L}_F - 1)$
r	radial distance
$\hat{r}$	r/r_s
R	r_s/r_{so}
t	time
T	temperature
$\hat{T}$	$C_p T/L_W$
u	velocity
$\hat{u}$	u/u_o

W_i	ratio of molecular weight of i to that of the noncondensable species
x	axial distance along chamber
$\hat{x}$	$x\rho_g D_g/(\rho_\ell u_o r_{so}^2)$
X_i	molar fraction
Y_i	mass fraction

Greek symbols

ε_i	m_i/m
ρ	density
ω_F	fractional amount of fuel vaporized , $(1 - R^3)$
ω_W	fractional amount of water condensed

Subscripts

c	state corresponding to constant droplet temperature solution
F	fuel
g	gas phase
i	index for species
ℓ	liquid phase
s	droplet surface
W	water
o	initial state

Superscript

*	fully vaporized or equilibrium state

I. INTRODUCTION

The rate of combustion of a fuel spray is frequently controlled by the rate with which the individual droplets within the spray interior vaporize. In general the primary driving force to effect vaporization is the sensible heat of the hot environment within which the spray is introduced. Through conductive-convective heat transport the originally cold fuel droplets subsequently heat up and vaporize, producing fuel vapor which is mixed with the oxidizer gas to render combustion possible.

There is, however, another potentially important source of heat whose utilization can significantly enhance the spray vaporization rate. This arises from the possibility that during vaporization the spray interior may be chilled to such an extent that the water vapor present in the gas medium may condense and release the associated heat of condensation, which can then supplement the heat needed for fuel vaporization.

This condensation-enhanced vaporization is expected to be particularly beneficial for spray vaporization in a relatively cold, humid, environment, for example during carburetion of the automotive engine. For systems similar to this it has been found [1,2,3] that under most situations the spray interior rapidly becomes saturated with fuel vapor, leading to complete termination of vaporization. Since it is generally recognized that incomplete fuel vaporization during carburetion causes maldistribution and other deleterious heterogeneous combustion characteristics, the possible minimization of these heterogeneous effects through water vapor condensation is significant. Similar arguments can also be extended to the direct injection systems because the environment of the spray core is likely to be cold and fuel rich due to the slow rate of entrainment.

It is also reasonable to expect that the extent of augmentation in the fuel spray vaporization rate can indeed be substantial. This is because firstly the air-fuel mass ratio for near-stoichiometric combustion of typical hydrocarbon fuels (e.g. gasoline) is usually a large number, around 15. Therefore for a sufficiently humid environment the moisture content is of the same order as the liquid fuel introduced. Furthermore the specific latent heat of vaporization of water is much larger than those of the hydrocarbon fuels. It is then obvious that the water vapor present in the environment does contain sufficient latent heat of condensation which when released can supply a significant portion of the energy needed for fuel vaporization. Finally, it is also of interest to note that since water is a major product of hydrocarbon combustion, the water vapor generated at the hot combustion zone may diffuse back to the cold, vaporization region where it condenses.

In the following we shall substantiate and quantize the above concepts through a study of monodisperse spray vaporization in an environment initially containing some water vapor. Two models will be formulated to bracket the limiting behavior of spray vaporization in the presence of water condensation. In the fastest limit, which is studied in Section II and is termed the heterogeneous condensation mode, condensation of water vapor is assumed to occur at the surface of the fuel droplets which, being colder than the gas, are ideally suited as heterogeneous nucleation sites. Since in this limit the condensation heat release is directly supplied to the droplet, the droplet vaporization rate is expected to be maximally enhanced. In the slowest limit, which is studied in Section III and is termed the homogeneous condensation mode, condensation occurs within the gas medium at the saturation temperature. This implicitly assumes that there exist some heterogeneous nucleation sites

(e.g. dust particles) in the gas other than the fuel droplets. In this limit the increase in the droplet vaporization rate is caused by an increase in the gas temperature relative to the case of no water condensation. Due to the large amount of air mass that needs to be heated, the extent of increase in the gas temperature, and hence the droplet vaporization rate, are not expected to be as significant as the heterogeneous mode. Finally, the transport of the spray in a quasi-one-dimensional chamber, with either mode of condensation, is formulated in Section V.

II. HETEROGENEOUS CONDENSATION MODE

(1) General Discussions

In this limit condensation of water vapor is assumed to take place at the droplet surface. In order to ascertain the maximum effects of water condensation on fuel vaporization, it is also assumed that the droplet surface is not covered by the condensed water so that fuel can vaporize uninhibited. This is a reasonable assumption due to the fact that since water and oil generally do not mix, the condensed water will contract under surface tension and hence offer minimum blockage of the droplet surface. Furthermore, since in realistic situations a relative velocity, and hence shear stress, exists between the droplet and the gas stream, it is reasonable to expect that these loosely attached water globules or caps tend to be stripped away from the fuel droplet if they are of any significant size.

An important quantity governing droplet vaporization is the temporal variation of the droplet temperature distribution, particularly its value at the surface, T_s, because it directly influences the amount of heat the droplet receives from the environment, the extent of droplet heating required, and the surface concentrations of the fuel and water vapor. An accurate

determination [4,5] of the droplet temperature distribution is difficult because it requires the knowledge of the internal circulatory motion responsible for convective transport. It has been found [6], however, that the bulk droplet vaporization characteristics are only minimally dependent on the detailed description of internal circulation. This is because as long as the massive surface layer is heated at approximately equal rates, the subsequent heating of the much lighter inner core constitutes only minor perturbations to the total heat budget at the droplet surface. Therefore for mathematical expediency we shall assume that the droplet temperature is spacially uniform but temporally varying, which is the simplest possible model allowing for droplet heating [7].

The problem of interest can then be stated as follows. At time $t = 0$ an ensemble of evenly-distributed pure fuel droplets of uniform radius r_{so} and temperature T_{so} start to vaporize within a stagnant gaseous environment characterized by its temperature T_{go}, and fuel and water vapor mass fraction, Y_{Fgo} and Y_{Wgo}, respectively. The initial mass fraction of the liquid fuel is $Y_{F\ell o}$. The subsequent behavior of this spray ensemble is determined by analyzing the vaporization of a single fuel droplet and the collective modification of the gaseous medium by all of them, as will be shown in the following.

(2) Fuel Droplet Vaporization with Water Condensation

To serve as input to the spray analysis, and neglecting the small interference effects caused by the presence of neighboring droplets [8,9], we are concerned herein with the spherically-symmetric vaporization of a single fuel droplet in an infinite expanse of gas which has temperature T_g and mass fractions of the fuel and water vapor Y_{Fg} and Y_{Wg} respectively. Since the states of the droplet and the environment change at rates much slower than the rate of gas-phase heat and mass transport in the vicinity of the droplet [5],

the droplet vaporization process can be considered to be quasi-steady with slowly-varying boundary conditions. By further assuming that the specific heat C_p and the conductivity coefficients are constants, and that the gas-phase Lewis number is unity, the non-dimensional gas-phase diffusive-convective conservation equations for fuel vapor, water vapor, and energy can be respectively written as [10],

$$\hat{m}Y_F - \hat{r}^2 dY_F/d\hat{r} = \hat{m}_F \tag{1}$$

$$\hat{m}Y_W - \hat{r}^2 dY_W/d\hat{r} = \hat{m}_W \tag{2}$$

$$\hat{m}(\hat{T} - \hat{T}_s) - \hat{r}^2 d\hat{T}/d\hat{r} = -(\hat{m}_F \hat{L}_F + \hat{m}_W + \hat{m}\hat{L}_H) \tag{3}$$

where $\hat{m} = m/(4\pi\rho_g D_g r_s)$, $\hat{r} = r/r_s$, $\hat{T} = C_p T/L_W$, $\hat{L}_F = L_F/L_W$, $\hat{L}_H = L_H/L_W$, $m = m_F + m_W$, m_i is the mass vaporization rate of species i, L_i the latent heat of vaporization of i, L_H the amount of heat utilized for droplet heating per unit change in the droplet mass, r the radial distance, ρ the density, and D the mass diffusivity.

Integrating Eqs. (1) to (3) from the droplet surface to the ambiance yields explicit expressions for the three parameters of interest,

$$\hat{m} = \ell n\ (1+B) \tag{4}$$

$$\epsilon_F = \frac{(Y_{Wg} - Y_{Ws})Y_{Fs} + (Y_{Fg} - Y_{Fs})(1 - Y_{Ws})}{(Y_{Fg} - Y_{Fs}) + (Y_{Wg} - Y_{Ws})} \tag{5}$$

and

$$\hat{L}_H = \epsilon_F(1 - \hat{L}_F) - \frac{(\hat{T}_g - \hat{T}_s)(\epsilon_F - Y_{Fs})}{(Y_{Fg} - Y_{Fs})} - 1 \tag{6}$$

where

$$B = \frac{(\hat{T}_g - \hat{T}_s)}{\epsilon_F \hat{L}_F + \epsilon_W + \hat{L}_H} \tag{7}$$

and $\epsilon_i = m_i/m$ such that $\epsilon_F + \epsilon_W = 1$.

Further realizing that the phase change processes occur at rates much faster than the gas-phase transport rates such that the vapor at the droplet surface can be considered to be saturated, and that water and oil do not mix such that they vaporize independently of each other, the vapor concentrations of fuel and water at the surface can be related to the droplet surface temperature through, say, the Antoine vapor pressure relation [11],

$$X_{is} = \frac{1}{760p} \exp\left[A_i - \frac{B_i}{(T_s + C_i)}\right] \tag{8}$$

where p is the system pressure expressed in units of atmospheres, A_i, B_i and C_i are constants for a given substance [11], X_i is the molar fraction which, for the present system, is related to the mass fraction Y_i through

$$Y_i = \frac{X_i W_i}{1 + \sum_i (W_i - 1)X_i}, \quad i = F,W \tag{9}$$

and W_i is the ratio of the molecular weight of i to that of the non-condensable species (e.g. dry air).

Equations (4) to (9) show that $\hat{m}$, ϵ_F, and $\hat{L}_H$ are functions of the droplet temperature $\hat{T}_s$ and the states of the ambiance characterized by $\hat{T}_g$ and Y_{ig}. These will be subsequently determined through coupling with the liquid-phase heat balance and overall conservation relations for the spray.

Finally, it may be noted that since we expect the fuel to vaporize and water to condense, $\epsilon_F \geq 1$ and $\epsilon_W \leq 0$. Therefore in situations where water condensation has not yet taken place, then $\epsilon_F = 1$, and Eq. (5) together with the water vapor pressure relation Eq. (8) are not needed.

(3) Droplet Temperature Transient

By definition

$$L_H = \frac{(4\pi/3)r_s^3 \rho_\ell C_p dT_s/dt}{-d[(4\pi/3)r_s^3 \rho_\ell]/dt} \quad , \tag{10}$$

which when expressed in non-dimensional form is

$$\hat{L}_H = -d\hat{T}_s/d(\ell n\, R^3) \quad , \tag{11}$$

where $R = r_s/r_{so}$. Therefore by equating Eq. (11) with the expression obtained through gas-phase energy conservation, Eq. (6), the rate of change of the droplet temperature as evaporation proceeds is given by

$$\frac{d\hat{T}_s}{d(\ell n\, R^3)} = 1 - \epsilon_F(1 - \hat{L}_F) + \frac{(\hat{T}_g - \hat{T}_s)(\epsilon_F - Y_{Fs})}{(Y_{Fg} - Y_{Fs})} \quad , \tag{12}$$

which is subject to the initial condition that $T_s = T_{so}$ when $R = 1$.

(4) Spray Conservation Relations

From energy conservation for the present adiabatic system, we have

$$\hat{T}_{go} + Y_{F\ell o}(\hat{T}_{so} - \hat{L}_F) = (1 + \omega_F Y_{F\ell o} - \omega_W Y_{Wgo})\hat{T}_g + (1 - \omega_F)Y_{F\ell o}(\hat{T}_s - \hat{L}_F) + \omega_W Y_{Wgo}(\hat{T}_s - 1) \tag{13}$$

where $\omega_F = 1 - R^3$ is the fractional amount of liquid fuel that has vaporized, and ω_W is the fractional amount of water vapor that has condensed. By definition they are related to Y_{Fg} and Y_{Wg} through

$$Y_{Fg} = \frac{Y_{Fgo} + \omega_F Y_{F\ell o}}{1 + \omega_F Y_{F\ell o} - \omega_W Y_{Wgo}} \quad , \tag{14}$$

$$Y_{Wg} = \frac{(1 - \omega_W)Y_{Wgo}}{1 + \omega_F Y_{F\ell o} - \omega_W Y_{Wgo}} \quad . \tag{15}$$

From conservation of water we can write

$$\frac{d(\omega_W Y_{Wgo})}{dt} = -\left[\frac{Y_{F\ell o}}{(4\pi/3)r_{so}^3 \rho_\ell}\right] \dot{m}_W \quad , \tag{16}$$

which states that the rate of depletion of the water vapor from the gas medium is equal to the rate of water condensation onto one droplet times the total number of droplets.

Similarly, conservation of fuel states that

$$\frac{d[(4\pi/3)r_{so}^3 \rho_\ell \omega_F]}{dt} = \dot{m}_F \quad . \tag{17}$$

Dividing Eq. (16) by Eq. (17), we have

$$\frac{d\omega_W}{dR^3} = \left(\frac{Y_{F\ell o}}{Y_{Wgo}}\right)\left(\frac{1}{\epsilon_F} - 1\right) \tag{18}$$

which is to be solved subject to the initial condition $\omega_W = 0$ when $R = 1$. When $Y_{Wgo} \to 0$, $\epsilon_F \to 1$; therefore the differential is finite.

This completes our formulation for the heterogeneous condensation mode. The final solution involves solving the coupled first order non-linear ordinary differential equations of Eqs. (12) and (18), with the inhomogeneous terms being functions of ω_W, R, and $\hat{T}_s$. If water does not condense, then Eq. (18) is not needed.

(5) Criterion for Complete Spray Vaporization

Without solving Eqs. (12) and (18), it is possible to derive an explicit criterion allowing a priori assessment of the ability of the spray to achieve total vaporization. Designating the fully vaporized state, $\omega_F = 1$, by the superscript "*", it is then required that $T_g^* > T_s^*$, $Y_{Wg}^* \geq Y_{Ws}^*$, and $Y_{Fs}^* > Y_{Fg}^*$. Therefore a sufficient, although not necessarily unique, criterion governing

full vaporization can be obtained by equating any two of the above three relations such that the remaining inequality will serve as the criterion.

As an illustration we have adopted $T_g^* = T_s^*$, $Y_{Wg}^* = Y_{Ws}^*$, and $Y_{Fg}^* < Y_{Fs}^*$ as our criterion. Using Eqs. (13), (14) and (15), it can be shown that the single inequality to be satisfied for complete spray vaporization is

$$\frac{Y_{Fgo} + Y_{F\ell o}}{1 + Y_{F\ell o} - Y_{Wgo}} < \frac{Y_{Fs}^*}{1 - Y_{Ws}^*} \tag{19}$$

where Y_{Fs}^* and Y_{Ws}^* are functions of $\hat{T}_g^*$ given by Eqs. (8) and (9), and $\hat{T}_g^*$ is to be iteratively determined from the relation

$$\hat{T}_g^*(1 + Y_{F\ell o}) = \hat{T}_{go} + Y_{F\ell o}(\hat{T}_{so} - \hat{L}_F) + [Y_{Wgo} - Y_{Ws}^*(1 + Y_{F\ell o})]/(1 - Y_{Ws}^*) \tag{20}$$

(6) Results

Equations (12) and (18) have been numerically integrated using the Runge-Kutta scheme. An n-heptane spray vaporizing in humid air, with $C_p = 0.35$ cal/gm-°K, $L_F = 75.8$ cal/gm, $L_W = 590$ cal/gm, $W_F = 3.46$, $W_W = 0.622$, is adopted for study. The Antoine coefficients A_i, B_i and C_i, for heptane and water, are listed in Ref. [11].

To limit the extent of our parametric study, we shall also consider fixed values of $T_{so} = 300°K$ and $Y_{Fgo} = 0$. The dependence of the system on T_{so} and Y_{Fgo} is physically obvious and hence need not be specially considered. Results will be presented for an environment which initially is either fully humid, or half humid (on molar basis), or completely dry. Corresponding to $T_{go} = 280°K$, 300°K, and 320°K, the saturation water contents are $Y_{Wgo} = 0.005979$, 0.02183, and 0.06722 for the fully-humid states, and 0.002984, 0.01084, and 0.03294 for the half-humid states.

Figures 1 and 2 show the variation of T_s with the fractional amount of liquid fuel vaporized, ω_F, which is an indication of the progress in the spray vaporization process. Since $T_{so} = 300^{\circ}K$ is higher than the wet bulb temperatures of heptane for the values of T_{go} considered, it is seen that T_s generally decreases as vaporization is initiated; the only exception here is the fully-humid case of $T_{go} = 320^{\circ}K$, for which the extent of condensation heat release causes an increase in the droplet temperature. The importance of water condensation is further illustrated by the fact that for a given T_{go}, curves representing different levels of initial humidity immediately branch off as condensation is initiated. For $T_{go} = 280^{\circ}K$, the half-humid curve coincides with the non-humid curve because condensation is not possible owing to the extremely low level of humidity in such a cold environment. For this case complete spray vaporization cannot be achieved; a state of equilibrium is reached with about 6% of the fuel still remaining in the liquid phase. However, for a fully-humid environment complete fuel vaporization can be attained through the additional condensation heat release. Therefore the potential of water condensation is particularly beneficial for cold mixtures which otherwise would not be able to achieve complete vaporization.

The present formulation assumes that the properties of the spray interior are uniform. In realistic situations, for example in the case of a spray jet, the cone region is much richer in fuel than the sheath region due to the finite rate of entrainment. To investigate effects due to this non-uniformity, Fig. 2 compares the variations of T_s for the near-stoichiometric and fuel-rich cases of $Y_{Fl_o} = 0.05$ and 0.2 respectively. It is seen that whereas T_s depends only weakly on Y_{Fl_o}, complete fuel vaporization for the rich case is very difficult to achieve. This is because not only there is now more fuel that

needs to be vaporized, but there is also less air and hence correspondingly less sensible and condensation heat available for vaporization.

An interesting result shown in Figs. 1 and 2 is that within 10-15% of the droplet lifetime the droplet temperature rapidly approaches a constant value. This behavior has also been observed in our previous studies [2,3] on fuel spray vaporization in non-humid environments, and can be explained as follows. When the droplet ensemble vaporizes, the gas medium is simultaneously chilled and enriched with fuel vapor. These two effects tend to suppress, and elevate, the droplet temperature in such proportions that the opposing trends cancel out. Therefore after the initial transient, the droplet attains a constant temperature. Similar argument can be extended to the present situation when there is the additional process of water condensation, which is just the reverse of vaporization.

It may also be emphasized that this constant droplet temperature is not the conventional wet-bulb temperature, which exists for droplet vaporization in a constant environment. In the present system the states of the environment, as well as the droplet vaporization rate, are continuously changing. The droplet temperature, however, is left unaffected. As will be subsequently shown, the establishment of this constant offers significant simplifications in the solution of the problem.

Figure 3 shows the variation of T_g as vaporization proceeds. During the initial 5-10% of the droplet lifetime T_g remains close to the initial values for those cases in which the droplet temperatures initially cool down. This is because even though their initial vaporization rates are relatively fast, the latent heat of vaporization is supplied by the sensible heat of the "hot" droplet rather than the environment. In fact the excessive heat contained in

the droplet may even produce an initial slight increase in T_g, as is found to be the case for $T_{go} = 280^{\circ}K$. On the other hand if the droplet temperature initially increases, then the environment actively supplies heat to the droplet from the beginning and therefore T_g starts to decrease immediately. In all cases, however, it is interesting to note that after the initial transient T_g decreases almost linearly with ω_F.

Figures 4 and 5 show the fuel vaporization rate, $\hat{m}_F$, as functions of ω_F. The qualitative behavior are as expected. It is again of interest to note the almost linear dependence of $\hat{m}_F$ on ω_F after the initial transient. The most significant result shown in these figures, and indeed for the present study, is the extent of augmentation in the spray vaporization rate in the presence of water condensation. For example, Fig. 4 shows that for $Y_{F\ell o} = 0.05$ at half-lifetime, a fully humid environment would enhance the fuel vaporization rate by about 30%, 70%, and 150% with $T_{go} = 280^{\circ}K$, $300^{\circ}K$, and $320^{\circ}K$, respectively.

Figure 6 shows that for situations in which T_s, and hence $\hat{m}_F$, initially decrease, an initially increasing ϵ_F results. This is because as T_s decreases, the rate of water condensation increases. But since $\hat{m}_W$ is inwardly directed, the net mass flow rate, $\hat{m}$, is reduced. This causes an increase in $\epsilon_F = \hat{m}_F/\hat{m}$. After the initial transient, ϵ_F assumes almost constant values for the rest of the vaporization process.

Figure 7 shows that after the initial transient the fractional amount of water vapor condensed varies almost linearly with the fractional amount of fuel vaporized, with slopes approximately being proportional to $(\epsilon_F - 1)/Y_{Wgo}$ (Eq. 22). Therefore even though a relatively hot spray may have a higher rate of vaporization, and hence higher rate of condensation, it also contains more water vapor initially. Hence the net effect can be a smaller slope than the case of an initially cold spray.

(7) Constant Droplet Temperature Solution

The observation that the droplet temperature rapidly approaches a constant value after initiation of spray vaporization renders possible analytical solution by assuming the droplet is at this characteristic temperature, T_{sc}, throughout its lifetime. Hence by setting $d\hat{T}_s/dR^3 = 0$ in Eq. (12), $\hat{T}_{sc}$ can be iteratively determined from the implicit algebraic relation

$$(Y_{Fgo} - Y_{Fsc})Q_c + (\epsilon_{Fc} - Y_{Fsc})[\hat{T}_{go} + Y_{F\ell o}\hat{T}_{so} - (1+Y_{F\ell o})\hat{T}_{sc}] = 0 \qquad (21)$$

where $Q_c = 1 + \epsilon_{Fc}(\hat{L}_F - 1)$ and ϵ_{Fc} is determined from the following.

Assuming that ϵ_F is a constant, Eq. (18) can be readily integrated, yielding

$$\omega_W = \left(\frac{Y_{F\ell o}}{Y_{Wgo}}\right)\left(1 - \frac{1}{\epsilon_{Fc}}\right)\omega_F \quad . \qquad (22)$$

Substituting Eq. (22) into Eq. (5), and using Eqs. (14) and (15), ϵ_{Fc} is given by

$$\epsilon_{Fc} = \frac{Y_{Fgo}(1 - Y_{Wsc}) - Y_{Fsc}(1 - Y_{Wgo})}{(Y_{Fgo} + Y_{Wgo}) - (Y_{Fsc} + Y_{Wsc})} \qquad (23)$$

which is only a function of $\hat{T}_{sc}$, and hence shows that the assumption $\epsilon_F = \epsilon_{Fc}$ used in deriving Eq. (22) is consistent. Equation (22) also shows that ω_W varies linearly with ω_F, as is found in Fig. 7.

The transfer number B is now given by

$$(1+B) = \frac{(1+B_c/Q_c)}{(1+\omega_F Y_{F\ell o}/\epsilon_{Fc})} \qquad (24)$$

where $$B_c = (\hat{T}_{go} - \hat{T}_{sc}) + Y_{F\ell o}(\hat{T}_{so} - \hat{T}_{sc}) \quad . \qquad (25)$$

For complete vaporization to occur, $B > 0$ at $\omega_F = 1$. From Eq. (24) the criterion for complete spray vaporization can now be simply stated as

$$B_c > Y_{F\ell o} Q_c / \epsilon_{Fc} \tag{26}$$

If Eq. (26) is not satisfied, then vaporization terminates when the droplets reach the equilibrium size

$$R = \{1 - (B_c \epsilon_{Fc})/(Y_{F\ell o} Q_c)\}^{1/3} \tag{27}$$

Finally, using Eqs. (4) and (24), it can be shown that for small values of $Y_{F\ell o}$, the variation of the fuel vaporization rate as vaporization proceeds is

$$\frac{d\hat{m}_F}{d\omega_F} \simeq - Y_{F\ell o} \quad . \tag{28}$$

Equation (28) agrees with the numerical results of Figs. 4 and 5, in which it is shown that after the initial transient curves with different T_{go} become parallel to each other, with a slope approximately equal to $Y_{F\ell o}$.

The problem can therefore be considered to be completely solved analytically, with the only numerical work involved being the initial, iterative determination of T_{sc} from Eq. (21). Results obtained from the variable and constant droplet temperature solutions will be compared in Section IV.

III. HOMOGENEOUS CONDENSATION MODE

(1) Formulation

In the slowest limit condensation of water vapor occurs in the gas medium, either homogeneous or heterogeneous on some dust particles. Without being unduly concerned about the detailed nucleation and condensation processes, we shall simply assume that the water vapor is always in a saturated state in the gas medium, which implies that the excessive amounts will have been condensed, at the prevailing gas temperature, with the attendant condensation heat release.

Most of the formulation for the heterogeneous condensation mode remain valid here by setting $\hat{m}_W = 0$, and hence $\hat{m} = \hat{m}_F$, $\epsilon_F = 1$, $\epsilon_W = 0$, etc. The energy conservation relation, Eq. (13), is slightly modified to become

$$\hat{T}_{go} + Y_{F\ell o}(\hat{T}_{so} - \hat{L}_F) = [1 + \omega_F Y_{F\ell o} - \omega_W Y_{Wgo}]\hat{T}_g + (1 - \omega_F)Y_{F\ell o}(\hat{T}_s - \hat{L}_F) - \omega_W Y_{Wgo} \quad (29)$$

The constraint on the saturation of the gas medium by water vapor is simply the Antoine relation evaluated at the gas temperature T_g, or

$$X_{Wg} = \frac{1}{760p} \exp\left[A_W - \frac{B_W}{(T_g + C_W)}\right] . \quad (30)$$

Furthermore, by definition

$$X_{Wg} = \frac{Y_{Wg}/W_W}{1 - (1 - 1/W_W)Y_{Wg} - (1 - 1/W_F)Y_{Fg}} \quad (31)$$

where Y_{Fg} and Y_{Wg} are given by Eqs. (14) and (15), and ω_W is obtained from Eq. (29). Hence by equating Eqs. (30) and (31), a transdendental equation

$$F(\hat{T}_g, \hat{T}_s, R^3) = 0 \quad (32)$$

results. The final solution then involves an iterative determination of $\hat{T}_g$ and $\hat{T}_s$ as functions of R^3 using Eqs. (12) and (32). If the solution yields $\omega_W < 0$, then the environment has not saturated. Hence $\omega_W = 0$ and only Eq. (12) is needed.

A criterion for complete spray vaporization similar to that derived for the heterogeneous case can also be obtained for the present case.

(2) Results

The system parameters adopted for illustration here are the same as those for the heterogeneous case. Figure 8 shows that for the fully-humid environment

condensation is initiated rapidly after the excessive heat initially contained in the droplets has been dissipated through vaporization. However, for the half-humid environment initiation of condensation can be quite delayed. Indeed for $Y_{F\ell o} = 0.05$ condensation fails to occur for the three initial gas temperatures investigated. The reason that condensation is difficult to start for the homogeneous mode is that an unsaturated gas medium has to be substantially chilled, through fuel vaporization, for water vapor to become saturated. This is particularly difficult to be achieved when $Y_{F\ell o}$ is small. However, for the heterogeneous mode condensation is induced by the concentration gradient between the gas medium and the droplet surface. Since the droplet surface is usually at a lower temperature than the environment so that fuel vaporization is possible, the water vapor concentration at the surface is likely to be lower than that in the environment, rendering condensation possible.

Figure 8 also shows that in the presence of condensation, the droplet temperature increases almost linearly with ω_F after the initial transient. The behavior of other system parameters are qualitatively similar with those of the heterogeneous case and hence will not be elaborated. Finally, Fig. 9 compares the fuel vaporization rate, $\hat{m}_F$, in a fully-humid environment for the heterogeneous, homogeneous, and non-condensing modes. In realistic situations the vaporization rate will be bounded by the homogeneous and heterogeneous curves.

IV. QUASI-ONE-DIMENSIONAL SPRAY TRANSPORT

In the following we shall consider the transport of the spray ensemble in an adiabatic, quasi-one-dimensional chamber with cross-sectional area A(x), where x is the axial distance. To focus our attention on effects due to heat and mass transfer, we shall also assume that there is no velocity lag between the gas and the droplets.

Using the definition of m_F and the identity $d/dt = ud/dx$, where u is the velocity, we have

$$R\hat{u}dR/d\hat{x} = - \epsilon_F \ell n\,(1+B) \tag{33}$$

where $\hat{u} = u/u_o$ and $\hat{x} = x\rho_g D_g/(\rho_\ell u_o r_{so}^2)$. Furthermore, continuity requires that

$$\hat{u}\hat{A} = 1 + \omega_F Y_{F\ell o} - \omega_W Y_{Wgo} \tag{34}$$

where $\hat{A} = A/A_o$.

Substituting Eq. (34) into Eq. (33) and integrating, we have

$$C(\hat{x}) = \int_R^1 \frac{(1+\omega_F Y_{F\ell o} - \omega_W Y_{Wgo})}{\epsilon_F \ell n\,(1+B)} R'dR' \tag{35}$$

where $C(\hat{x})$ is the chamber function defined as

$$C(\hat{x}) = \int_o^{\hat{x}} \hat{A}(x')dx' \quad , \tag{36}$$

which is a measure of the axial distance travelled.

Figure 10 shows $C(\hat{x}^*)$ as a function of the inlet gaseous temperature T_{go} for the heterogeneous, homogeneous, and non-condensing modes, where $\hat{x}^*$ is the location of either complete or equilibrium fuel vaporization. It is obvious that the shortening of the chamber length required to achieve complete spray vaporization as a result of condensation is significant, particularly for the heterogeneous mode and at higher inlet temperatures.

By further invoking the constant droplet temperature assumption for the heterogeneous condensation mode, Eq. (35) becomes

$$C(\hat{x}) = \int_R^1 \frac{(1+\omega_F Y_{F\ell o}/\epsilon_{Fc})}{\epsilon_{Fc}\,\ell n\left[(1+B_c/Q_c)/(1+\omega_F Y_{F\ell o}/\epsilon_{Fc})\right]} R'dR' \tag{37}$$

Equation (37) can be integrated by assuming that the spray is not rich ($Y_{F\ell o} \ll 1$) and the evaporator is sufficiently efficient ($Y_{F\ell o} \ll B_c/Q$), yielding

$$C(\hat{x}) = \hat{m}_{Fc}^{-1}[0.5(1+z)(1-R^2) - 0.2z(1-R^5)] \quad (38)$$

where

$$\hat{m}_{Fc} = \epsilon_{Fc} \ell n\,(1+B_c/Q_c) \quad (39)$$

and

$$z = \left(\frac{1}{\epsilon_{Fc}} + \frac{1}{\hat{m}_{Fc}}\right) Y_{F\ell o} \quad (40)$$

Therefore in order to achieve complete spray vaporization, the chamber length needs to have a minimum length

$$C(\hat{x}^*) = \hat{m}_{Fc}^{-1}(0.5+0.3z) \quad . \quad (41)$$

Figure 11 compares $C(\hat{x}^*)$ given by the exact expression Eq. (35), the constant temperature expression Eq. (37), and the efficient evaporation limit of Eq. (41). It is found that results from the constant droplet temperature integral agree with those from the exact integral to within 5% and hence can be considered to be accurate. Results from the efficient evaporation limit agree well with the exact results at higher inlet temperatures, although the agreement deteriorates as T_{go} decreases and completely breaks down near the fuel saturation limit, as should be.

V. CONCLUSIONS

In this paper we have investigated, and bracketed, the effects of water vapor condensation during the vaporization of a fuel spray in a humid environment. It is demonstrated that for the heterogeneous mode the effect of condensation is indeed significant and can substantially hasten the fuel vaporization process. For the homogeneous case the effect is relatively smaller because of the large amount of air mass that absorbs the condensation

heat release. For both modes the potential of water condensation in enabling an initially cold spray to achieve complete vaporization, and therefore minimizing the deleterious heterogeneous combustion effects, are particularly significant.

The present results also indicate that caution should be exercised when experimentally measuring spray properties. The condensation process not only introduces an additional heat source, but it can also give a larger value of the fuel droplet size in the presence of heterogeneous nucleation, and a larger value of the droplet number density in the presence of homogeneous nucleation. In both cases inaccurate data will be taken on the spray vaporization rate, the droplet distribution function, the total amount of fuel available for combustion, and its relative amounts in the gas and liquid phases. The difficulty in avoiding this masquerading effect is further compounded by realizing that even if the gas mixture is dried before using, water vapor can still be generated in the combustion region and possibly diffuse back to the vaporization region. It seems a necessary precaution to take in ascertaining the accuracy of the data is to ensure that the data do not violate the requirement of atom or species conservation.

Finally, considerations should also be given to gaseous experiments in which seedings are introduced for optical measurement purposes. These seedings may serve as heterogeneous nucleation sites and hence may become larger than assumed. Subsequently their velocity may not always be in phase with that of the gas, and therefore yielding inaccurate data on the gas velocity.

Acknowledgment

This work was sponsored by the Office of Basic Energy Sciences, Department of Energy, under Contract No. EG-77-S-02-4433.

REFERENCES

1. D. R. Dickenson and W. R. Marshall, "The Rates of Evaporation of Spray," AIChE J. 14, 541-552 (1968).

2. C. K. Law, "A Theory for Monodisperse Spray Vaporization in Adiabatic and Isothermal Systems," Intl. J. Heat Mass Transfer 18, 1285-1292 (1975).

3. C. K. Law, "Adiabatic Spray Vaporization with Droplet Temperature Transient," Combust. Sci. Tech. 15, 65-73 (1977).

4. C. K. Law, S. Prakash and W. A. Sirignano, "Theory of Convective, Transient, Multicomponent Droplet Vaporization," Sixteenth Symposium (International) on Combustion, pp. 605-617, The Combustion Institute, Pittsburgh, Pa. (1977).

5. W. A. Sirignano and C. K. Law, "A Review of Transient Heating and Liquid-Phase Mass Diffusion in Fuel Droplet Vaporization," ACS Advances in Chemistry Series, Vol. 166: Evaporation and Combustion of Fuels, American Chemical Society, N.Y. (1977).

6. C. K. Law and W. A. Sirignano, "Unsteady Droplet Combustion with Droplet Heating. II: Conduction Limit," Combust. Flame 28, 175-186 (1977).

7. C. K. Law, "Unsteady Droplet Combustion with Droplet Heating," Combust. Flame 26, 17-22 (1976).

8. M. Labowsky, "A Formation for Calculating the Evaporation Rates of Rapidly Evaporating Interacting Particles," Combust. Sci. Tech. 18, 145-151 (1978).

9. R. Samson, D. Bedeaux, M. J. Saxton and J. M. Deutch, "A Simple Model of Fuel Spray Burning I: Random Sprays," Combust. Flame 31, 215-221 (1978).

10. C. K. Law, "A Model for the Combustion of Oil/Water Emulsion Droplets," Combust. Sci. Tech. 17, 29-38 (1977).

11. R. C. Reid, J. M. Prausnitz and T. K. Sherwood, The Properties of Gases and Liquids, McGraw-Hill, N.Y., 1977.

FIGURE CAPTIONS

Figure 1. Influence of initial gas temperature and humidity on droplet temperature variation for the heterogeneous condensation mode.

Figure 2. Influence of initial liquid fuel concentration and humidity on droplet temperature variation for the heterogeneous condensation mode.

Figure 3. Influence of initial gas temperature and humidity on subsequent gas temperature variations for the heterogeneous condensation mode.

Figure 4. Influence of initial gas temperature and humidity on fuel vaporization rate variation for the heterogeneous condensation mode.

Figure 5. Influence of initial liquid fuel content and humidity on fuel vaporization rate variation for the heterogeneous condensation mode.

Figure 6. Influence of initial gas temperature and humidity on the variation of fractional vaporization rate of fuel for the heterogeneous condensation mode.

Figure 7. Influence of initial gas temperature and humidity on the variation of the fractional amount of water vapor condensed for the heterogeneous condensation mode.

Figure 8. Influence of initial liquid fuel concentration and humidity on droplet temperature variation for the homogeneous condensation mode.

Figure 9. Comparison of fuel vaporization rate variations for heterogeneous, homogeneous, and non-condensing modes for varying initial gas temperature.

Figure 10. Comparison of the chamber function for complete fuel vaporization for the heterogeneous condensation, homogeneous condensation, and non-condensing modes.

Figure 11. Comparison of the accuracy of different solutions in predicting the chamber function for complete fuel vaporization for the heterogeneous condensation mode.

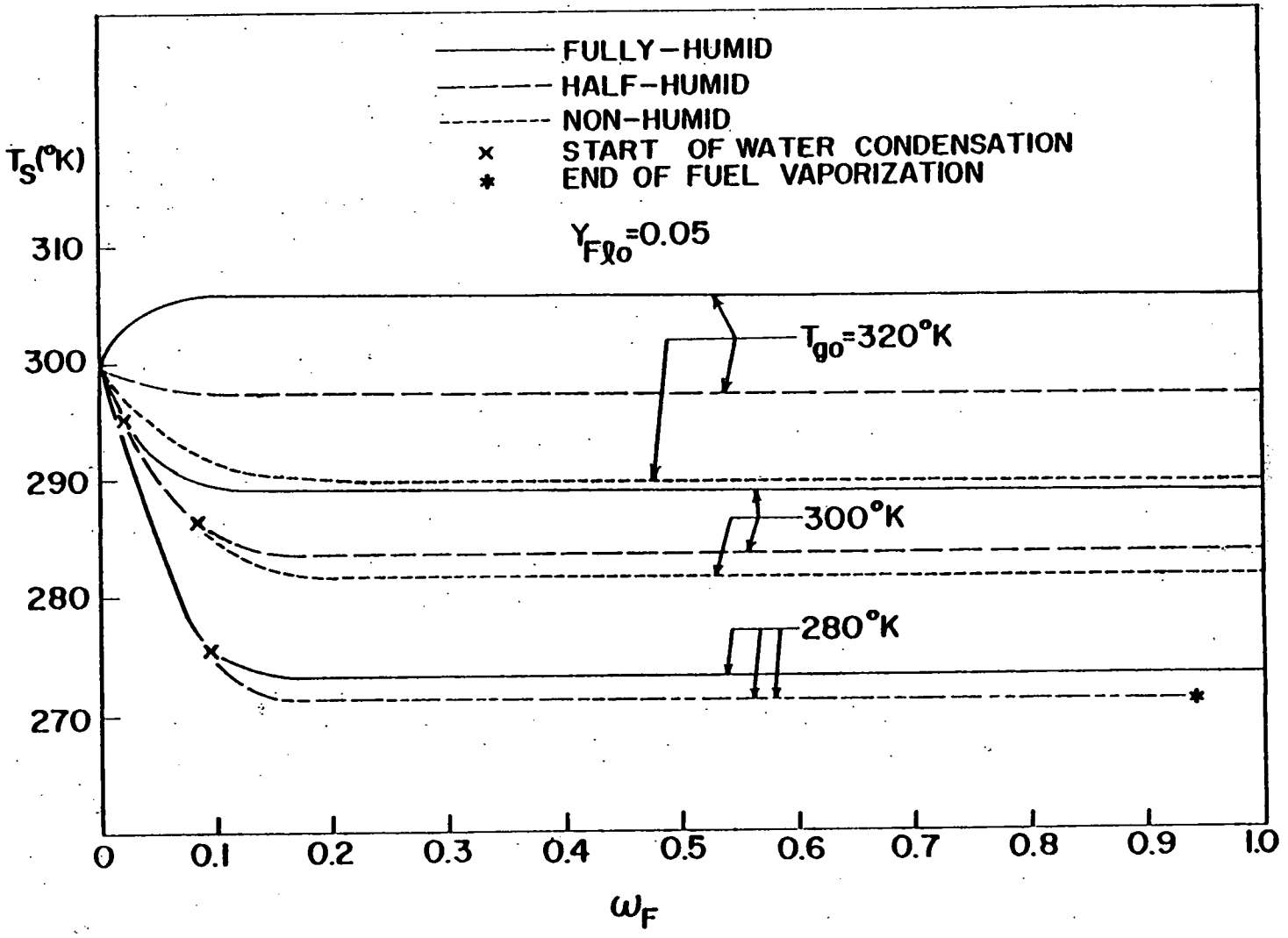

Figure 1. Influence of initial gas temperature and humidity on droplet temperature variation for the heterogeneous condensation mode.

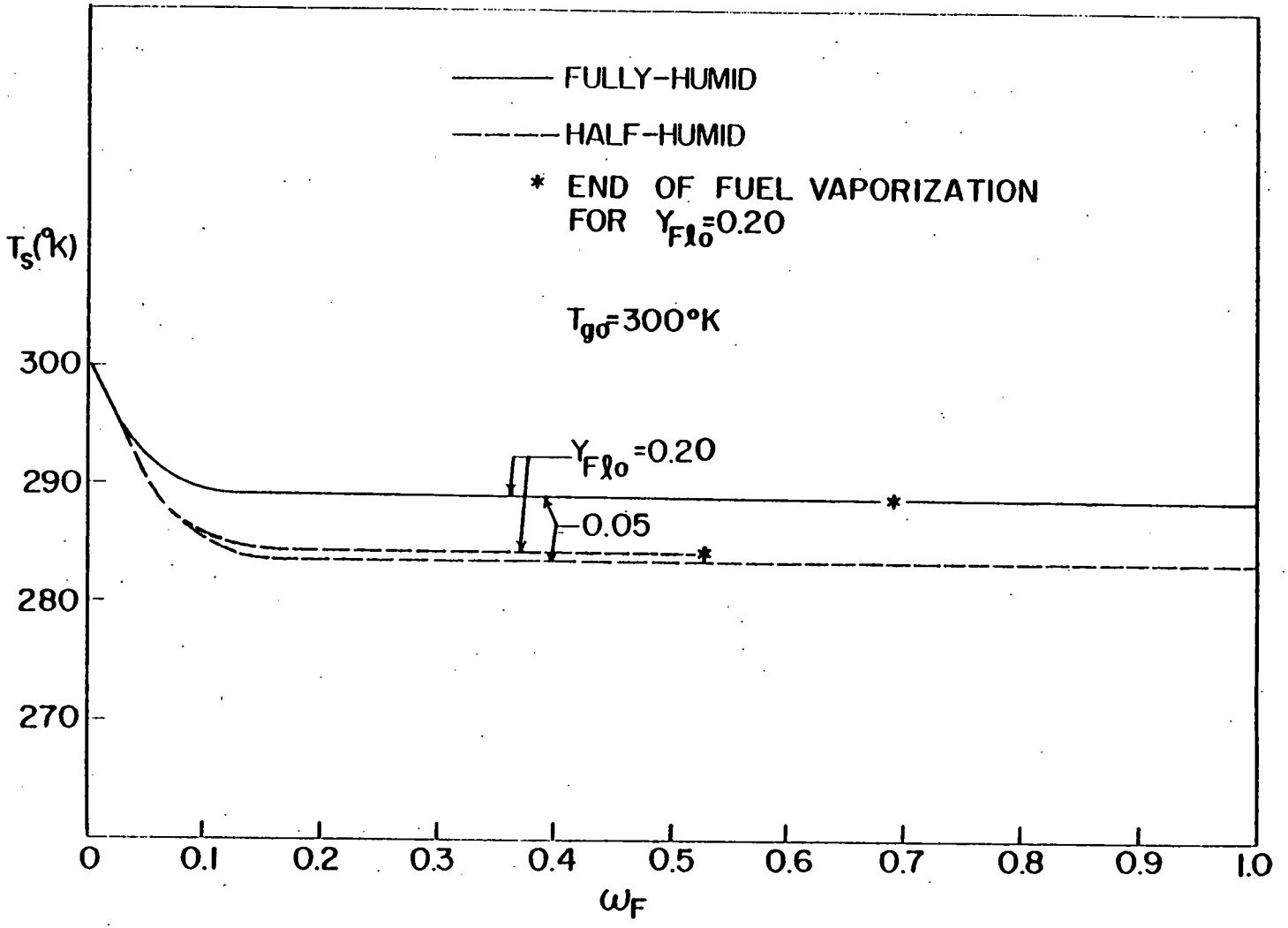

Figure 2. Influence of initial liquid fuel concentration and humidity on droplet temperature variation for the heterogeneous condensation mode.

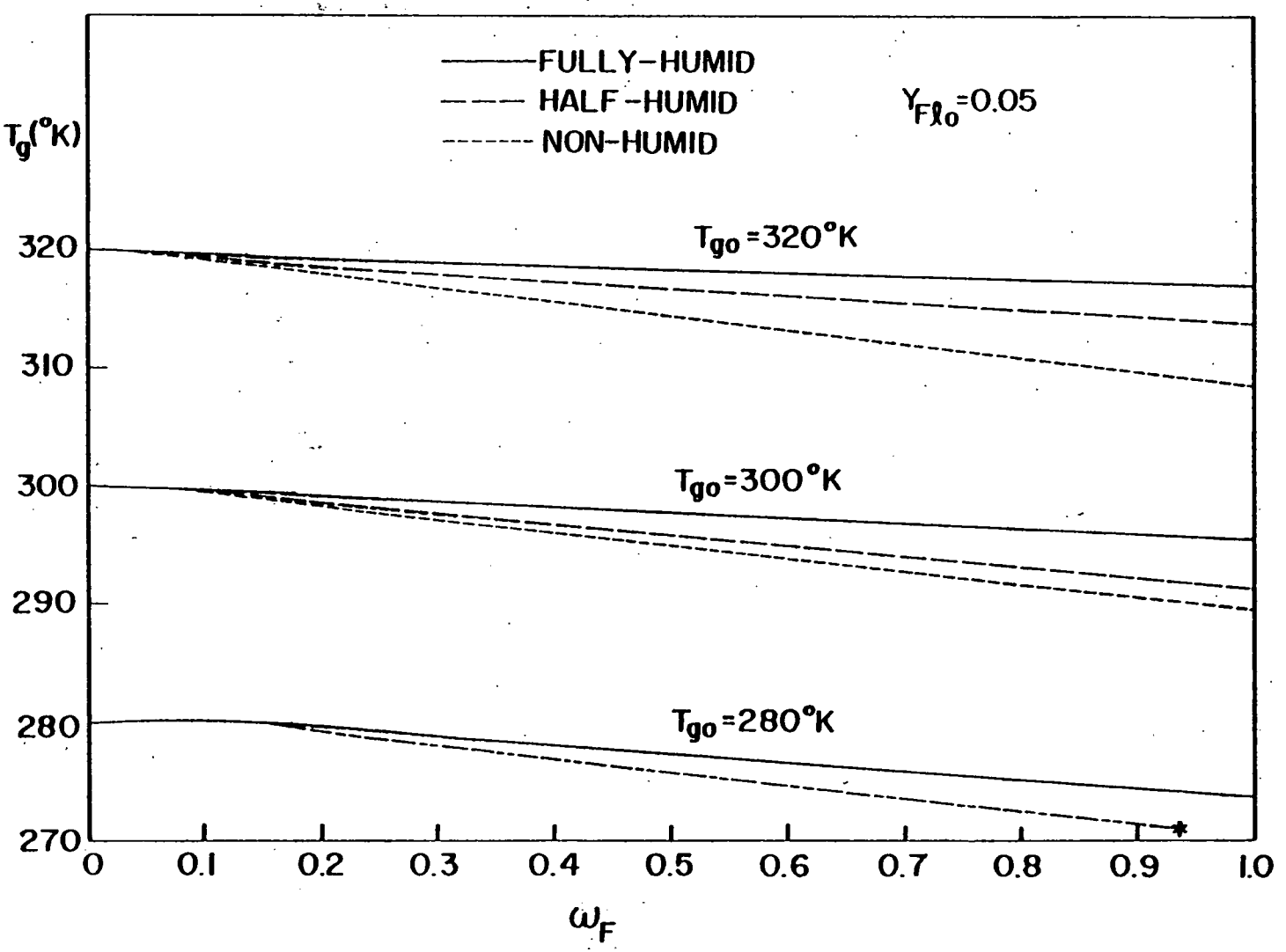

Figure 3. Influence of initial gas temperature and humidity on subsequent gas temperature variations for the heterogeneous condensation mode.

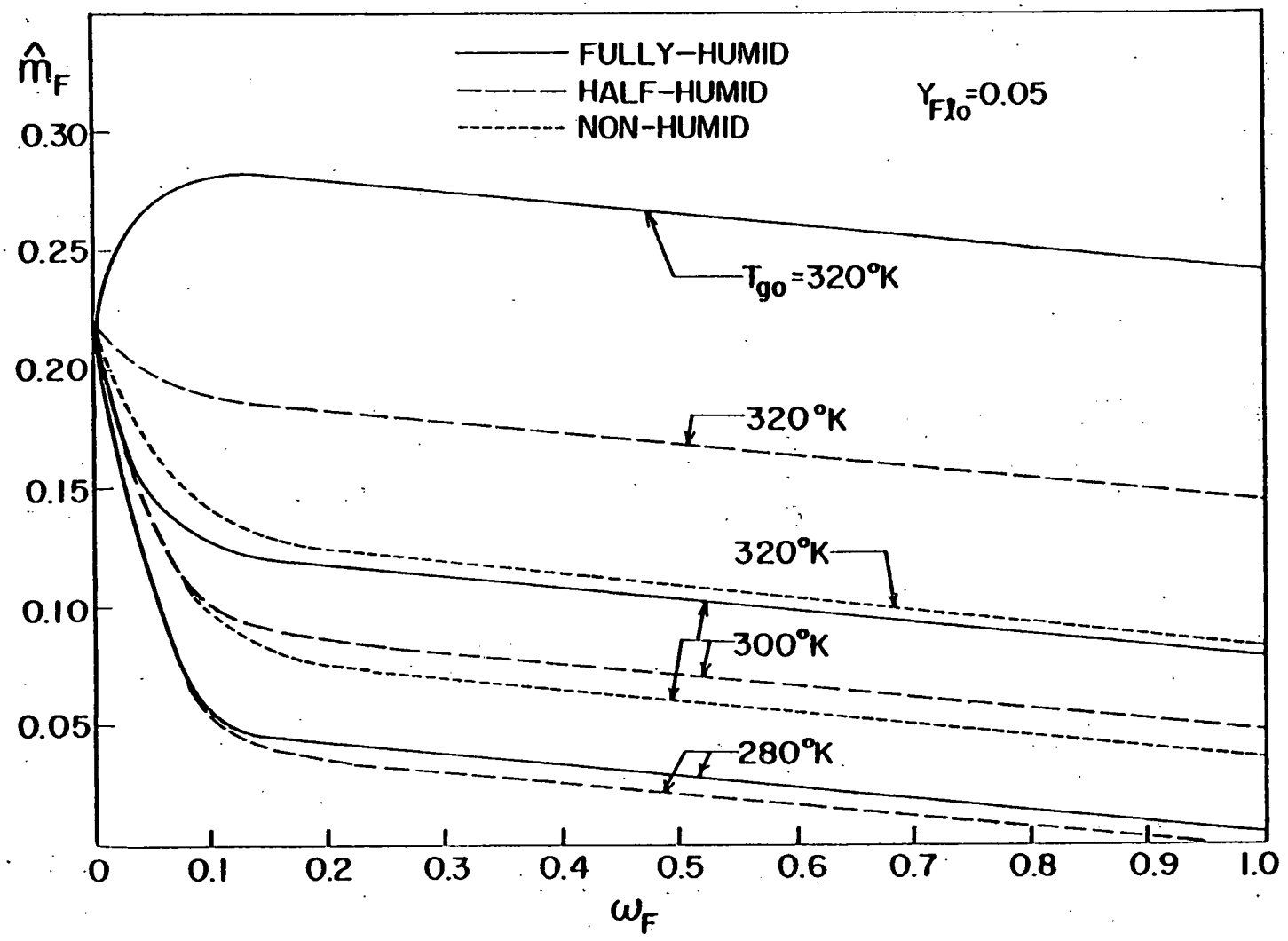

Figure 4. Influence of initial gas temperature and humidity on fuel vaporization rate variation for the heterogeneous condensation mode.

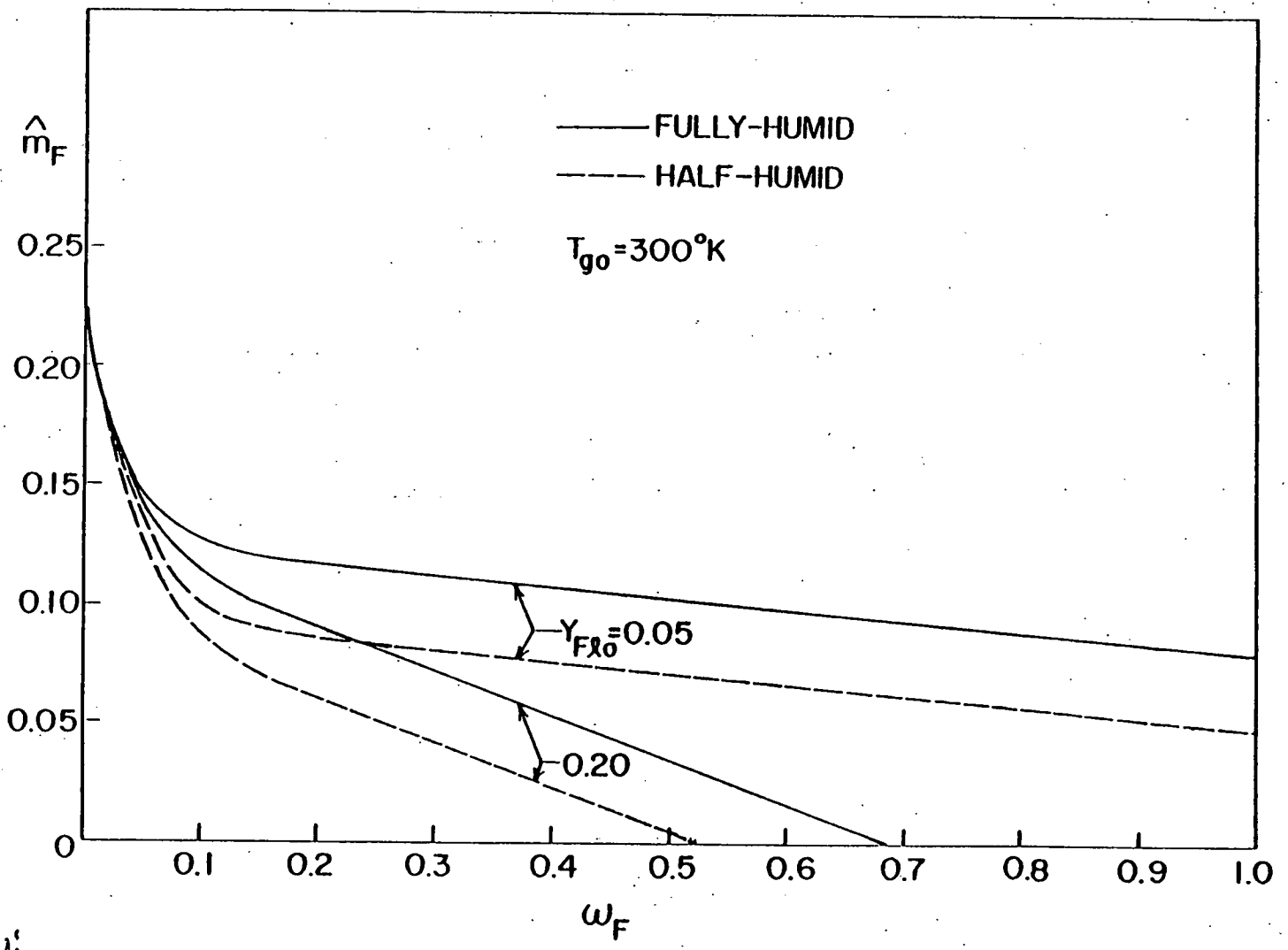

Figure 5. Influence of initial liquid fuel content and humidity on fuel vaporization rate variation for the heterogeneous condensation mode.

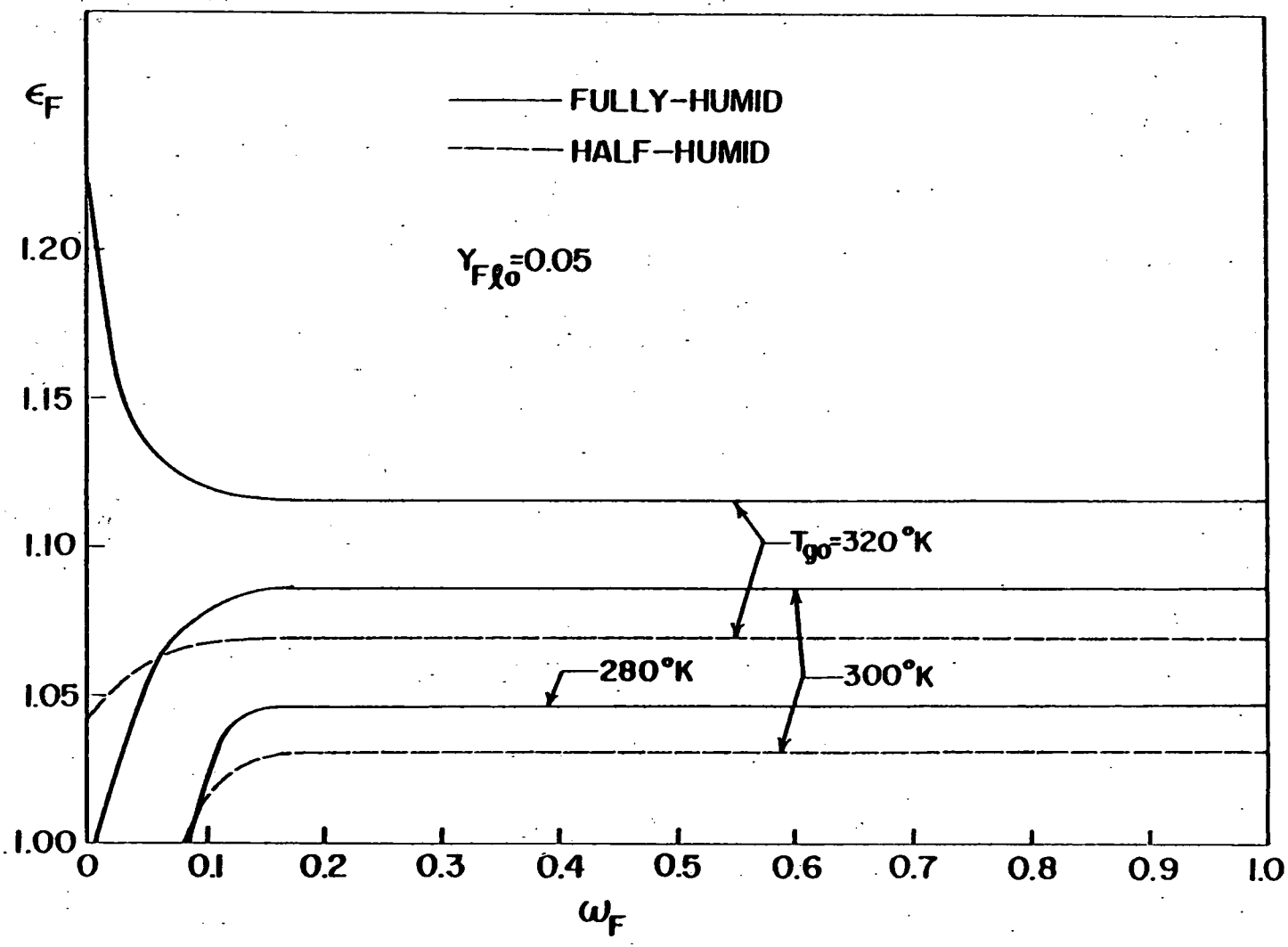

Figure 6. Influence of initial gas temperature and humidity on the variation of fractional vaporization rate of fuel for the heterogeneous condensation mode.

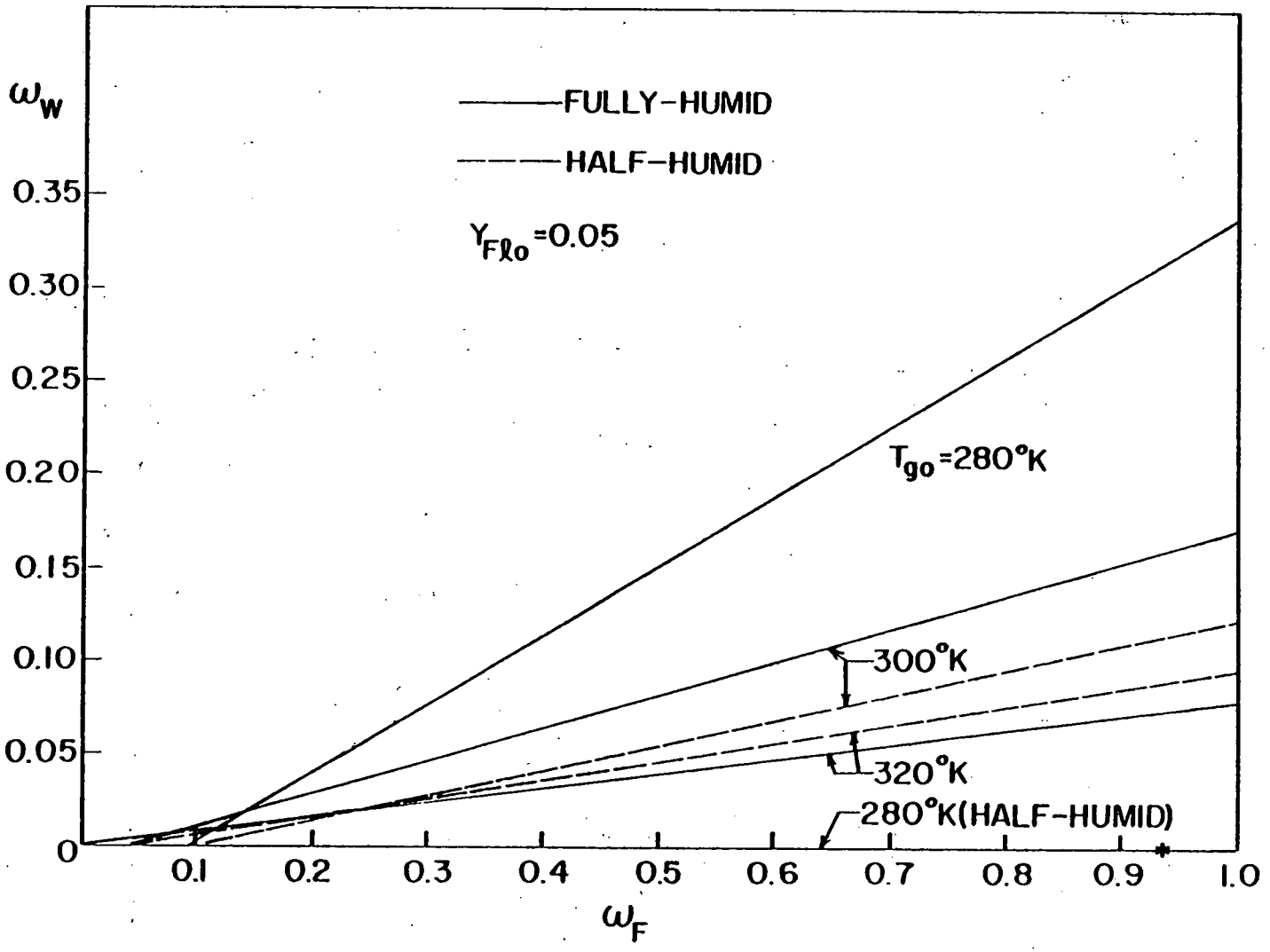

Figure 7. Influence of initial gas temperature and humidity on the variation of the fractional amount of water vapor condensed for the heterogeneous condensation mode.

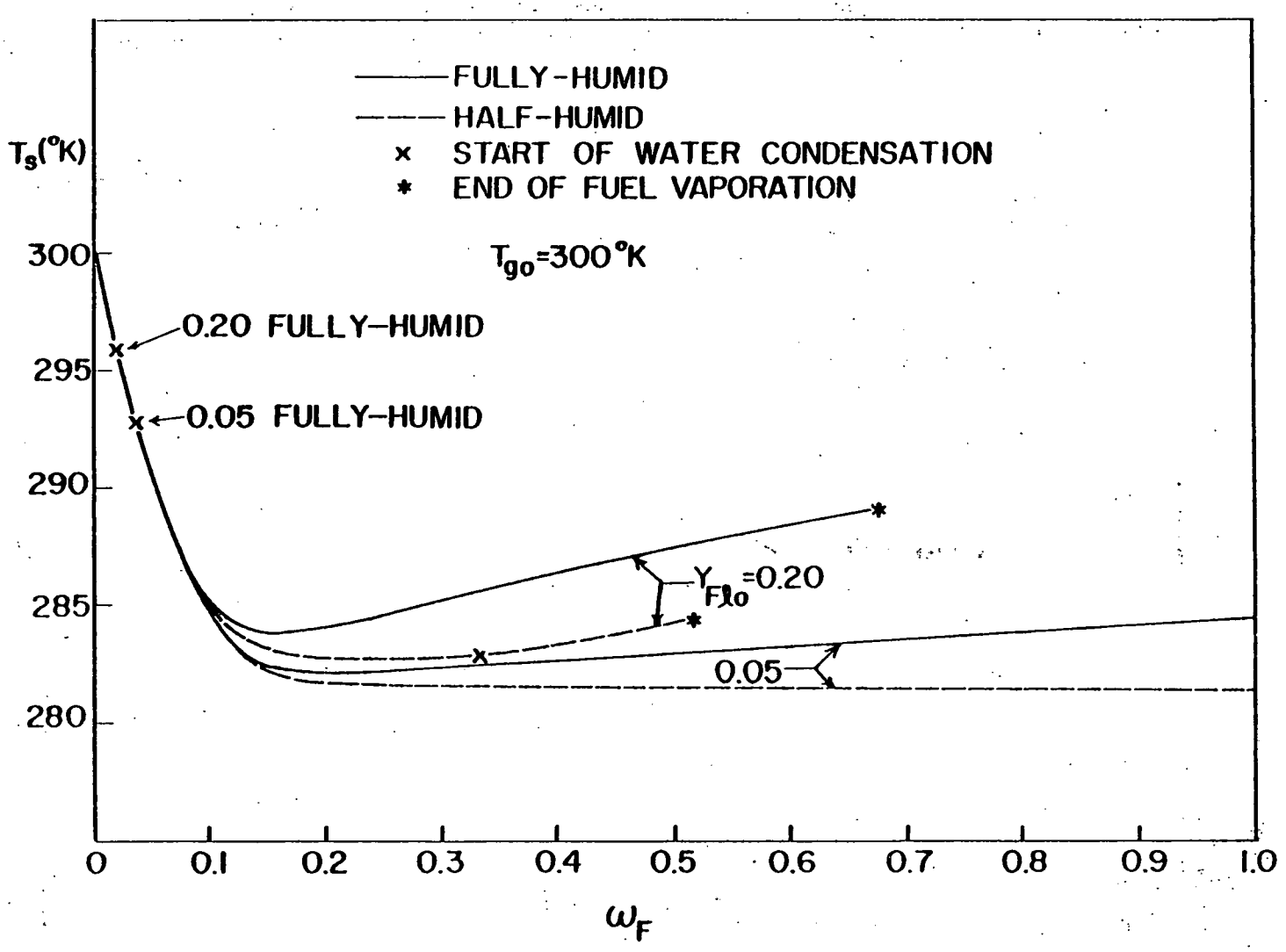

Figure 8. Influence of initial liquid fuel concentration and humidity on droplet temperature variation for the homogeneous condensation mode.

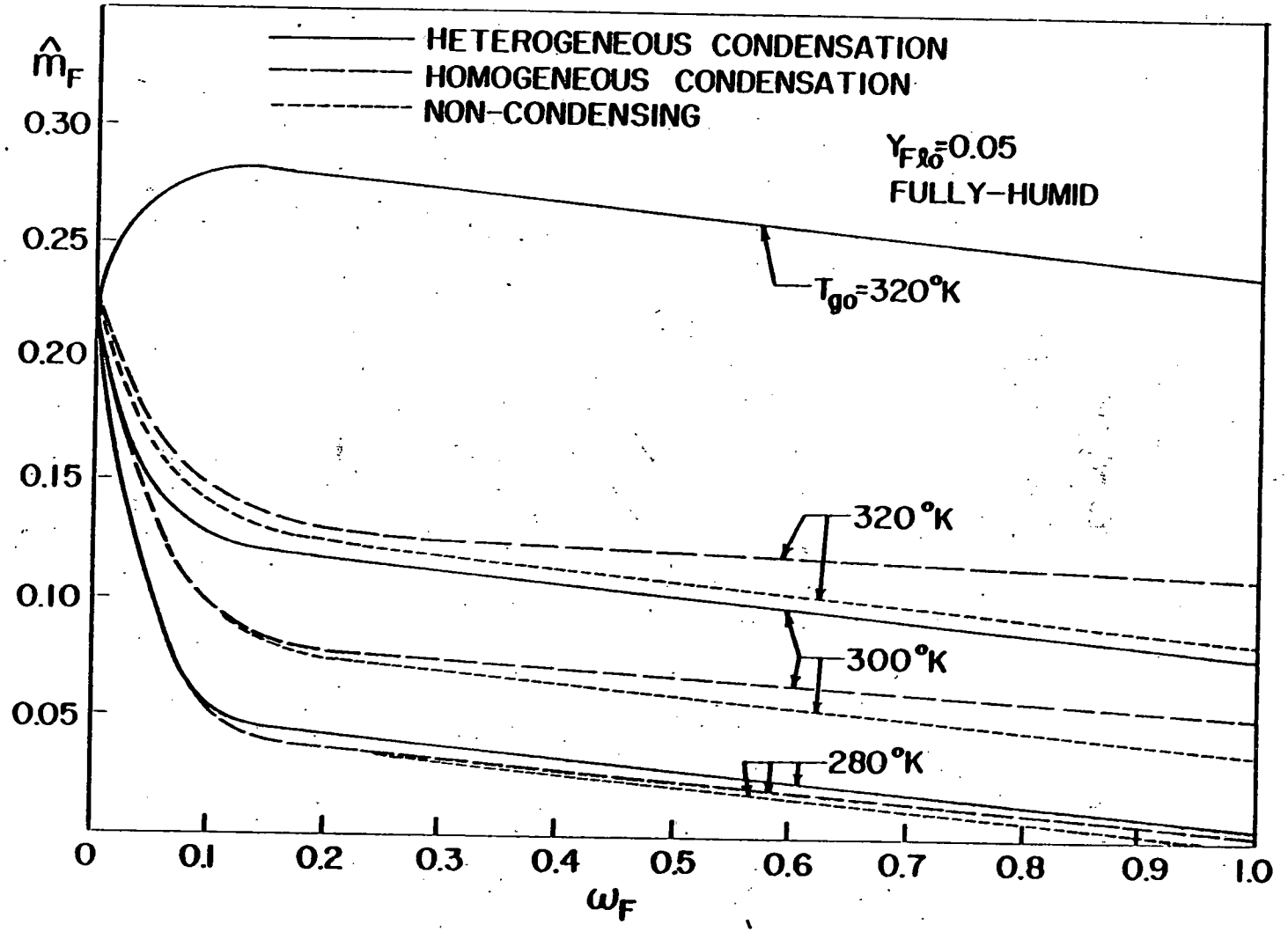

Figure 9. Comparison of fuel vaporization rate variations for heterogeneous, homogeneous, and non-condensing modes for varying initial gas temperature.

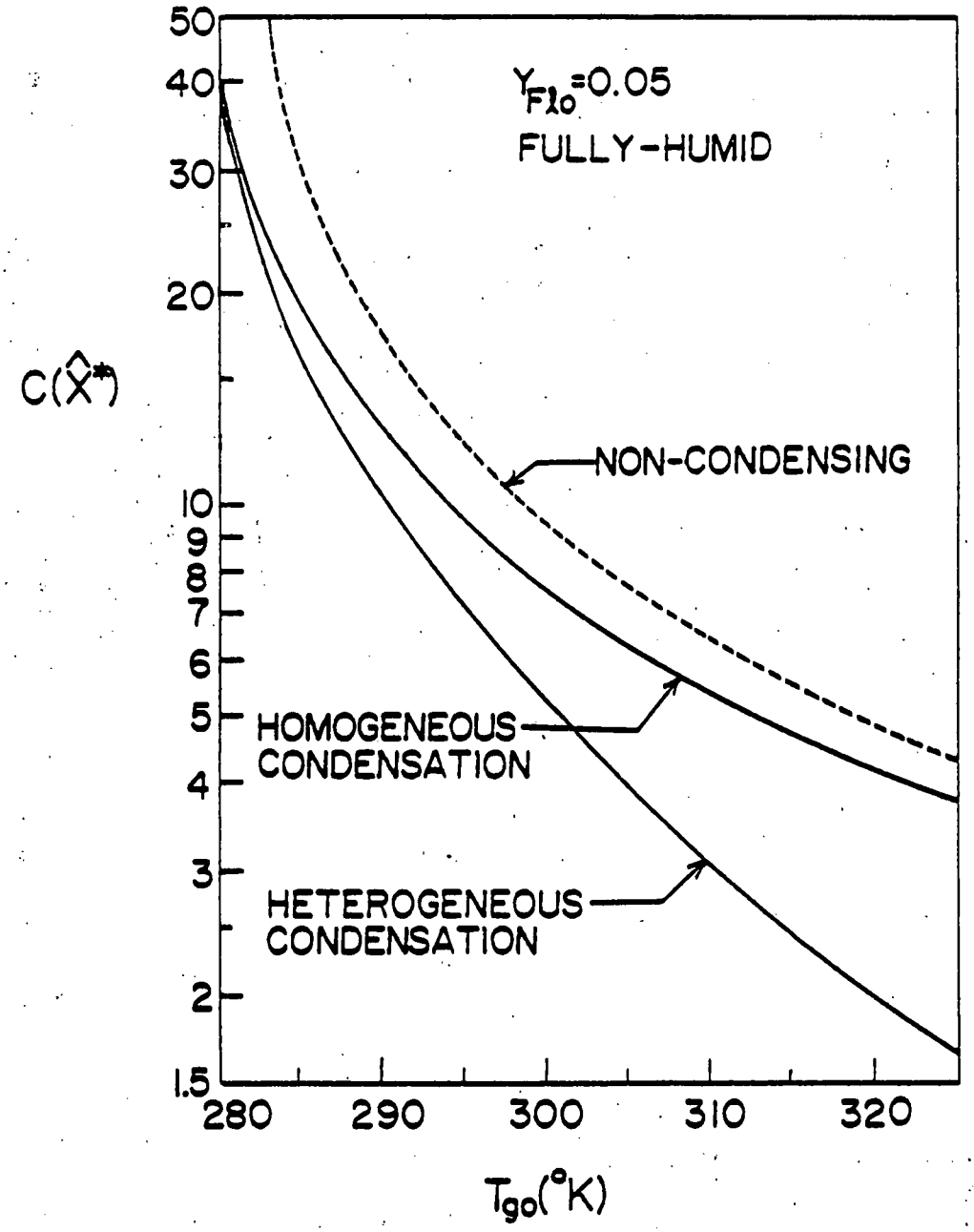

Figure 10. Comparison of the chamber function for complete fuel vaporization for the heterogeneous condensation, homogeneous condensation, and non-condensing modes.

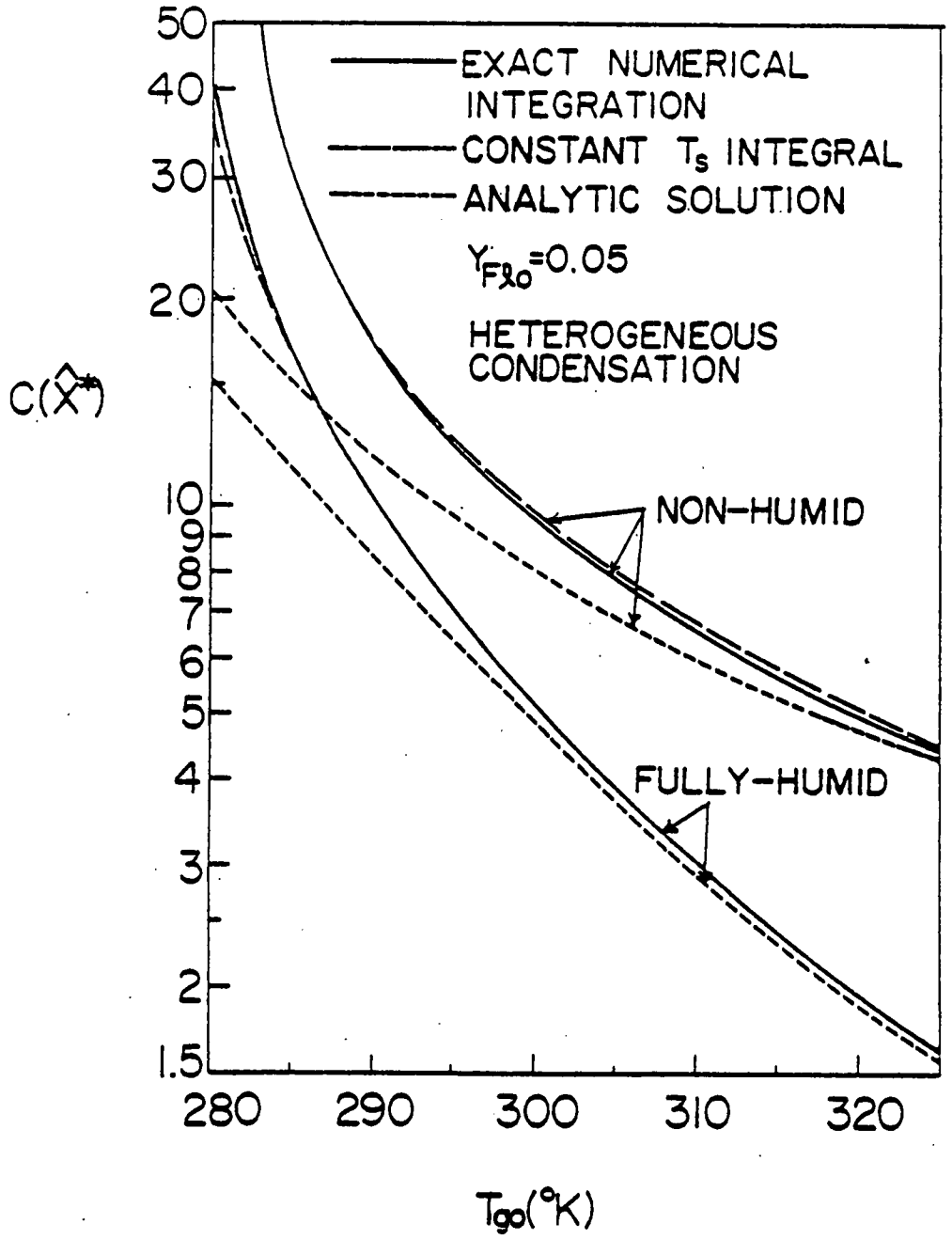

Figure 11. Comparison of the accuracy of different solutions in predicting the chamber function for complete fuel vaporization for the heterogeneous condensation mode.

☆U.S. GOVERNMENT PRINTING OFFICE: 1979 .640 .092/ 1088